

CS&SE@SW 2022

5th Workshop for Young Scientists in

Computer Science & Software Engineering

December 16, 2022
Kryvyi Rih, Ukraine

PROCEEDINGS

EDITORS

Orken Mamyrbayev
Natalia Morkun
Andrey Kupin
Serhiy Semerikov
Victoria Solovieva
Andrii Striuk

CS&SE@SW 2022

Proceedings of the
5th Workshop for
Young Scientists in Computer Science and Software
Engineering

Kyiv - Ukraine

December 16, 2022

Copyright © 2023 by SCITEPRESS – Science and Technology Publications, Lda.
Under CC license (CC BY-NC-ND 4.0)

Edited by Orken Mamyrbayev, Natalia Morkun, Andrey Kupin, Serhiy Semerikov, Victoria Solovieva and
Andrii Striuk

Printed in Portugal

ISBN: 978-989-758-653-8

DOI: 10.5220/0000166700003561

Depósito Legal: 514392/23

<https://cssesw.ccjournals.eu>

BRIEF CONTENTS

ORGANIZING COMMITTEES	IV
PROGRAM COMMITTEE	V
FOREWORD	VII
CONTENTS	IX

ORGANIZING COMMITTEES

ORGANIZING COMMITTEE

Dr. Andrii Striuk, Head of Simulation and Software Engineering department, Kryvyi Rih National University, Ukraine (chair)

Prof. Dr. Serhiy Semerikov, Professor of Computer Science and Educational technology, Kryvyi Rih State Pedagogical University, Ukraine (co-chair)

Prof. Dr. Tetiana Vakaliuk, Professor of Software Engineering and Educational Technology, Zhytomyr Polytechnic State University, Ukraine (co-chair)

Dr. Orken Mamyrbayev, Deputy Director-General of the Institute of Information and Computational Technologies, Kazakhstan

Prof. Dr. Natalia Morkun, Professor at Faculty of Engineering Sciences, Bayreuth University, Germany

Prof. Dr. Andrey Kupin, Kryvyi Rih National University, Ukraine

Dr. Victoria Solovieva, Head of Department of Economics and Digital Business, State University of Economics and Technology, Ukraine

PROGRAM COMMITTEE

Emrah Atilgan, Eskişehir Osmangazi University, Turkey

Kevin Matthe Caramancion, University at Albany, State University of New York, United States

Nadire Cavus, Near East University, North Cyprus

Stuart Charters, Lincoln University, New Zealand

Pavlo Hryhoruk, Khmelnytskyi National University, Ukraine

Oleksii Ignatenko, Institute of Software Systems, Ukraine

Oleksandr Kolgatin, Simon Kuznets Kharkiv National University of Economics, Ukraine

Pavlo Merzlykin, Kryvyi Rih State Pedagogical University, Ukraine

Vasyl Oleksiuk, Ternopil Volodymyr Hnatiuk National Pedagogical University, Ukraine

Viacheslav Osadchyi, Borys Grinchenko Kyiv University, Ukraine

İlker Özçelik, Eskişehir Osmangazi University, Turkey

James Procter, University of Dundee, United Kingdom

Marco Roveri, University of Trento, Italy

Antonii Rzhеuskyi, Lviv Polytechnic National University, Ukraine

Nataliia Veretennikova, Lviv Polytechnic National University, Ukraine

FOREWORD

Workshop for Young Scientists in Computer Science & Software Engineering (CS&SE@SW) is a peer-reviewed computer science workshop focusing on research advances, applications of information technologies. The vision of the CS&SE@SW 2022 is provides an expert environment for young researchers, who are at the beginning of their career, to present and discuss the most recent of ideas and early results of research projects. Young researchers, who will join us to take part in discussions and/or present their papers, will be offered an opportunity to exchange and discuss their research ideas with their peers, supervisors, and senior scientists working in the fields that are within the scope of CS&SE@SW.

CS&SE@SW topics of interest are:

1. Software engineering
 - Software requirements
 - Software design
 - Software construction
 - Software testing
 - Software maintenance
 - Software configuration management
 - Software engineering management
 - Software development process
 - Software engineering models and methods
 - Software quality
 - Software engineering professional practice
 - Software engineering economics
 - Computing foundations
 - Mathematical foundations
 - Engineering foundations
2. Theoretical computer science
 - Data structures and algorithms
 - Theory of computation
 - Information and coding theory
 - Programming language theory
 - Formal methods
3. Computer systems
 - Computer architecture and computer engineering
 - Computer performance analysis
 - Concurrent, parallel and distributed systems
 - Computer networks
 - Formal methods
 - Databases

4. Computer applications

- Computer graphics and visualization
- Human–computer interaction
- Scientific computing
- Artificial intelligence

1. Software engineering • Software requirements • Software design • Software construction • Software testing • Software maintenance • Software configuration management • Software engineering management • Software development process • Software engineering models and methods • Software quality • Software engineering professional practice • Software engineering economics • Computing foundations • Mathematical foundations • Engineering foundations 2. Theoretical computer science • Data structures and algorithms • Theory of computation • Information and coding theory • Programming language theory • Formal methods 3. Computer systems • Computer architecture and computer engineering • Computer performance analysis • Concurrent, parallel and distributed systems • Computer networks • Formal methods • Databases 4. Computer applications • Computer graphics and visualization • Human–computer interaction • Scientific computing • Artificial intelligence

This volume represents the proceedings of the 5th Workshop for Young Scientists in Computer Science & Software Engineering, held in Kryvyi Rih, Ukraine, on December 16, 2022. It comprises 11 contributed papers that were carefully peer-reviewed and selected from 19 submissions. Each submission was reviewed by at least 2, and on average 2.2, program committee members. The accepted papers present a state-of-the-art overview of successful cases and provide guidelines for future research.

We are thankful to all the authors who submitted papers and the delegates for their participation and their interest in CS&SE@SW as a platform to share their ideas and innovation. Also, we are also thankful to all the program committee members for providing continuous guidance and efforts taken by peer reviewers contributed to improve the quality of papers provided constructive critical comments, improvements and corrections to the authors are gratefully appreciated for their contribution to the success of the workshop. We would like to thank the developers of HotCRP, who made it possible for us to use the resources of this excellent and comprehensive conference management system, from the call of papers and inviting reviewers, to handling paper submissions, and communicating with the authors. And last but not least, we are grateful to the SCITEPRESS team for their fruitful cooperation in preparing and publishing the workshop proceedings.

Orken Mamyrbayev

Institute of Information and Computational Technologies, Kazakhstan

Natalia Morkun

Kryvyi Rih National University, Ukraine

Andrey Kupin

Kryvyi Rih National University, Ukraine

Serhiy Semerikov

Kryvyi Rih State Pedagogical University, Ukraine

Victoria Solovieva

State University of Economics and Technology, Ukraine

Andrii Striuk

Kryvyi Rih National University, Ukraine

CONTENTS

PAPERS





FULL PAPERS

Algorithm and Model of Intelligent Classification for Optimizing the Parameters of Beneficiation Technology <i>Andrey Kupin, Dmytro Zubov, Yuriy Osadchuk and Vadym Saiapin</i>	5
Experimental Verification of Collocation Detection Methods <i>Galiya S. Ybytayeva, Nina F. Khairova, Orken Zh. Mamyrbayev, Kuralay Zh. Mukhsina and Bagashar Zh. Zhumazhanov</i>	13
An Improved Diagonal Loading-Based Minimum Variance Distortionless Response Beamformer <i>Quan Trong The</i>	19
A Spectral Mask for Generalized Sidelobe Canceller Beamformer <i>Quan Trong The</i>	27
A Different Phase-Based Improved Performance of Differential Microphone Array <i>Quan Trong The</i>	34
The System of Automated Diabetes Control <i>Vitalii L. Levkivskiy, Galyna V. Marchuk, Oleksandr V. Kuzmenko and Anton Yu. Levchenko</i>	41
An Intelligent Robotic Platform for Conducting Geodetic and Ecological Surveys of Water Bodies <i>Andrii Tkachuk, Mariia Hrynevych, Tetiana A. Vakaliuk, Oksana A. Chernysh and Mykhailo G. Medvediev</i>	50
Drill String Vibration Monitoring as an Element of Automatic Control of Drilling <i>Vladimir Morkun, Natalia Morkun, Vitalii Tron, Alona Haponenko, Iryna Haponenko and Evhen Bobrov</i>	57
Simulator of Computer Networks and Basic Network Protocols <i>Tetiana A. Vakaliuk, Oleksii V. Chyzhmotria, Olena H. Chyzhmotria, Dmytro S. Antoniuk, Valerii V. Kontsedailo and Viacheslav Kryvohyzha</i>	63
Ultrasonic Cleaning of Ore Particles and Disintegration of Flocculation Formations <i>Vladimir Morkun, Natalia Morkun, Vitalii Tron, Oleksandra Serdiuk, Iryna Haponenko and Alona Haponenko</i>	78
NFTs: An Overhyped Gimmick or a Promising Technology of the 21st Century <i>Savelii Lukash, Nonna N. Shapovalova and Andrii M. Striuk</i>	86
AUTHOR INDEX	93

PAPERS

FULL PAPERS

Algorithm and Model of Intelligent Classification for Optimizing the Parameters of Beneficiation Technology

Andrey Kupin¹^a, Dmytro Zubov²^b, Yuriy Osadchuk¹^c and Vadym Saiapin¹^d

¹Kryvyi Rih National University, 11 Vitalii Matusevych Str., Kryvyi Rih, 50027, Ukraine

²University of Central Asia, 310 Lenin Str., Naryn, 722918, Kyrgyzstan

kupin.andrew@gmail.com, dzubovua@mail.ru, u.osadchuk@knu.edu.ua, ksn.vadim@gmail.com

Keywords: Optimization, Beneficiation Processes, Magnetite Quartzite, Intellectual Classification and Control.

Abstract: Based on the application of the classification control approach, a generalized algorithm for optimization of beneficiation processes is proposed. The results of computer modelling of the classification optimization process on the example of real indicators of magnetite quartzite beneficiation are presented. The results of classification and evolutionary optimization procedures are compared. It was concluded that the proposed intelligent classification method is able to determine the vector of settings and predict the TP beneficiation with satisfactory accuracy. It is confirmed that the developed algorithms and control principles can be applied to determine the required parameter values in modern ICS.

1 INTRODUCTION

The question of optimization of parameters of technological process (TP) of magnetite quartzites (iron ore) beneficiation in industrial conditions of the mining and processing plant (MPP) for the purpose of definition of settings of regulators as a part of intelligent control system (ICS) is considered. The multidimensional and multiconnected mathematical model of TP, which is obtained as a result of the identification procedure using the neural network approach (Kupin and Senko, 2015), is considered to be known. The relevance and general formulation of such a task is presented in the works of the authors (Bublikov and Tkachov, 2019; Kupin, 2014).

Various modifications of gradient algorithms are now mainly used as search methods for multifactor optimization of technological functions of targets, optimal and adaptive automatic control systems (AACS) (Morkun et al., 2018; Livshin, 2019). However, it is well known that in the case of poor conditionality of the optimization problem, which is typical in the case of an attempt to approximate technological functions (especially in non-stationary processes), there are some problems

with the coincidence of the extremum search process appear (Livshin, 2019). A good enough alternative to this is the use of intelligent approaches: classification control and evolutionary calculations (Rudenko and Bezsonov, 2018; Trunov and Malcheniuk, 2018).

2 PROBLEM STATEMENT


Taking into account listed above, in the work (Kupin, 2014) a combined ICS with multi-stage TP beneficiation was developed. Features of the offered decisions are a rational combination of approaches of classification control and genetic optimization. The purpose of this article is to develop a generalized algorithm of intellectual classification, its research by computer modelling and verification on the principle of comparison with the results of genetic optimization.


To implement the classification algorithm in terms of TP beneficiation, we apply the problem statement according to (Rudenko and Bezsonov, 2018). Let the following categories be known in advance:


- 1) an alphabet of recognition classes for technological situations in the form of a set


$$\{X_m^0 | m = 1, M\}, \quad (1)$$

which characterizes M functional states of TP and let the class X_l^0 characterize the most desirable

^a <https://orcid.org/0000-0001-7569-1721>

^b <https://orcid.org/0000-0002-5601-7827>

^c <https://orcid.org/0000-0001-6110-9534>

^d <https://orcid.org/0000-0002-7415-5158>

(search, close to ideal or quasi-optimal) state of TP;

- 2) a training matrix of the type “object-property”, which characterizes the m -th state of ICS in the form

$$\|y_{m,i}^{(j)}\| = \begin{pmatrix} y_{m,1}^{(1)} & y_{m,2}^{(1)} & \dots & y_{m,l}^{(1)} & \dots & y_{m,N}^{(1)} \\ y_{m,1}^{(2)} & y_{m,2}^{(2)} & \dots & y_{m,l}^{(2)} & \dots & y_{m,N}^{(2)} \\ \dots & \dots & \dots & \dots & \dots & \dots \\ y_{m,1}^{(j)} & y_{m,2}^{(j)} & \dots & y_{m,l}^{(j)} & \dots & y_{m,N}^{(j)} \\ \dots & \dots & \dots & \dots & \dots & \dots \\ y_{m,1}^{(n)} & y_{m,2}^{(n)} & \dots & y_{m,l}^{(n)} & \dots & y_{m,N}^{(n)} \end{pmatrix} \quad (2)$$

$i = \overline{1, N}, j = \overline{1, n}$, where each row is an implementation of the image $\{y_{m,i}^{(j)} | i = \overline{1, N}\}$ and the column of the matrix is a training sample from the technological database (DB) $\{y_{m,i}^{(j)} | j = \overline{1, n}\}$; N, n are the numbers of signs of recognition and testing (sample size), respectively.

In the result of training it is necessary to build a division of the feature space into recognition classes Ω in order to optimize and stabilize the functional state of the ICS. In our case, for TP beneficitation according to (Kupin and Senko, 2015), the feature space is formed on the basis of the state vector of the system, which contains all the necessary previously normalized indicators (regime, control effects, output, etc.).

3 RESULTS

Based on the above statement of the problem, the next procedure of intellectual classification will have the following stages.

1. The algorithm of intelligent classification begins to work in case of a special situation (state). This state is fixed when the current values of the initial indicators (qualitative or quantitative i -th stage) at the current (k -th) step of the system $y_i(k)$ are significantly different from the planned settings $y_i^*(k)$. That is, none of the following conditions are met (or several at a time):

$$|y_i(k) - y_i^*(k)| \leq \Delta_y \Leftrightarrow \begin{cases} |Q_i - Q^*| \leq \Delta_Q \\ |\beta_i - \beta^*| \leq \Delta_\beta \\ |\beta x_i - \beta x_i^*| \leq \Delta_{\beta x} \end{cases}, \quad (3)$$

where $Q_i, \beta_i, \beta x_i$ are the current values of stage productivity, the quality of the intermediate or final product and the loss of useful in the tails,

respectively. In addition, the yield indicators (γ_i) can be additionally taken into account as similar criteria and separation indicators (ε_i). $Q_i^*, \beta_i^*, \beta x_i^*$ are the corresponding setting values. $\Delta Q, \Delta \beta, \Delta \beta x$ are the maximum permissible values of deviations between the values of the settings and the corresponding output values.

2. The main cause of special situations is perturbations caused by constant fluctuations in the quality composition and properties of primary raw materials (charges) (Bublikov and Tkachov, 2019). The peculiarity is that these effects in the conditions of modern MPP are almost impossible to measure accurately enough during the TP in real time. Therefore, we apply the method of inverse prediction using inverse models of short-term neural network predictors (Kupin and Senko, 2015). For this purpose, on the basis of the known values of the initial indicators $y_i(k)$ from (3), obtained at the k -th step of the system of the i -th stages, the corresponding values of the input perturbations at the previous step ($k-1$) are predicted. Thus, the inverse model for the neuroemulator has the form

$$v_i(k-1) \approx \hat{v}_i(k-1) = NN^{-1} \left(\begin{array}{c} y_i(k), y_i(k-1), \dots, y_i(k-l_1), \\ u_i(k), u_i(k-1), \dots, u_i(k-l_2-1), \\ v_i(k), v_i(k-1), \dots, v_i(k-l_2-1) \end{array} \right), \quad (4)$$

where $NN(\cdot)$ is nonlinear function that performs neural network transformation (direct or inverse, depending on the direction of study); l_1, l_2 are the numbers of delayed signals at the input and output, respectively.

The rest of the indicators, which are mode or controlled, are determined by direct measurement by appropriate means.

3. To implement the classification procedure, it is necessary to form a sample of data for training (parameterization) of the classifier. Such a sample is formed on the basis of records of the technological database, which is constantly updated during the TP. Therefore, to improve the speed and quality of training classifier with technological database dimension M_{DB} records is selected a limited cluster with the number of C_S records. In the process of ISC, a neural network classifier is used, so the sample size for training can be determined using expressions from (Bublikov and Tkachov, 2019). Therefore, with this in mind, the size of the cluster for classification under TP beneficitation will be $[180 \leq C_S \leq 900]$. If this amount of information is not in the technological database (for example, at the beginning of the ICS), the classification is impossible.

The selection of the specified number of cluster elements from the technological database is by the

method of the nearest neighbours based on the analysis of vectors with a minimum value of the Hamming radius (Rudenko and Bezsonov, 2018)

$$\min_m \left[d_m = \sum_{i=1}^N (x_{m,i} \oplus \lambda_i) \right], \quad (5)$$

where $x_{m,i}$ is the i -th coordinate of the reference (current) state vector from (1); λ_i is the i -th coordinate of an arbitrary vector from the technological database that is a candidate for the cluster.

Therefore, as a result of a successful clustering procedure, the C_S of records (vectors) that are closest (similar) to the current technological situation according to criterion (5) will be selected for the training sample (training cluster). In this case, as alternative clustering methods the Kohonen network or the principle of K-means may be used (Rudenko and Bezsonov, 2018).

4. Synthesis and training of the classifying neural network. Artificial neural networks today are one of the most effective means for automatic classification and clustering due to their sufficiently flexible learning capabilities and generalization properties (Kupin and Senko, 2015; Bublikov and Tkachov, 2019).

To solve the problem of classification (1) - (2), a neural network based on a multilayer perceptron is created (figure 1). The network contains 1-2 hidden layers, the size of which is determined by setting up the circuit empirically from a range of $18 \leq n_h \leq 450$ neurons in total (Bublikov and Tkachov, 2019).

As a learning algorithm in the scheme (figure 1) used one of the varieties of the algorithm with inverse error propagation. An example of a two-class classification shows that the root mean square error (MSE) does not exceed 0.4 (Class 1) and 1.2 (Class 2). This indicates a sufficient quality of classification.

5. The main task in the course of classification (or classification optimization) of the current technological situation is the final choice from the cluster of the best vector (X^*), which satisfies the following two conditions:

- according to the input features most corresponds to the current technological situation in the cluster X_i^0 on the basis of the statement (1-2);
- according to the corresponding initial indicators from the technological database best of all corresponds to the value of the global criterion type (7).

Therefore, on the basis of these conditions we obtain

$$\begin{aligned} X^* &= \arg \operatorname{extr} [J(y_1(k+1), y_2(k+1), y_3(k+1)) \\ &\quad \bar{u}(k), \bar{v}(k)] \\ &= J(Q, \beta, \beta_X), \end{aligned} \quad (6)$$

where the criterion $J(Q, \beta, \beta_X)$ is selected by the system or operator (technologist, dispatcher, etc.) based on the modification of expression (7), for example,

$$J(Q, \beta, \beta_X) = \begin{cases} Q \rightarrow \max \\ \beta^{\min} \leq \beta \leq \beta^{\max} \\ \beta_X^{\min} \leq \beta_X \leq \beta_X^{\max} \end{cases}, \quad (7)$$

where Q is the output of the control stage or section; β ; β^{\min} ; β^{\max} are the content of the useful component and the corresponding restrictions (minimum and maximum); β_X ; β_X^{\min} ; β_X^{\max} are the loss of useful in tails and corresponding restrictions.

The value of the expression of the main (first) local criterion in expression (7) may change in the process of ICS on a marginal principle. For example, $Q \rightarrow \max$, $\beta \rightarrow \max$, $\beta_X \rightarrow \min$ with restrictions on the rest of the local criteria. Therefore, the ideal class formed on the basis of (1-2) and (7) will have the form

$$X_i^0 : |y_{m,l}^{(j)}| = \{Q^{\max}, \beta^{\max}, \beta_X^{\min}\}, \quad (8)$$

where Q^{\max} the maximum value of the output performance in the cluster.

With this in mind, the distribution function from the current class analyzed in the classification process will look like

$$S(X_m^0) = \begin{cases} 1(\text{true}), \text{ if } \left| \frac{y_{m,l}^{(j)} - y_{m,i}^{(j)}}{y_{m,l}^{(j)}} \right| < \delta_{K_i} \\ 0(\text{false}), \text{ otherwise.} \end{cases}, \quad (9)$$

where $\{\delta_{K_i} | i = \overline{1, N}\}$ is the limit values of control tolerance fields for normalized recognition features.

After substitution (8) to (9) we obtain

$$S(X_m^0) = \begin{cases} 1, \left[\left[\frac{Q^{\max} - Q}{Q^{\max}} \right] < \delta_Q \right] \wedge \\ \left[\left[\frac{\beta^{\max} - \beta}{\beta^{\max}} \right] < \delta_\beta \right] \\ \wedge \left[\left[\frac{\beta_X^{\min} - \beta_X}{\beta_X^{\min}} \right] < \delta_{\beta_X} \right] \\ 0 \end{cases}, \quad (10)$$

where $\delta_Q, \delta_\beta, \delta_{\beta_X}$ are the limit normalized values of fields of control tolerances on the corresponding signs of recognition (productivity, quality, losses); \wedge is logical conjunction operation.

Functions (9 - 10) take only two logical values of value: 1 (true - true), if the current class belongs (close) to the ideal (8) or 0 (false) – otherwise (technological situation is far from ideal).

6. Making a final decision on the suitability (or unsuitability) of the classification results. For the successful implementation of the automated neural network classification procedure, the following conditions must be consistently met:

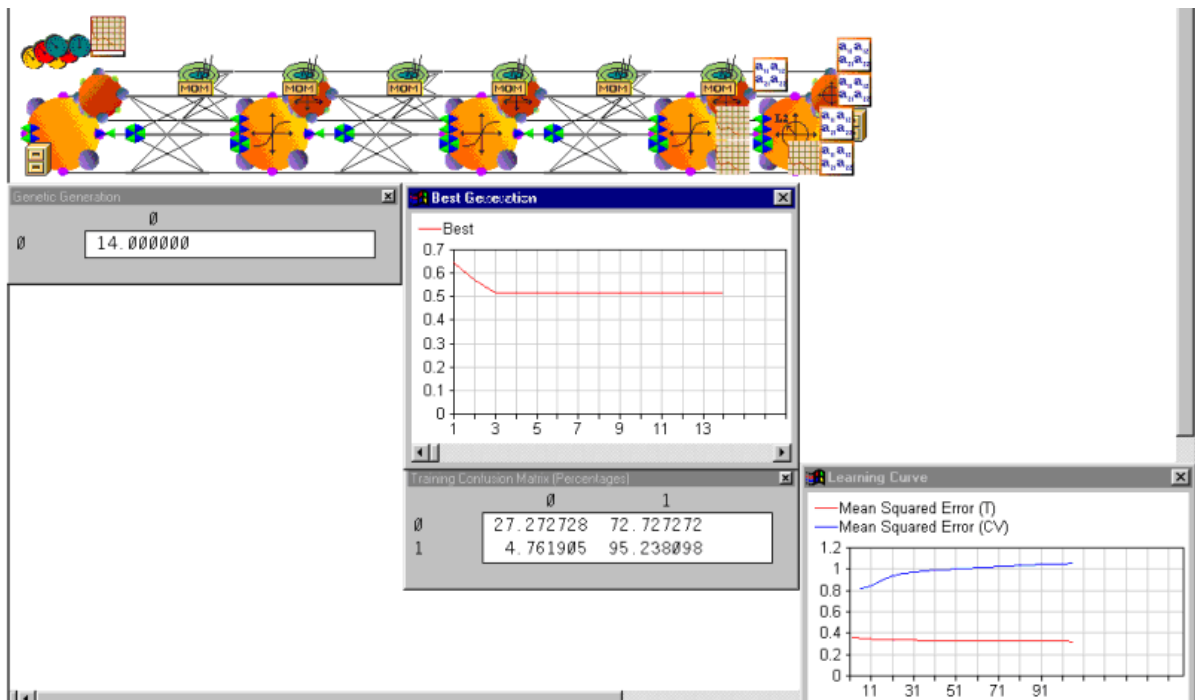


Figure 1: ICS classification neural network implemented in the environment of a specialized package of Neuro Solutions.

- the cluster for parameterization (training) of the classifying neural network must contain not less than the C_S of vectors from the technological database;
- if the precondition is fulfilled, it is necessary to check the quality of classification on the basis of calculating the value of the maximum measure of control tolerance fields for normalized recognition $\{\delta_{K_i} | i = \overline{1, N}\}$ features defined (2) and allowable forecast error ϵ_f , which according to (Rudenko and Bezsonov, 2018)

$$\begin{cases} \max [\delta_{K_i}] \leq \delta_K^* \\ \epsilon_f = |y(X^*) - y(X_l^0)| \leq \epsilon_f^* \end{cases}, \quad (11)$$

where δ_K^* , ϵ_f^* are permissible values of tolerance fields and forecast errors respectively.

- it is finally checked whether the obtained classification solution X^* can satisfy the global criterion of type (9), especially by constraints (second and third local criteria).

If all these requirements are met, the final decision on the success of the classification procedure is made (return code 0 – “successful”). Otherwise, the classification is impossible or unsuccessful (returns an error code other than 0).

7. In case of successful classification according to the algorithm, the class closest to the ideal development of the technological situation according

to the global criterion is selected as a potential solution (9).

Consider a computer model of the classification algorithm for decision-making in the ISC on the example of one stage of TP beneficiation. To do this, we use a sample of statistical indicators of the second stage in the 14-th section of the ore beneficiation plant (OBP) No. 2 Southern MPP (Kryvyi Rih, Ukraine) (Telenyk et al., 2018).

Table 1 shows an example of the current technological situation (state vector X) at a certain point in time. All factors are divided into three groups:

- 1) a perturbations – input indicators that are not subject to regulation at the current (second) stage (output for the previous first stage);
- 2) the control effects and regime indicators that may change or be regulated at the current stage;
- 3) the initial indicators to be optimized in the ICS at the current stage in accordance with (9).

Therefore, in the first step, according to the above algorithm, the cluster elements are selected according to the degree of their similarity (proximity) to the current technological situation (table 1) on the basis of criterion (7). Table 2 shows a fragment of such a cluster, which was selected from the current technological database. The total volume of the

Table 1: Instant sampling of indicators of the current technological situation.

N ^o	Marking	Explanation	Value
1.1	d ₁ , %	Particle size distribution of the product at the output of the 1st stage by class -0,074mm	48,57
1.2	Q ₁ , t/h	Processing (productivity) of the 1st stage of ore beneficiation	172,86
1.3	β _{nn1} (β ₁), %	Mass fraction (content) of total iron (magnetic) in the industrial product of the 1st stage	47,64
1.4	β _{x1} , %	Loss of iron (mass fraction) in the tails of the 1st stage	12,98
1.5	γ ₁ , %	The yield of iron in the industrial product of the 1st stage	57,85
1.6	ε ₁ , %	Extraction (extraction) of iron in the industrial product of the 1st stage	85,28
2.1	C ₂ , %	Circulating load of the second stage	288,65
2.2	d ₂ , %	Particle size distribution of the intermediate product at the output of the 2nd stage of beneficiation by class -0,074mm	76,08
2.3	Ph ₂ , %	The solids content in the mill of the 2nd stage	76,85
2.4	ρ _{k2} , %	The density of the pulp in the TP classification of the 2nd stage (hydrocyclone)	17,43
2.5	ρ _{c2} , %	The density of the pulp in the process of magnetic separation of the 2nd stage	20,43
2.6	Bm ₂ , t/h	Water consumption in the mill of the 2nd stage	26,57
2.7	Bk ₂ , t/h	Water consumption in the hydrocyclone of the 2nd stage	102,86
2.8	Bc ₂ , t/h	Water consumption for magnetic separation of the 2nd stage	92,86
3.1	Q ₂ , t/h	Processing (productivity) of the 2nd stage of ore beneficiation	301,46
3.2	β _{nn2} (β ₂), %	Mass fraction (content) of total iron (magnetic) in the industrial product of the 2nd stage	51,15
3.3	β _{x2} , %	Loss of iron (mass fraction) in the tails of the 2nd stage	10,17
3.4	γ ₂ , %	The yield of iron in the industrial product of the 2nd stage	65,74
3.5	ε ₂ , %	Extraction of iron in the industrial product of the 2nd stage	81,64
3.6	Q, t/h	Productivity (average) for the processing of ore beneficiation	237,16
3.7	γ, %	The yield of iron (average) for the processing of ore beneficiation	61,80
3.8	ε, %	Extraction of iron (average) for the processing of ore beneficiation	83,46

Table 2: A fragment of a cluster with elements that best correspond to the current technological situation in the vector of input indicators (perturbations).

N ^o	d ₁ , %	Q ₁ , t/h	β _{nn1} (β ₁), %	β _{x1} , %	γ ₁ , %	ε ₁ , %	Criterion min[d _m]
1	49,51	173,95	47,83	13,36	59,00	85,66	0,0802
2	48,98	178,73	47,59	12,88	57,56	85,18	0,0552
3	48,88	176,67	47,69	13,09	58,18	85,39	0,0433
4	48,82	179,67	47,55	12,80	57,31	85,10	0,0690
5	49,91	173,32	47,92	13,55	59,57	85,85	0,1123
6	49,62	175,61	47,76	13,23	58,61	85,53	0,0727
7	49,56	175,39	47,78	13,26	58,68	85,56	0,0744
8	48,94	171,89	47,93	13,57	59,61	85,87	0,0982
9	48,43	178,58	47,66	13,03	57,99	85,33	0,0416
10	48,55	171,03	47,98	13,66	59,90	85,96	0,1095

specified cluster, taking into account the requirements (Bublikov and Tkachov, 2019) was C_S = 250 records.

Therefore, the ideal class of initial (qualitative) indicators, formed using the requirements (10) and the data of table 3 will be as follows

$$|y_{m,l}^{(j)}| = \{Q^{\max}; \beta^{\max}; \beta_X^{\min}\} = \{330; 53, 3; 9, 8\}$$

To automate the classification process, a

multilayer neural network of direct propagation is used (figure 2), which is implemented in the Neuro Solutions as neurosimulator. On the basis of sample data from the cluster (tables 2-4) training (parameterization) of the neural network is carried out (figure 2).

To reduce the number of recognized classes in the classification process, it is necessary to rationally

Table 3: A fragment of a cluster with elements that best correspond to the current technological situation in the vector of output.

№	Q ₂ , t/h	β _{nn2} (β ₂), %	β _{x2} , %	γ ₂ , %	ε ₂ , %	Limitation [min-max]	
						β ₂ , %	β _{x2} , %
1	305,81	52,30	10,66	65,93	82,90	50,3-53,3	9,8-11,1
2	324,93	50,86	10,04	65,69	81,32	50,3-53,3	9,8-11,1
3	316,70	51,48	10,31	65,79	82,00	50,3-53,3	9,8-11,1
4*	328,69	50,61	9,93	65,65	81,04	50,3-53,3	9,8-11,1
5	303,31	52,87	10,91	66,02	83,53	50,3-53,3	9,8-11,1
6	312,47	51,91	10,50	65,86	82,48	50,3-53,3	9,8-11,1
7	311,58	51,98	10,53	65,88	82,55	50,3-53,3	9,8-11,1
8	297,56	52,91	10,93	66,03	83,58	50,3-53,3	9,8-11,1
9	324,34	51,29	10,23	65,76	81,79	50,3-53,3	9,8-11,1
10	294,15	53,20	11,05	66,08	83,89	50,3-53,3	9,8-11,1

Table 4: A fragment of a cluster with the corresponding elements according to the vector of control influences and mode indicators.

№	C ₂ , %	d ₂ , %	Ph ₂ , %	ρ _{k2} , %	ρ _{c2} , %	Bm ₂ , t/h	Bk ₂ , t/h	Bc ₂ , t/h
1	326,75	78,07	78,00	19,33	22,60	27,33	106,67	96,67
2	278,90	75,58	76,56	16,94	19,87	26,37	101,89	91,89
3	299,53	76,65	77,18	17,97	21,05	26,79	103,95	93,95
4**	270,38	75,13	76,31	16,51	19,39	26,20	101,03	91,03
5	345,86	79,06	78,57	20,29	23,69	27,71	108,58	98,58
6	313,97	77,40	77,61	18,69	21,87	27,07	105,39	95,39
7	316,19	77,52	77,68	18,80	22,00	27,12	105,61	95,61
8	347,32	79,14	78,61	20,36	23,77	27,74	108,73	98,73
9	293,27	76,33	76,99	17,66	20,69	26,66	103,32	93,32
10	356,73	79,63	78,90	20,83	24,31	27,93	109,67	99,67

Notes: where (*) is the class closest to the ideal on the basis of the analysis of values of initial (qualitative) indicators; (**) is the corresponding vector of setting values (control effects and mode indicators) to ensure quasi-optimal (close to ideal) output.

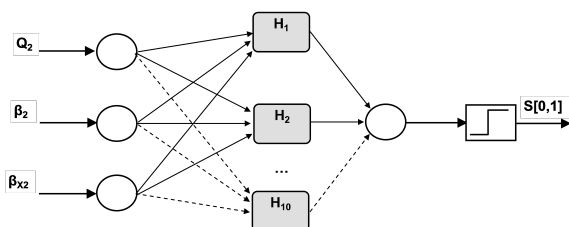


Figure 2: Neural network implementation scheme (3: 10: 1) for classification procedure.

choose the appropriate values of tolerance fields. This can be done by varying the value of the tolerance and its further study (figure 5).

As can be seen from figure 5 the number of classes that are recognized linearly depends on the tolerance values. This is evidenced by the linear trend, which is determined on the basis of the known method of least squares. The value of the coefficient of determination $R^2 = 99.8\%$ indicates a sufficiently high reliability of the approximation.

Analysis of the results of intellectual classification

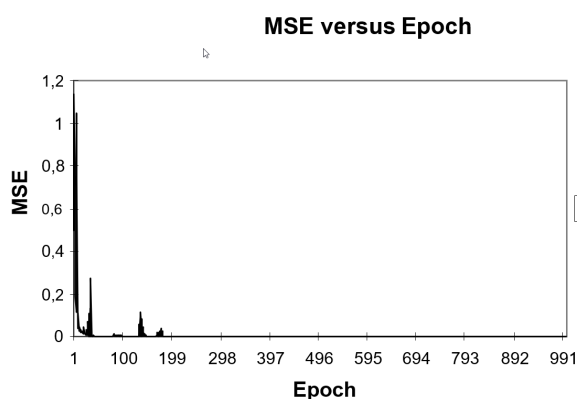


Figure 3: Report on the course of parameterization of the classification process.

(figures 3, 4, 5) and table 5 indicates the sufficient quality of such a procedure. Thus, when changing the normalized average tolerance fields within 4-4.5%, it is possible to determine with sufficient adequacy from 1 to 13 vectors with potentially quasi-optimal settings

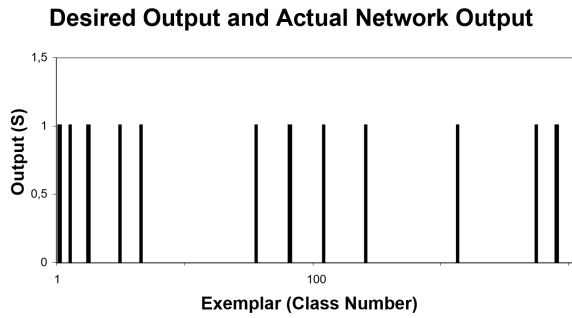


Figure 4: Report on the number of recognized classes in the classification process.

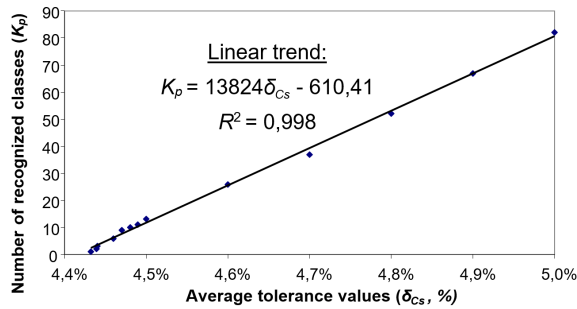


Figure 5: Dependence of tolerance field values on the number of recognized classes in the classification process.

Table 5: The resulting indicators of the adequacy of neural network classification.

Marking (Input/ Output)	S=0	S=1
1. MSE	1,49245E-10	3,78047E-07
2. NMSE	8,6783E-06	7,66892E-06
3. MAE	9,21927E-06	0,000205495
4. Min Abs Error	7,36317E-08	1,70942E-07
5. Max Abs Error	5,31987E-05	0,006554622
6. r	0,999995787	0,999996284
7. S=0 (rejected classes)	237	0
8. S=1 (classes are close to ideal)	0	13

that are close to the ideal sample. In this case, based on the application of the empirical linear dependence of the trend, the quality of such a classification can be significantly improved and brought to 1-3 samples. The rate of convergence in the parameterization of the circuit (figure 3) allows you to apply this approach in real time.

Analysis of the results of the comparison of dependencies (figure 6) shows their satisfactory convergence. As expected, more accurate control results are given by genetic optimization. On the other hand, the classification approach has a higher rate of coincidence. Therefore, both methods have demonstrated the ability to determine the required settings, both in the individual stages of TP

beneficiation, and for several stages simultaneously. Depending on the quantity and quality of a priori information in the technological database at the current time it may be appropriate to use a certain method. Therefore, the rational combination and application in the ICS of two alternative strategies (classification control and global optimization using genetic algorithms) is appropriate and justified.

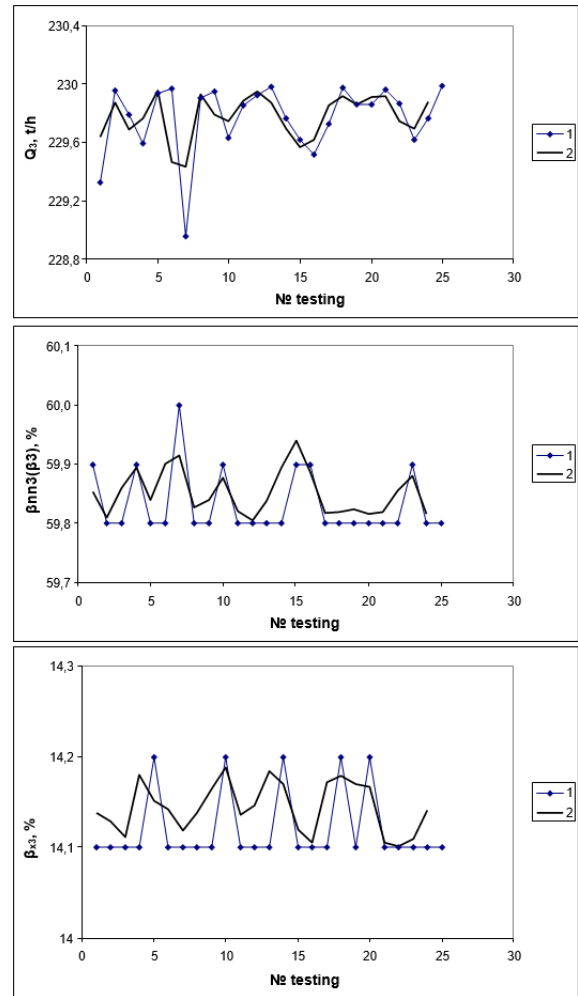


Figure 6: Comparative characteristics of the results of classification and evolutionary optimization of the 3rd stage of TP beneficiation of magnetite quartzites on productivity (Q₃) at restrictions on quality (β₃) and losses in tails (β_{x3}): 1 – classification solution (Neuro Solutions); 2 – optimization solution (NeuroShell2 + GeneHunter).

4 CONCLUSIONS

The analysis of results of computer modelling allows to make certain generalisations in the form of such

conclusions.

1. Intelligent classification using multilayer neural networks and preceding cluster selection of the training sample while ensuring the appropriate number of cluster elements allows to determine the vector of settings and predict the TP beneficiation with satisfactory accuracy, which relative error does not exceed the average normalized tolerance field within 4-4.5%.
2. The results of computer simulation using neurosimulators such as Neuro Solutions, NeuroShell2 and genetic optimizer type GeneHunter proved that the developed algorithms and control principles using evolutionary optimization methods, genetic algorithms and automated intelligent classification can be applied to the practical implementation of modern ICS in conditions of complex multistage TP to determine the required values of the settings.

REFERENCES

Aggarwal, C. C. (2018). *Neural Networks and Deep Learning*. Springer Cham, London. <https://doi.org/10.1007/978-3-319-94463-0>.

Bublikov, A. V. and Tkachov, V. V. (2019). Automation of the control process of the mining machines based on fuzzy logic. *Naukovyi Visnyk Natsionalnoho Hirnychoho Universytetu*, 2019(3):112–118. <https://doi.org/10.29202/nvngu/2019-3/19>.

Hu, Z., Bodyanskiy, Y., and Tyshchenko, O. K. (2019). Self-learning Procedures for a Kernel Fuzzy Clustering System. In Hu, Z., Petoukhov, S., Dychka, I., and He, M., editors, *Advances in Computer Science for Engineering and Education*, pages 487–497, Cham. Springer International Publishing. https://link.springer.com/chapter/10.1007/978-3-319-91008-6_49.

Kupin, A. (2014). Research of properties of conditionality of task to optimization of processes of concentrating technology is on the basis of application of neural networks. *Metallurgical and Mining Industry*, 6(4):51–55. <https://www.metaljournal.com.ua/assets/Journal/11.2014.pdf>.

Kupin, A. and Senko, A. (2015). Principles of intellectual control and classification optimization in conditions of technological processes of beneficiation complexes. *CEUR Workshop Proceedings*, 1356:153–160. https://ceur-ws.org/Vol-1356/paper_34.pdf.

Livshin, I. (2019). *Artificial Neural Networks with Java*. Apress Berkeley, CA, 1 edition. <https://doi.org/10.1007/978-1-4842-4421-0>.

Morkun, V., Morkun, N., Tron, V., and Dotsenko, I. (2018). Adaptive control system for the magnetic separation process. *Sustainable Development of Mountain Territories*, 10(4):545–557. <http://naukagor.ru/Portals/4/233%202018/E2%84%964,%202018.pdf?ver=2019-02-21-091240-697>.

Rudenko, O. G. and Bezsonov, A. A. (2018). Neural network approximation of nonlinear noisy functions based on coevolutionary cooperative-competitive approach. *Journal of Automation and Information Sciences*, 50(5):11–21. <https://doi.org/10.1615/JAutomatInfScien.v50.i5.20>.

Semerikov, S. O., Vakaliuk, T. A., Mintii, I. S., Hamaniuk, V. A., Soloviev, V. N., Bondarenko, O. V., Nechypurenko, P. P., Shokaliuk, S. V., Moiseienko, N. V., and Ruban, V. R. (2021). Development of the computer vision system based on machine learning for educational purposes. *Educational Dimension*, 5:8–60. <https://doi.org/10.31812/educdim.4717>.

Telenyk, S., Zharikov, E., and Rolik, O. (2018). Modeling of the Data Center Resource Management Using Reinforcement Learning. In *2018 International Scientific-Practical Conference Problems of Infocommunications. Science and Technology (PIC S&T)*, pages 289–296. <https://doi.org/10.1109/INFOCOMMST.2018.8632064>.

Trunov, A. and Malcheniuk, A. (2018). Recurrent network as a tool for calibration in automated systems and interactive simulators. *Eastern-European Journal of Enterprise Technologies*, 2(9 (92)):54–60. <https://doi.org/10.15587/1729-4061.2018.126498>.

Experimental Verification of Collocation Detection Methods

Galiya S. Ybytayeva¹^a, Nina F. Khairova²^b, Orken Zh. Mamyrbayev³^c,
Kuralay Zh. Mukhsina³^d and Bagashar Zh. Zhumazhanov³^e

¹*Satbayev University, 22 Satpayev Street, Almaty, 050000, Kazakhstan*

²*National Technical University “Kharkiv Polytechnic Institute”, 2 Kirpichov Str., Kharkiv, 61000, Ukraine*

³*Institute of Information and Computational Technologies, 28 Shevchenko Str., Almaty, 050010, Kazakhstan*
ybytayeva.galiya@gmail.com, nina.khajrova@yahoo.com, morkenj@mail.ru, kuka_ai@mail.ru, bagasharj@mail.ru

Keywords: Collocation, Corpus, Corpus Linguistics, Corpora, Association Measures.

Abstract: The article describes the results of a study to determine the correct phrases in the Kazakh language. The experiment consisted in the search and analysis of bigrams with frequent verbs, adjectives and nouns of the Kazakh language. Applying a statistical method to corpus material allows researchers to quantify the data obtained. The article provides an overview of MI, t-score indicators for calculating the strength of links within phrases, including their main characteristics. The purpose is to study the combinability characteristics of these lexical units, to correlate the results obtained on the basis of various association measures on different corpus, to compare the most popular association measures.

1 INTRODUCTION


In the process of penetration of modern information and communication technologies into all areas of science, in particular, into philological science, the popularity of using linguistic corpora of texts in the study of various aspects of the language is growing. In recent years, a whole range of methodological studies has appeared in the methodological literature on teaching schoolchildren and students the lexical and grammatical side of a foreign language using various linguistic corpora (Sysoyev, 2010; Chernyakova, 2012; Ryazanova, 2012). An analysis of this and other studies shows that the authors have reached a certain agreement on the conceptual content of the term “corpus linguistics”. It refers to an organized collection of texts selected and tagged according to a specific methodology and presented electronically.


The main attention in our research is paid to the corpus of parallel texts. In our study, we understand the corpus of parallel texts as a type of corpus linguistics consisting of a source text in one language and its translation into another language or languages.


This is a linguistic corpus of texts that allows you to study lexical connectivity or the phenomenon of word combinations in context.


Recently, in connection with the increasing need for automated systems, much attention is paid to the problem of automatic segmentation of word combinations in texts. There are various statistical indicators to evaluate the compatibility of words. Some dimensions are called associative measures or association measures. They allow you to calculate the strength of the connection between the elements of word combinations and are based on the frequency of these word combinations and the individual words included in them. Thus, it is possible to calculate some characteristics of the stability of lexical units, which allows them to be arranged on a conditional scale: from free combinations to phraseological units. In total, there are more than 80 measures to assess the strength of the connectedness of word combinations (Pecina, 2009).


The article is organized as follows. Section 2 is devoted to the literature review. Section 3 provides an overview of the statistical method, Section 4 presents the research methodology, and the final section discusses the research findings and suggests future plans.

^a  <https://orcid.org/0000-0002-4243-0928>

^b  <https://orcid.org/0000-0002-9826-0286>

^c  <https://orcid.org/0000-0001-7569-1721>

^d  <https://orcid.org/0000-0002-8627-1949>

^e  <https://orcid.org/0000-0002-5035-9076>

2 RELATED WORKS

Although the term “collocation” has recently come into regular use, it occupies one of the most important places in modern linguistics. In a broad sense, it is a combination of two or more words that tend to co-occur. Currently, collocations play a leading role in lexicographic practice (Atkins and Rundell, 2008; Kilgarriff, 2006). Recently, special collocation dictionaries are being created abroad and in Kazakhstan (Krishnamurthy, 2006; Smagulova, 2010; Zhanuzak et al., 2011).

However, existing dictionaries of regular expressions, firstly, do not contain their complete list, and secondly, they often do it in an insufficiently consistent manner. This is especially true for the Kazakh language. Therefore, the relevance of works on automatic detection of collocations from texts is undeniable.

Currently, we see several important application tasks that require automated methods for extracting collocations from large corpora of texts. In particular, these tasks include the creation of dictionaries and other lexicographic tools, the creation of ontologies, language learning, repair of linguistic processors, and information retrieval.

Let us briefly discuss the concept of the word combination. There are different definitions of this concept. In general, many definitions of collocation are based on the phenomenon of semantic and grammatical interdependence of phrase elements (Iordanskaya and Mel’chuk, 2007).

The term “collocation” in the Russian scientific literature was first used by Akhmanova (Akhmanova, 1996) in the Dictionary of Linguistic Terms. The first work in Russian linguistics devoted to the study of the concept of collocation in the material of the Russian language was the monograph of Borisova (Borisova, 1995).

Kozhakhmetova et al. (Kozhakhmetova et al., 1988) were worked on the problem of translation of correct word combinations from the Kazakh language to a foreign language without loss of meaning and national-cultural aspect. The scholars published a dictionary of some 2,300 regular expressions. It is effective to use in verbal translation, but we believe that it would be more effective if the regular word combinations were divided into meaning categories.

3 STATISTICAL METHOD

Nowadays the term “collocation” is widely used in corpus linguistics, in which the concept of collocation

is reinterpreted or simplified compared to traditional linguistics. This approach can be called statistical. Priority is given to the frequency of coincidences, so word combinations in corpus linguistics can be defined as statistically persistent phrases. In addition, a statistically persistent combination can be phraseological and arbitrary. In recent years, a lot of research and development on collocations has appeared, addressing both the theoretical aspects of a statistical approach to this notion and practical methods of phrase detection.

This is the emergence of a large representative corpus of texts, allowing to obtain reliable information on the frequency of a particular combination in the language as a whole. A high value of the frequency of matches seems to indicate the stability of the combination. However, this description is not sufficient to talk about the preferred combinability of certain words. Therefore, a number of statistical measures (called “association measures”) have been created to calculate the strength of the relationship between elements in a word combination. In general, these measures take into account both the frequency of matching and other parameters, primarily the frequency in a given corpus of each individual element.

However, statistics are not enough. The question needs to be answered as to what other requirements such statistically stable combinations should meet.

Most corpus managers are able to calculate the frequency of occurrence of words or word forms and the frequency of matches. Based on this data, there are many measures of association.

The total number of these dimensions is counted in dozens. The values of associative measures can be seen as indicators of the strength of the syntagmatic relationship between phrasal elements. See (Evert, 2004) for a description of the most common measures. MI, t-score is used more frequently than others. Some case managers allow the calculation of these measures.

The MI (mutual information) measure introduced in (Church and Hanks, 1990) compares context-dependent frequencies, such as randomly occurring words in a text, with independent frequencies:

$$MI(n, c) = \log_2 \frac{f(n, c) \cdot N}{f(n) \cdot f(c)}, \quad (1)$$

here: n – keyword (node); c – collocation; $f(n, c)$ – frequency of occurrence of keyword n paired with collocation c ; $f(n)$, $f(c)$ – absolute (independent) frequency of keyword n and word c in the corpus (text); N – total number of word uses in the corpus (text).

If the value of $MI(n, c)$ is greater than a certain value, then the expression can be considered statisti-

cally significant. If $MI(n, c)$ is less than zero, then n and c are called complementary.

The t-score also takes into account the frequency of occurrence of a keyword and its combination, answering the question of how non-random the strength of the association between the word combinations is:

$$t - score = \frac{f(n, c) - \frac{f(n) \cdot f(c)}{N}}{\sqrt{f(n, c)}} \quad (2)$$

4 IDENTIFICATION OF WORD COMBINATIONS BASED ON THE STATISTICAL METHOD

The aim of the work is a comparative analysis of different associative measures based on the corpus of the Kazakh language. In addition, the dependence of the results (the list of word combinations derived from the same measure) on the text material (text type) is investigated.

Our dataset includes a parallel Russian-Kazakh corpus, which has been developed over three years (Khairova et al., 2019), and an XML dictionary of synonyms with criminally related vocabulary (Khairova et al., 2021). The parallel Kazakh-Russian corpus includes texts from four news sites of the Kazakh information Internet space zakon.kz, caravan.kz, lenta.kz, nur.kz for the period from April 2018 to June 2021.

At the moment the volume of the parallel Kazakh-Russian corpus is 3000 texts in Russian and 3000 in Kazakh, including two thousand texts containing agreed Kazakh-Russian sentences.

We extracted the vocabulary for our XML dictionary of synonyms manually from the English, Ukrainian, Kazakh and Russian texts on criminal matters. Seven main thematic categories were identified for the terms, Movement, Traffic Accident, Injure, Offense, Arrest, Trial, PD. The choice of categories was due to the fact that the information resources from which the texts were taken contained the largest amount of data on the three criminal areas of “Police”, “Transfer”, “Crime” and their aforementioned subspecies. This made it possible to make our dictionary narrowly focused. All terms were also divided by parts of speech, i.e. only nouns, verbs, adjectives and word combinations were included in the dictionary. Figure 1 shows a fragment of the dictionary, which now includes about 650 basic words (over 320 nouns, over 100 adjectives, about 170 verbs and 40 word combinations) and over 2500 synonyms. It is currently still under active development.

Our study was based on the corpus of news texts “nur.kz”, “zakon.kz”, “patrul.kz”, “caravan.kz”, “inform.kz”, which includes 857 texts.

Table 1 contains data for 15 word combinations with word “police” sorted by value of MI parameter. The columns of the table, in addition to the word combination itself, show the following characteristics: Freq Word 1 & Word 2 – frequency of matching, Freq Word 1 – frequency of word combination, Freq Word 2 – key word, MI – MI value, T-score – t-score value.

The analysis of the data in table 1 (15 word combinations in total) shows that the ranks of the word combinations obtained using different indicators do not coincide.

It should also be noted that different dimensions affect the frequency of the words composing a word combination and the frequency of their combinability. Thus, MI is considered to be sensitive to low-frequency words, while t-score is useful for finding high-frequency word combinations.

We compared the automatically generated word combinations on different association indices with data from different dictionaries. The material served as collections of 2 nouns without homonyms (sozdik.kz) and 1 adjective (Kazakh-Russian, Russian-Kazakh Terminological Dictionary. Jurisprudence).

We call the above word combinations “correct”.

Below are graphs showing MI values, t-score measurements on the ordinate axis and bigram ranks on the abscissa axis. Black colour indicates “correct” word combinations from the dictionary “sozdik.kz” (4, 10 ranks) and “Kazakh-Russian, Russian-Kazakh terminological dictionary. Jurisprudence” (rank 7) indicates an additional phrase found in the dictionary.

The same tendency is observed for all obtained word combinations: the smaller the value of the measure, the greater the probability that these word combinations will not be registered as regular word combinations in dictionaries of the Kazakh language. Thus, we can say that the compatibility data given in dictionaries corresponds to the data obtained on the basis of associative measures.

As a result of the experiment, it seems important to identify phrases that are not registered in any of the dictionaries. The analysis of such word combinations shows that the bigrams located at the top of the list by degree of probability (sorted in descending order of one of the dimensions) turn out to be stable, so they can be included in the list.

As mentioned above, other statistical criterion methods based on linguistic models should also work. This idea has been adopted and implemented in the fa-

```

<term id="27">
<lemma lang="ru">сотрудник полиции</lemma>
<domain>PD</domain>
<synset lang="ru">агент полиции, сотрудник милиции, полицейский чиновник, офицер полиции, полиция
</synset>
<definition lang="ru">управление государственных служб и органов по охране общественного порядка
</definition>
<example lang="ru">Местные жители сообщали, что выживший сотрудник полиции родом из райцентра
Кыринского района</example>
<lemma lang="en">police officer</lemma>
<synset lang="en">policeman, patrolman, peace officer</synset>
<definition lang="en">a person whose job is to enforce laws, investigate crimes, and make arrests: a
member of the police</definition>
<example lang="en">But cadets and police officers deployed at the residence rapidly resorted to
sustained and excessive lethal force</example>
<lemma lang="ka">полиция қызметкері</lemma>
<synset lang="ka">полиция агенті, милиция қызметкері, полиция офицері, полиция, полицей</synset>
<definition lang="ka">қоғамдық тәртіпті сақтау, қылмыспен күресу, халық пен мемлекеттің
қауіпсіздігін қамтамасыз ету, қоғамдық және мемлекеттік құрылысты қорғау міндеттері жүктелген мекемелер мен
лауазымдардың және әскерлендірілген жасақтардың жиынтық атауы</definition>
<example lang="ka">Әлеуметтік желілерде полиция қызметкері өз тойында аспанға қарудан оқ атты деген
ақпарат тараған болатын</example>
<lemma lang="ua">співробітник поліції</lemma>
<synset lang="ua">агент поліції, співробітник міліції, поліцейський чиновник, офіцер поліції,
поліція</synset>
<definition lang="ru">орган державної влади, що займається охороною громадського порядку і боротьбою
з правопорушеннями</definition>
<example lang="ru">У Польщі співробітники поліції викрили три плантації марихуани на суму понад 2,4
мільйона злотих</example>
</term>

```

Figure 1: The fragment of the multilingual synonyms dictionary.

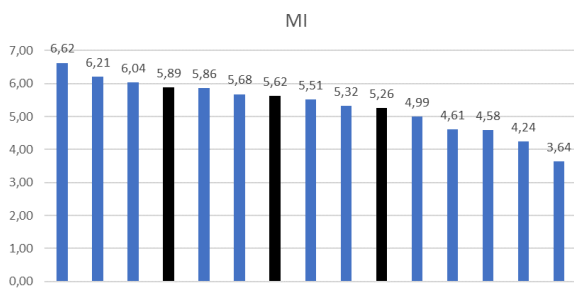


Figure 2: Values of the MI measure for collocations with the word "Police".

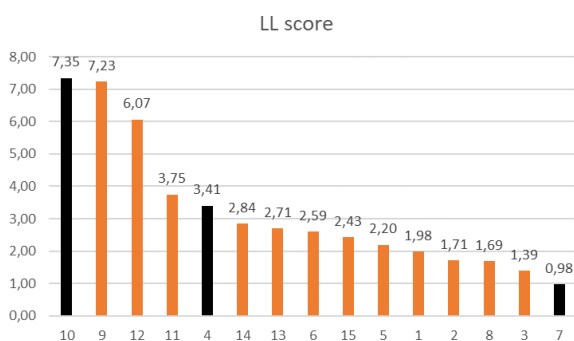


Figure 3: Values of the t-score measure for collocations with the word "Police".

mous Sketch Engine (Kilgarriff et al., 2004). It yields typical word combinations for a given keyword, on the one hand, due to a syntax restricting the compatibility of words in a given language, and on the other

hand, due to possible laws related to semantics and linguistic origin.

It turns out that there are few "correct" collocations, but this is because the vocabulary we have been relying on is too small, so it needs to be expanded. We can say that a new vocabulary is needed, which should contain various regular expressions.

The results of searching and identifying word combinations of this type are useful for lexicographers who know how to select different examples for dictionaries, and for linguists who study vocabulary and syntax in a certain aspect.

5 CONCLUSION

When comparing the phrases obtained using statistical methods with dictionaries, the same tendency is observed: the lower the value of the measure, the more these phrases are not recorded in dictionaries of the Kazakh language, and vice versa. Most of the phrases recorded in dictionaries are at the top of the list based on one of the measures of association. Thus, it can be said that the data on stable compatibility given in dictionaries coincide with the data obtained on the basis of measures of association, or, in other words, statistical measures of association better determine the real semantic-syntagmatic relations.

A comparative analysis of different association

Table 1: Values of associative measures for the word “Polisia”.

Nº	Collocation	Word 1	Word 2	Freq Word 1 & Word 2	Freq Word 1	Freq Word 2	Word in Corpus	MI	T- score
1	Patrúldik polisia	patrúldik	polisia	4	8	906	178645	6,62	1,98
2	Qarjy polisiasy	qarjy	polisiasy	3	8	906	178645	6,21	1,71
3	Polisia jasaǵy	polisia	jasaǵy	2	906	6	178645	6,04	1,39
4	Polisia bólimi	polisia	bólimi	12	906	40	178645	5,89	3,41
5	Polisiaǵa júginý	polisiaǵa	júginý	5	906	17	178645	5,86	2,20
6	Polisia shaqyrý	polisia	shaqyrý	7	906	27	178645	5,68	2,59
7	Áskerı polisia	áskerı	polisia	1	4	906	178645	5,62	0,98
8	Turǵylyqty polisia	turǵylyqty	polisia	3	13	906	178645	5,51	1,69
9	Polisia qyzmetkeri	polisia	qyzmetkeri	55	906	272	178645	5,32	7,23
10	Polisia basqarmasy	polisia	basqarmasy	57	906	294	178645	5,26	7,35
11	Polisia qyzmeti	polisia	qyzmeti	15	906	93	178645	4,99	3,75
12	Polisia departamenti	polisia	departamenti	40	906	323	178645	4,61	6,07
13	Polisiaǵa habarlasý	polisiaǵa	habarlasý	8	906	66	178645	4,58	2,71
14	Polisia basshysy	polisia	basshysy	9	906	94	178645	4,24	2,84
15	Polisia kóligi	polisia	kóligi	7	906	111	178645	3,64	2,43

measures carried out on a set of all data obtained for different word classes shows the following.

The MI measure can give the best average result. It makes it possible to distinguish between correct phraseological collocations as well as collocations in which proper names act as collocations, as well as low-frequency special terms. The disadvantages of using the t-score are primarily related to the fact that it determines the frequency with collocations, in particular with auxiliary words. Therefore, in order to “remove” the most frequent words for t-score, it is necessary to set up a list of stop words whose combinations are always at the top of the table: auxiliary words, pronouns or conjunctions. However, this also applies to other dimensions.

Whether statistical measures should be taken into account when searching for a lemma or a phrase remains an open question. The structural syntactic formulas and semantic constraints underlying the phrases also need to be taken into account.

In the future it is planned to test the effectiveness of the method on a large corpus.

ACKNOWLEDGEMENTS

This work was carried out with the financial support of the Committee of Science of the Ministry of Education and Science of the Republic of Kazakhstan (No. AR09259309).

REFERENCES

- Akhmanova, O. S. (1996). *Slovar' lingvisticheskikh terminov*. Editorial URSS, Moscow.
- Atkins, B. T. S. and Rundell, M. (2008). *The Oxford Guide to Practical Lexicography*. Oxford University Press.
- Borisova, Y. G. (1995). *Kollokatsii. Chto eto takoye i kak ikh izuchat'*. Filologiya, Moscow, 2 edition.
- Chernyakova, T. A. (2012). *Metodika formirovaniya leksicheskikh navykov studentov na osnove lingvisticheskogo korpusa*. The thesis for the degree of candidate of pedagogical sciences.
- Church, K. W. and Hanks, P. (1990). Word Association Norms, Mutual Information, and Lexicography. *Computational Linguistics*, 16(1):22–29. <https://aclanthology.org/J90-1003>.
- Evert, S. (2004). *The Statistics of Word Co-occurrences: Word Pairs and Collocations*. PhD thesis, Institut für Maschinelle Sprachverarbeitung (IMS), Universität Stuttgart, Stuttgart.
- Iordanskaya, L. N. and Mel'chuk, I. A. (2007). *Smysl i sochetayemost' v slovare*. Yazyki slavyanskikh kul'tur, Moscow.
- Khairova, N., Kolesnyk, A., Mamyrbayev, O., and Mukhsina, K. (2019). The Aligned Kazakh-Russian Parallel Corpus Focused on the Criminal Theme. In Lytvyn, V., Sharonova, N., Hamon, T., Cherednichenko, O., Grabar, N., Kowalska-Styczen, A., and Vysotska, V., editors, *Proceedings of the 3rd International Conference on Computational Linguistics and Intelligent Systems (COLINS-2019). Volume I: Main Conference, Kharkiv, Ukraine, April 18-19, 2019*, volume 2362 of *CEUR Workshop Proceedings*, pages 116–125. CEUR-WS.org. <http://ceur-ws.org/Vol-2362/paper11.pdf>.

- Khairova, N., Kolesnyk, A., Mamyrbayev, O., Ybytayeva, G., and Lytvynenko, Y. (2021). Automatic multilingual ontology generation based on texts focused on criminal topic. In Sharonova, N., Lytvyn, V., Cherednichenko, O., Kupriianov, Y., Kanishcheva, O., Hamon, T., Grabar, N., Vysotska, V., Kowalska-Styczen, A., and Jonek-Kowalska, I., editors, *Proceedings of the 5th International Conference on Computational Linguistics and Intelligent Systems (COLINS 2021). Volume I: Main Conference, Lviv, Ukraine, April 22-23, 2021*, volume 2870 of *CEUR Workshop Proceedings*, pages 108–117. CEUR-WS.org. <http://ceur-ws.org/Vol-2870/paper11.pdf>.
- Kilgarriff, A. (2006). Collocationality (and how to measure it). In Corino, E., Marellò, C., and Onesti, C., editors, *Proceedings of the 12th EURALEX International Congress*, pages 997–1004, Torino, Italy. Edizioni dell’Orso. <https://euralex.org/publications/collocationality-and-how-to-measure-it/>.
- Kilgarriff, A., Rychlý, P., Smrz, P., and Tugwell, D. (2004). The Sketch Engine. In Williams, G. and Vessier, S., editors, *Proceedings of the 11th EURALEX International Congress*, pages 105–115, Lorient, France. Université de Bretagne-Sud, Faculté des lettres et des sciences humaines. <https://euralex.org/publications/the-sketch-engine/>.
- Kozhakhmetova, K. K., Zhaysakova, R. E., and Kozhakhmetova, S. O. (1988). *Kazakh-Russian phraseological dictionary*. Mektep, Almaty.
- Krishnamurthy, R. (2006). *Collocations*, pages 596–600. Elsevier, Netherlands, 2nd edition. <https://doi.org/10.1016/B0-08-044854-2/00414-4>.
- Pecina, P. (2009). *Lexical Association Measures: Collocation Extraction*. Studies in Computational and Theoretical Linguistics. Institute of Formal and Applied Linguistics, Prague. https://ufal.mff.cuni.cz/books/preview/pecina_preview.pdf.
- Ryazanova, Y. A. (2012). *Metodika formirovaniya grammaticheskikh navykov rechi studentov na osnove lingvisticheskogo korpusa*. The thesis for the degree of candidate of pedagogical sciences.
- Smagulova, G. S. (2010). *Magynalas frazeologizmder sozdigi*. Yeltanym baspasy, Almaty.
- Sysoyev, P. V. (2010). Lingvisticheskiy korpus v metodike obucheniya inostrannym yazykam. *Yazyk i kul'tura*, 1(9):99–111.
- Zhanuzak, T., Omarbekov, S., and Zhunisbek, A. (2011). *Kazak adebetinin sozdigi. On bes tomdyk*. Almaty.

An Improved Diagonal Loading-Based Minimum Variance Distortionless Response Beamformer

Quan Trong The^a

Digital Agriculture Cooperative, No. 15 Lane 2, Tho Thap, Dich Vong, Cau Giay, Hanoi, Viet Nam
quantrongthe1984@gmail.com

Keywords: Microphone Array, Speech Enhancement, Minimum Variance Distortionless Response, Diagonal Loading, Desired Target Speaker, Dual-Microphone System, the Signal-to-Noise Ratio.

Abstract: The MVDR beamformer has more prominent solution and much better noise reduction and interference suppression capability than the conventional beamforming method, which required that the associated microphone array steering vector to sound source is accurately known. However, whenever the a priori information about the direction of arrival of the interest signal is not imprecise, microphone mismatch or different microphone sensitivities; the evaluation of MVDR beamformer is often degraded, thus speech distortion, which decreases the speech quality, is unavoidable. For mitigating the drawbacks, diagonal loading has been imposed to enhance MVDR's performance in terms of improving the signal-to-noise ratio (SNR) and removing background noise. So diagonal loading has been a common widely used method to enhance the robustness of MVDR beamformer. The inherent problem of diagonal loading is the choice of optimal parameter λ to increase the effective working of diagonal loading in complex acoustical situation. In this correspondence, the author presented a method for calculating the necessary parameter λ to improve the speech enhancement in dual-microphone system. The illustrated experiment has proven the capability of considered technique via a numerical example.

1 INTRODUCTION

Separation and speech enhancement are the most popular challenging task in digital signal processing. In real environment, target speech signal is often distorted, cause: third-party speaker, noise, transport vehicle, interference. Separation speech refers to the task of saving the target speech speaker and suppressing the unwanted different noisy environment. In this context, speech enhancement is extracting one or more target speakers, and mitigate the effect of annoying noise, interfering environment or reduce some types of speech distortions due to reverberation, the complex surrounding recording scenario. So that, the terms of "signal enhancement" and "source separation" are very necessary in almost industry application. Audio device, hearing aid, teleconference, communication.

Conference has several speakers, which can be considered as target source speech, that requires separating each component from a complicated mixture. Moreover, speech enhancement is the most crucial pre-processing for further speech application, such as:

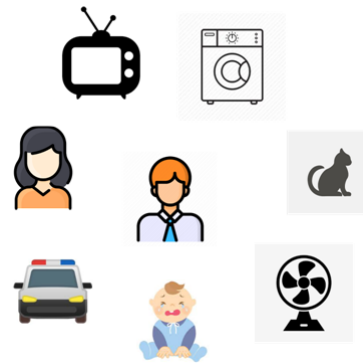


Figure 1: Extracting the desired speech is an essential task in speech enhancement.

dialogue, speech recognition, distant remote, GPS, surveillance device, video game. For dealing these problems, the microphone array (MA) (Benesty et al., 2008, 2016, 2017; Lockwood et al., 2004; Brandstein and Ward, 2001) is used for using the advantage of microphone array geometry, the spatial information of direction-of-arrival (DOA), the coherence between microphones, the characteristics of environment to alleviate the effect of noise while saving the target speaker. MA allows more input signals are multi-

^a <https://orcid.org/0000-0002-2456-9598>

channel. The number of microphones has increased in many applications in the last few years. Most of telephone, tablets or hearing-aid require 2-3 microphones.

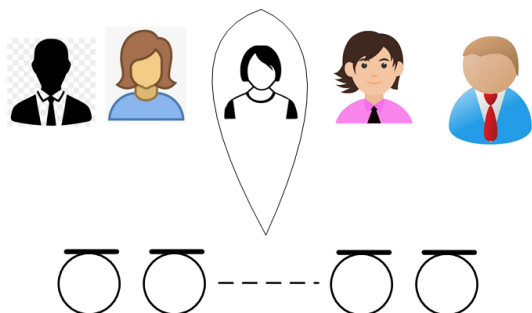


Figure 2: The using of microphone array technology.

The enhancement capabilities of MA are often higher than single-channel method. Because of the designed spatial filter to extract the target directional source speaker while eliminating all interference and noise. MA exploit the spatial a priori information about position, configuration user-defined of MA, difference of phase, more general the different acoustic properties between MA to achieve the better noise reduction while keeping the target speech. In contrast, the single – channel approach doesn't have knowledge of source or noise, so in results, the smaller quality obtained signal.

Minimum Variance Distortionless Response (MVDR) (Pan et al., 2014; Ba et al., 2007; Erdogan et al., 2016; Xiao et al., 2017a,b) has an attractive performance, which is the most widely studied and the basic to some commerce available acoustic devices. MVDR utilizes the information of DOA of target desired speaker for forming beam pattern toward this direction while minimizing the output noise power. Based on the precise knowledge of interest signal's DOA, MVDR has ability of extracting the only target directional useful speech component. In practice, the DOA of target speaker if usually is not determined exactly, due to many reasons: position of MA, influence of interference or noisy environment, that degrades seriously performance of MVDR beamformer. A lot of research has been developed to overcome this problem, by extending the region where the target directional sound source can be determined. In this paper, the author proposed the using of diagonal method for solving the problem of imprecise DOA of interest signal to improve speech enhancement.

There are some research directions for enhancing the evaluation of MVDR beamformer. One of the most important parameters is a steering vector,

which present the acoustic of sound propagation in environment from the desired source to all element of MA. More generally, a normalized of relative transfer function (RTFs) (Gannot et al., 2001b,a) is used for further signal processing. To improve performance of MVDR beamformer, RTF may be measured a priori or based on knowledge of microphone properties, room acoustic, speaker location, position.

However, in complex situation with presence of microphone mismatches or error of preferred DOA, the diagonal loading (DL) (Wu and Zhang, 1999; Vorobyov et al., 2003; Lorenz and Boyd, 2005; Shahbazpanahi et al., 2003; Chen and Vaidyanathan, 2007) technique is developed to address the problem of degraded performance of MVDR beamformer. DL technology is not only known provides the robustness, which against the DOA mismatch but also to the imprecise steering vector. Several research of DL have been proposed to force the magnitude of final signal in complex recording environment to exceed or equal to the original microphone array signal. The one well-known disadvantage of DL is the way of choosing the exact parameters is still lacking.

In this contribution, the author introduces an improvement of MVDR beamformer (imMVDR) that can be integrated into multi-microphone system for extracting the target directional speaker while eliminating all non-target directional noise or interference.

The rest of this paper is organized as: The next section is the model signal of MVDR beamformer. The proposed method, which use the diagonal technique is presented in section 3. The enhanced evaluation of the suggested method is illustrated in section 4, a comparison the quality output signal between the traditional MVDR beamformer (traMVDR) and imMVDR provides the robustness for separating interested speech source signal. Finally, concluding remarks and the future research of this approach are conducted.

Hundreds of microphone phones have been used for acoustic acquisition sound source from distance. However, dual-microphone array (DMA2) is more popular widely applied in almost speech application, due to it's simplicity, low computational load, compact, and easily installed in almost audio equipment. In experiment, DMA2 is used for verifying and illustrating the effectiveness of suggested method in term of increasing the signal-to-noise ratio (SNR) in real environment.

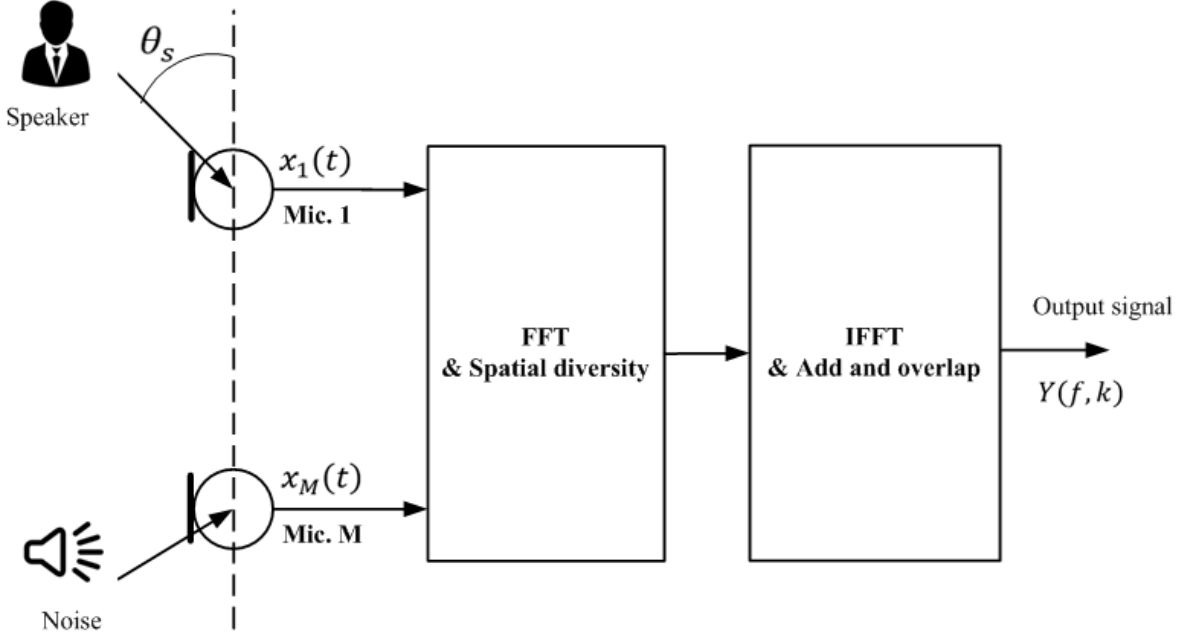


Figure 3: The scheme of beamforming in the frequency domain.

2 THE MVDR BEAMFORMER

In a noisy acoustic recording situation, it is very importance to capture the speech signal from target directional talker, therefore the only capable method is using MA beamforming to acquire the desired signal. It is assumed that a DMA2 is used to record speaker and acoustic environment. With f, k index frequency and frame, a target speaker $S(f, k)$ from a certain direction θ_s , an unwanted noise $V(f, k)$ are captured by DMA2, the observed microphone signals $X_1(f, k), X_2(f, k)$ can be written by in the frequency domain as:

$$X_1(f, k) = S(f, k)e^{j\Phi_s} + V_1(f, k) \quad (1)$$

$$X_2(f, k) = S(f, k)e^{-j\Phi_s} + V_2(f, k) \quad (2)$$

where $e^{j\Phi_s}, e^{-j\Phi_s}$ is the transfer function of target talker relative to microphone 1,2 respectively. $\Phi_s = \pi f \tau_0 \cos(\theta_s)$, $\tau_0 = d/c$, d distance between two microphones, $c = 343(m/s)$ speed of sound propagation in the air, τ_0 is the time delay.

We denote $\mathbf{X}(f, k) = [X_1(f, k) \ X_2(f, k)]^T$, $\mathbf{D}(f, \theta_s) = [e^{j\Phi_s} \ e^{-j\Phi_s}]^T$, $\mathbf{V}(f, k) = [V_1(f, k) \ V_2(f, k)]^T$ with $()^T$ indicates transpose operator, equation (1-2) can be rewritten by:

$$\mathbf{X}(f, k) = S(f, k)\mathbf{D}(f, \theta_s) + \mathbf{V}(f, k) \quad (3)$$

The steering vector $\mathbf{D}(f, \theta_s)$ play a major role in all MA algorithm. Due to, $\mathbf{D}(f, \theta_s)$ contains the information of DOA desired talker.

The digital signal processing is necessary to find an optimum weight vector $\mathbf{W}(f, k)$, which ensures the final output signal $Y(f, k)$ approximate the original signal $S(f, k)$:

$$Y(f, k) = \mathbf{W}^H(f, k)\mathbf{X}(f, k) \quad (4)$$

where $()^H$ is the symbol of Hermitian conjugation.

MVDR beamformer is aiming to minimizing the power of noise at the output without speech distortion, therefore, the optimum problem is described by the following equation:

$$\begin{aligned} \min_{\mathbf{W}(f, k)} \quad & \mathbf{W}(f, k)^H \Phi_{VV}(f, k) \mathbf{W}(f, k) \\ \text{s.t.} \quad & \mathbf{W}(f, k)^H \mathbf{D}(f, \theta_s) = 1 \end{aligned} \quad (5)$$

where $\Phi_{VV}(f, k) = E\{\mathbf{V}^H(f, k)\mathbf{V}(f, k)\}$ is the covariance matrix of noise. The optimum criteria of preserving the target directional speech signal leads to the solution:

$$\mathbf{W}(f, k) = \frac{\Phi_{VV}^{-1}(f, k)\mathbf{D}(f, \theta_s)}{\mathbf{D}^H(f, \theta_s)\Phi_{VV}^{-1}(f, k)\mathbf{D}(f, \theta_s)} \quad (6)$$

In realistic speech application, due to not available information about noise, the covariance matrix of observed microphone array signals is used instead of noise $\Phi_{XX}(f, k) = E\{\mathbf{X}^H(f, k)\mathbf{X}(f, k)\}$. So, the final optimum weight vector is:

$$\mathbf{W}(f, k) = \frac{\Phi_{XX}^{-1}(f, k)\mathbf{D}_s(f, \theta_s)}{\mathbf{D}_s^H(f, \theta_s)\Phi_{XX}^{-1}(f, k)\mathbf{D}_s(f, \theta_s)} \quad (7)$$

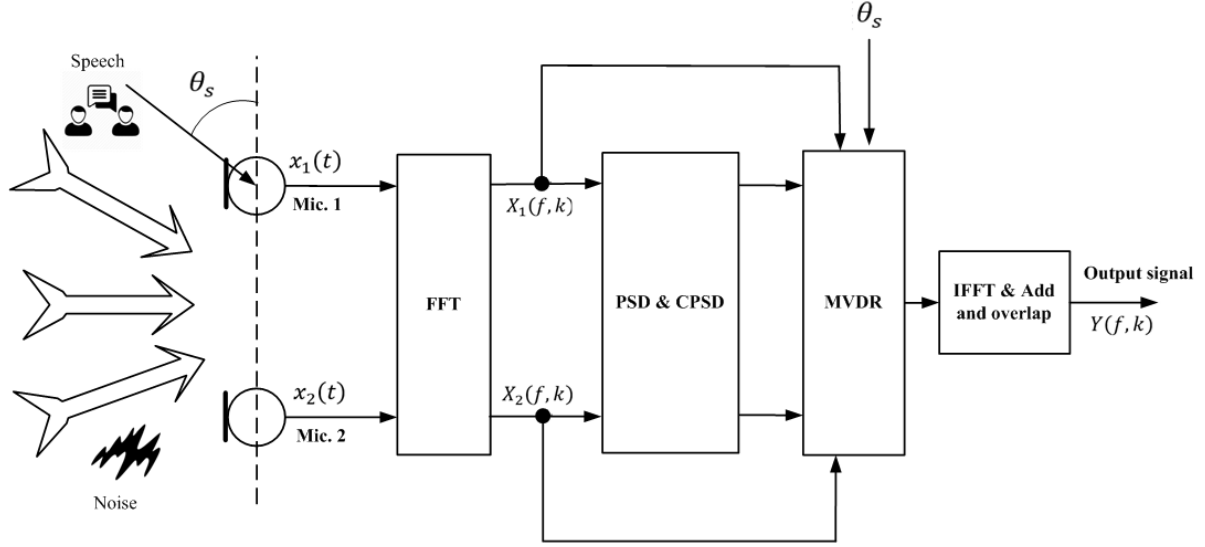


Figure 4: The scheme of MVDR beamformer.

$$\Phi_{XX}(f, k) = \begin{Bmatrix} E\{X_1^*(f, k)X_1(f, k)\} * 1.001 & E\{X_1^*(f, k)X_2(f, k)\} \\ E\{X_2^*(f, k)X_1(f, k)\} & E\{X_2^*(f, k)X_2(f, k)\} * 1.001 \end{Bmatrix} \quad (8)$$

$$P_{X_i X_j}(f, k) = (1 - \alpha)P_{X_i X_j}(f, k - 1) + \alpha X_i^*(f, k)X_j(f, k) \quad (9)$$

where $\Phi_{XX}(f, k)$ is denoted by equation (8).

With the power spectral density, $E\{X_i^*(f, k)X_j(f, k)\} = P_{X_i X_j}(f, k)$ is calculated as (9), where α is the smoothing parameter.

3 THE DIAGONAL LOADING-BASED PROPOSED METHOD

The matrix covariance $\Phi_{XX}(f, k)$ is one of the most common enhanced for MVDR beamformer. Diagonal loading technique is an efficient method for increasing the robustness of signal processing and speech quality of the output beamformer, while alleviating all surrounding background noise. Matrix covariance

$$\Phi_{XX}(f, k)$$

is added $\lambda \mathbf{I}$, where λ is unknown parameter in range $\{0..1\}$, \mathbf{I} is the unity matrix. The problem of determining λ still the most challenging in speech enhancement.

As a result, the speech distortion often occurs in frame, where the signal-to-noise ratio (SNR) high. Due to, the necessary information of noise is more required than target directional speech, the author uses

the information the speech presence probability (SPP) (Gerkmann and Hendriks, 2012a,b) and SNR to form an appropriate value of λ .

$$\lambda = SPP(f, k) * \frac{1}{1 + SNR(f, k)} \quad (10)$$

where $SPP(f, k)$ was calculated from (Gerkmann and Hendriks, 2012a,b).

In the scenario with these criteria: the speech component of target speaker and noise are uncorrelated, the noise is the same and uncorrelated between two microphones. An estimation of speech covariance $\sigma_s^2(f, k)$ (Zelinski, 1988) can be expressed as:

$$\sigma_s^2(f, k) = \frac{Re\{P_{X_1 X_2}(f, k) + P_{X_2 X_1}(f, k)\}}{2} \quad (11)$$

where $Re\{\cdot\}$ is the mathematical operator, which gets the real part.

And an estimation of noise covariance:

$$\sigma_n^2(f, k) = \frac{P_{X_1 X_1}(f, k) + P_{X_2 X_2}(f, k)}{2} - \sigma_s^2(f, k) \quad (12)$$

The temporal $SNR(f, k)$ is computed by:

$$SNR(f, k) = \frac{\sigma_s^2(f, k)}{\sigma_n^2(f, k)} \quad (13)$$

From the equation (7), the denominator plays a role as equalizer for MVDR beamformer. Therefore,

the author proposed the modified MVDR beamformer as the following equation:

$$\mathbf{W}(f, k) = \frac{(\Phi_{XX} + \lambda \mathbf{I})^{-1}(f, k) \mathbf{D}_s(f, \theta_s)}{\mathbf{D}_s^H(f, \theta_s) (\Phi_{XX} + \lambda \mathbf{I})^{-1}(f, k) \mathbf{D}_s(f, \theta_s)} \quad (14)$$

The diagonal loading technique is suitable with complex recording scenarios in presence of diffuse, coherent, incoherent noise field or interference. With an adaptive determined addition to covariance matrix of observed data, the performance of beamformer will rapidly adapt to the change of considered environment.

The next section will analyze the improvement of the proposed technique for reducing speech distortion and enhance speech quality.

4 EXPERIMENTS AND DISCUSSION

In experiment, a DMA2 is used for recording the target directional speech talker in presence of surrounding noise, interference of real situation. The purpose of this experiment is verifying the capability of saving target directional speech in comparison with the conventional MVDR. The distance between two microphones $d = 5(cm)$. The model of experiment is illustrated in figure 5. The desired speaker stand at the direction $\theta_s = 90(deg)$ relative to the axis of DMA2. For further digital signal processing, the author used Hamming window, $\alpha = 0.1$, $FFT = 512$, overlap 50%, the sampling frequency $F_s = 16kHz$. A measurement SNR (Ellis, 2011) is used for estimating the speech quality of obtained signal. The configuration of experiment is shown in figure 5.

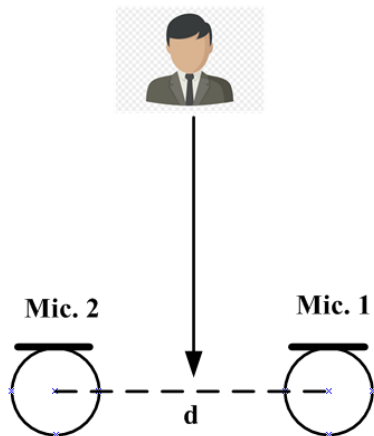


Figure 5: The scheme of experiment.

The author will compare the waveform and energy of microphone array signal and processed signals by

traMVDR, imMVDR to realize the effectiveness of the proposed method. The observed microphone signal is shown in figure 6.

The obtained signal by traMVDR and imMVDR are presented in figure 7, 8. The effectiveness of the proposed method is preserving the original speech component while mitigating all background noise. In comparison with the convention MVDR, as we can see, traMVDR removes noise, but the it's weakness is speech distortion due to several reasons. imMVDR has deal it perfectly, and help keeping the original speech signal. With an appropriate addition, which has the information of speech presence probability and the SNR, MVDR beamformer has achieved a better result in extracting the target directional useful speech signal while removing the background noise or coherence noise. MVDR beamformer has the capability of minimizing the noise at the beamformer's output, but because of some reasons, such as the error of direction of arrival (DOA) of target speaker, the microphone mismatches, the different sensitivities of microphones, that degrade the performance of MVDR beamformer. In figure 7, all of surrounding noise are suppressed, but the beamformer has cancelled original signal.

Therefore, as the following of diagonal loading technique, the author has expropriated a small value, which depends on the speech presence probability and temporal SNR. The effectiveness of the proposed has increased the amplitude of received signal. Figure 9 presents the energy of microphone array, traMVDR and imMVDR. imMVDR reduces speech distortion to 3.5 (dB).

The comparison in term of speech quality between two output signals depicted in table 1. The speech quality is increased from 1.8 to 5.4 (dB).

Table 1: The signal-to-noise ratio (dB)

Method Estimation	Microphone array signal	traMVDR	imMVDR
NIST STNR	9.5	24.0	25.8
WADA SNR	6.8	20.4	25.8

So, in the complicated environment, the suggested diagonal loading technique has improved the performance of MVDR beamformer and enhanced the speech quality and intelligibility. The effectiveness of imMVDR was verified and numerical result confirmed the capability of this approach, which uses the information of speech presence probability and instantaneous SNR. The obtained numerical results have satisfied the aim of evaluated experiment.

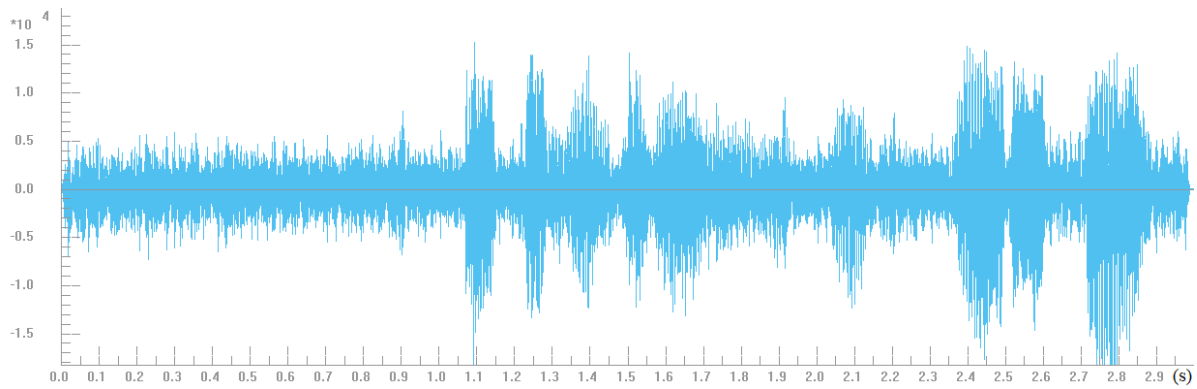


Figure 6: The waveform of the observed microphone array signal.

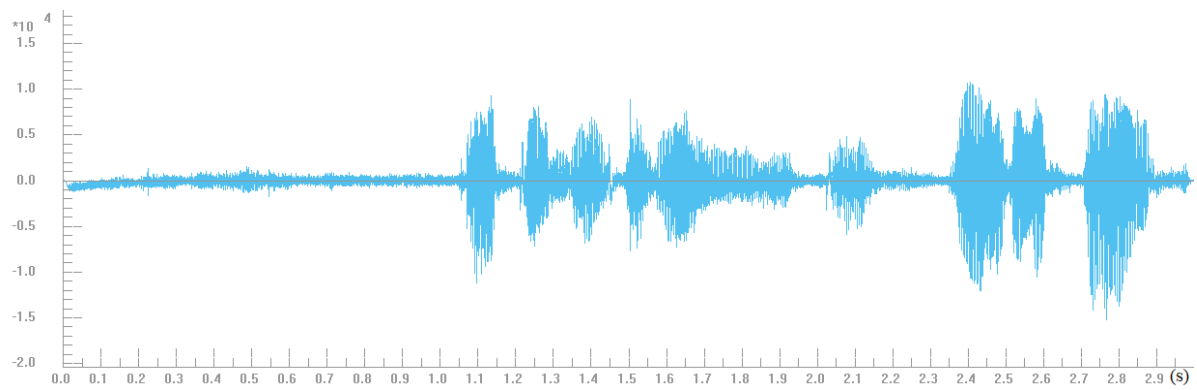


Figure 7: The obtained signal by traMVDR.

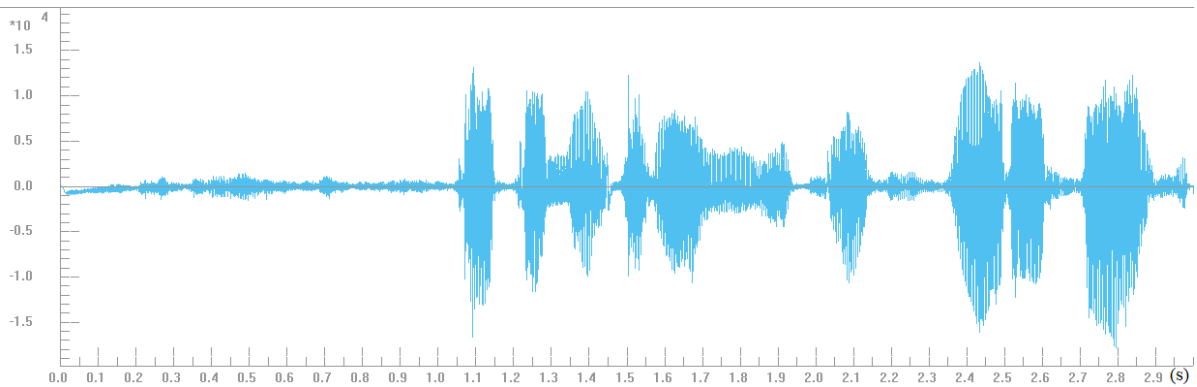


Figure 8: The obtained signal by imMVDR.

5 CONCLUSION

In many speech applications, such as hearing aids, audio devices; extracting of desired speech signal is a challenging problem from a mixture of corrupted signal with surrounding interference and different noise at low SNR. The performance of microphone array signal processing usually significantly deteriorated in the presence of unwanted noise, different speaker or complex recording scenario. Therefore, improvement

of diagonal loading is a promising method for enhancing MVDR beamformer to extract useful target signal. This contribution presents an improved of diagonal loading that takes into account the calculation of necessary parameter. Objective experiment was carried out to confirm the ability of suggested technique in increasing of speech quality, noise reduction and the signal-to-noise ratio from 1.8 to 5.4 (dB). The numerical result has ensured that the proposed method can be integrated into multi-microphone system. The es-

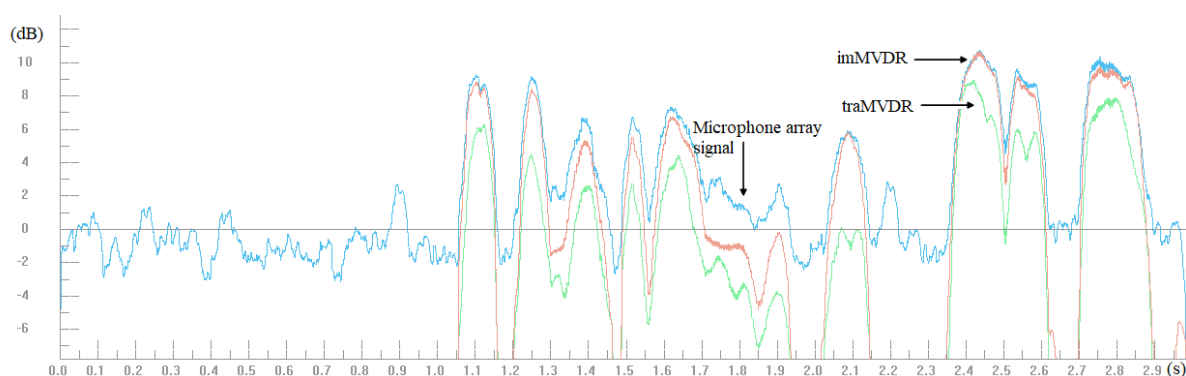


Figure 9: The illustrated energy of microphone array signal and traMVDR, imMVDR.

timization of speech presence probability can be more applied into several approaches to enhance the performance of speech enhancement system.

ACKNOWLEDGEMENTS

This research was supported supported by Digital Agriculture Cooperative. The author thank our colleagues from Digital Agriculture Cooperative, who provided insight and expertise that greatly assisted the research.

REFERENCES

- Ba, D. E., Florencio, D., and Zhang, C. (2007). Enhanced MVDR Beamforming for Arrays of Directional Microphones. In *2007 IEEE International Conference on Multimedia and Expo*, pages 1307–1310. <https://doi.org/10.1109/ICME.2007.4284898>.
- Benesty, J., Chen, J., and Huang, Y. (2008). *Microphone Array Signal Processing*, volume 1 of *Springer Topics in Signal Processing*. Springer Berlin, Heidelberg. <https://doi.org/10.1007/978-3-540-78612-2>.
- Benesty, J., Chen, J., and Pan, C. (2016). *Fundamentals of Differential Beamforming*. SpringerBriefs in Electrical and Computer Engineering. Springer Singapore. <https://doi.org/10.1007/978-981-10-1046-0>.
- Benesty, J., Cohen, I., and Chen, J. (2017). *Fundamentals of Signal Enhancement and Array Signal Processing*. John Wiley & Sons Singapore. <https://doi.org/10.1002/9781119293132>.
- Brandstein, M. and Ward, D., editors (2001). *Microphone Arrays: Signal Processing Techniques and Applications*. Digital Signal Processing. Springer Berlin, Heidelberg. <https://doi.org/10.1007/978-3-662-04619-7>.
- Chen, C.-Y. and Vaidyanathan, P. P. (2007). Quadratically Constrained Beamforming Robust Against Direction-of-Arrival Mismatch. *IEEE Transactions on Signal Processing*, 55(8):4139–4150. <https://doi.org/10.1109/TSP.2007.8944402>.
- Ellis, D. (2011). Objective measures of speech quality/SNR. <https://labrosa.ee.columbia.edu/projects/snreval/>.
- Erdogan, H., Hershey, J. R., Watanabe, S., Mandel, M. I., and Roux, J. L. (2016). Improved MVDR Beamforming Using Single-Channel Mask Prediction Networks. In *Proc. Interspeech 2016*, pages 1981–1985. <https://doi.org/10.21437/Interspeech.2016-552>.
- Gannot, S., Burshtein, D., and Weinstein, E. (2001a). Signal enhancement using beamforming and nonstationarity with applications to speech. *IEEE Transactions on Signal Processing*, 49(8):1614–1626. <https://doi.org/10.1109/78.934132>.
- Gannot, S., Burshtein, D., and Weinstein, E. (2001b). Theoretical Performance Analysis of the General Transfer Function GSC. In *Proc. Int. Workshop Acoustic Echo Noise Control*. <https://www.eng.biu.ac.il/~gannot/articles/Perf.pdf>.
- Gerkmann, T. and Hendriks, R. C. (2012a). Unbiased MMSE-Based Noise Power Estimation With Low Complexity and Low Tracking Delay. *IEEE Transactions on Audio, Speech, and Language Processing*, 20(4):1383–1393. <https://doi.org/10.1109/TASL.2011.2180896>.
- Gerkmann, T. and Hendriks, R. C. (2012b). Unbiased MMSE-Based Noise Power Estimation With Low Complexity and Low Tracking Delay. *IEEE Transactions on Audio, Speech, and Language Processing*, 20(4):1383–1393. <https://doi.org/10.1109/TASL.2011.2180896>.
- Lockwood, M. E., Jones, D. L., Bilger, R. C., Lansing, C. R., O'Brien, W. D., Wheeler, B. C., and Feng, A. S. (2004). Performance of time- and frequency-domain binaural beamformers based on recorded signals from real rooms. *The Journal of the Acoustical Society of America*, 115(1):379–391. <https://doi.org/10.1121/1.1624064>.
- Lorenz, R. G. and Boyd, S. P. (2005). Robust minimum variance beamforming. *IEEE Transactions on Signal Processing*, 53(5):1684–1696. <https://doi.org/10.1109/TSP.2005.845436>.
- Pan, C., Chen, J., and Benesty, J. (2014). On the noise-reduction performance of the MVDR beamformer in noisy and reverberant environments. In *2014 IEEE International Conference on Acoustics, Speech and*

- Signal Processing (ICASSP)*, pages 815–819. <https://doi.org/10.1109/ICASSP.2014.6853710>.
- Shahbazpanahi, S., Gershman, A., Luo, Z.-Q., and Wong, K. M. (2003). Robust adaptive beamforming for general-rank signal models. *IEEE Transactions on Signal Processing*, 51(9):2257–2269. <https://doi.org/10.1109/TSP.2003.815395>.
- Vorobyov, S. A., Gershman, A. B., and Luo, Z.-Q. (2003). Robust adaptive beamforming using worst-case performance optimization: a solution to the signal mismatch problem. *IEEE Transactions on Signal Processing*, 51(2):313–324. <https://doi.org/10.1109/TSP.2002.806865>.
- Wu, S. Q. and Zhang, J. Y. (1999). A new robust beamforming method with antennae calibration errors. In *WCNC. 1999 IEEE Wireless Communications and Networking Conference (Cat. No.99TH8466)*, volume 2, pages 869–872 vol.2. <https://doi.org/10.1109/WCNC.1999.796795>.
- Xiao, X., Zhao, S., Jones, D. L., Chng, E. S., and Li, H. (2017a). On time-frequency mask estimation for MVDR beamforming with application in robust speech recognition. In *2017 IEEE International Conference on Acoustics, Speech and Signal Processing (ICASSP)*, pages 3246–3250. <https://doi.org/10.1109/ICASSP.2017.7952756>.
- Xiao, Y., Yin, J., Qi, H., Yin, H., and Hua, G. (2017b). MVDR Algorithm Based on Estimated Diagonal Loading for Beamforming. *Mathematical Problems in Engineering*, 2017:7904356. <https://doi.org/10.1155/2017/7904356>.
- Zelinski, R. (1988). A microphone array with adaptive post-filtering for noise reduction in reverberant rooms. In *ICASSP-88., International Conference on Acoustics, Speech, and Signal Processing*, pages 2578–2581 vol.5. <https://doi.org/10.1109/ICASSP.1988.197172>.

A Spectral Mask for Generalized Sidelobe Canceller Beamformer

Quan Trong The ^a

Digital Agriculture Cooperative, No. 15 Lane 2, Tho Thap, Dich Vong, Cau Giay, Hanoi, Viet Nam
quantrongthe1984@gmail.com

Keywords: Generalized Sidelobe Canceller, Main Signal, Reference Signal, the Signal-to-Noise Ratio, Spectral Mask, Speech Enhancement, Speech Quality.

Abstract: High quality of transmitted signals is the most important task in communication when using mobile telephone, even in complicated challenging situations with presence of third-party speaker, transport vehicle, diffuse noise field, imperfect propagating of acoustic sound. Microphone array (MA) processing has become attractive technology for noise suppression in acoustic audio device by utilizing the spatial information, the properties of geometry MA, the direction-of-arrival (DOA) of interest signal without speech distortion of useful signal. GSC beamformer is one the most popular method, which applied in almost acoustic device for extracting target speaker and suppress noise from different directions. However, in realistic scenario, the error of phase or microphone mismatches often lead to speech leakage in the reference signal, that significantly deteriorates the performance of GSC beamformer, decrease the speech quality of final signal. In this paper, the author proposed a spectral mask for alleviating the speech leakage at the output of BM block to improve speech quality of GSC beamformer. Experimental results show the effective usage of suggested method (GSC-sp) in comparison between conventional GSC beamformer (GSC-ctl) and GSC-sp. Numerical results ensures that the author's approach can be integrated into multi-microphone system for solving other complicated tasks in practical situations and increases the signal-to-noise ratio to 2.3 (dB).


1 INTRODUCTION

Many acoustic devices in human life, such as stereo-sound systems, hand-free mobile phone, hearing aids, require an appropriate signal processing technique to achieve the original desired speech signal while suppressing as much as possible background noise or interfering signal. The speech intelligibility or quality indicates the degree of effective developed method. In general, signal processing method or optimum technique are chosen based on the constrained criteria, the characteristic of environment. Speech enhancement is one of the most attractive problem by numerous scholars. Saving the desired speech component while removing noise is the essential task of all speech enhancement system. The single-channel approach usually uses spectral subtraction, which convenient in suppressing noise, but leads to speech distortion.

In recent years, acoustic audio device has significant increasing in numerous speech application. However, the observed signal is frequently immersed by unwanted acoustic noise, annoying interference,

third-party talker, transport vehicle, house equipment, fan, telephone. These above factors also effect and deteriorate the speech quality and intelligibility of received signal. Method, algorithm, technology digital signal processing for assisted listening is desired to increase the efficient of speech communication, suppress background noise, third-party talker, listener fatigue to obtain hearing protection, listening comfort. However, in real life, with several undetermined interferences, noise sources; single-channel approach can't solve all necessary requirement for listening.

By utilizing array signal processing, beamforming becomes a ubiquitous task for solving the above problem. Otherwise, beamforming is used in radar, astronomy, medical imaging or communication. The usage of this beamforming helps dealing many complex tasking and gives us the benefit of eliminating noise without speech distortion. The spatial diversity, which is the major advantage of beamforming, uses a priori information of DOA, the distribution of microphone array, the properties of surrounding noise to obtain a significant noise reduction or a good pre-processing step for further processing. Meanwhile, array processing can be applied additive post-

^a  <https://orcid.org/0000-0002-2456-9598>

filtering technique to improve the beamforming’s performance. The designed microphone array with an arbitrary geometry or precise microphone sensitivity allow easily extracting the desired speech source and suppress background floor noise.

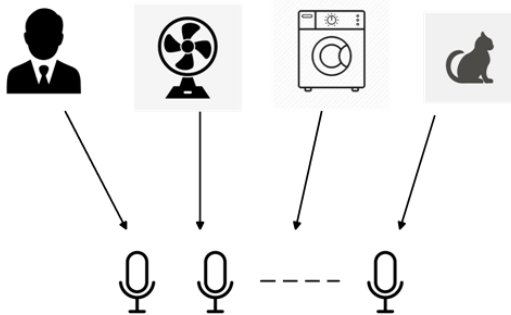


Figure 1: The complex surrounding environment affects on acquisition of target speaker.

MA (Brandstein and Ward, 2001; Benesty et al., 2008, 2017; Elko and Pong, 1997) is use in a large speech application. Because of, it’s compact, easy to implement, exploiting of the spatial diversity, DOA, a priori knowledge of environment, coherence between two microphone signals.

Beamforming approach can be categorized as two main directions: the fixed beamformer, where coefficients are constant or defined according to the DOA and adaptive beamformer, which has an adaptive filter for obtaining the desired speech.

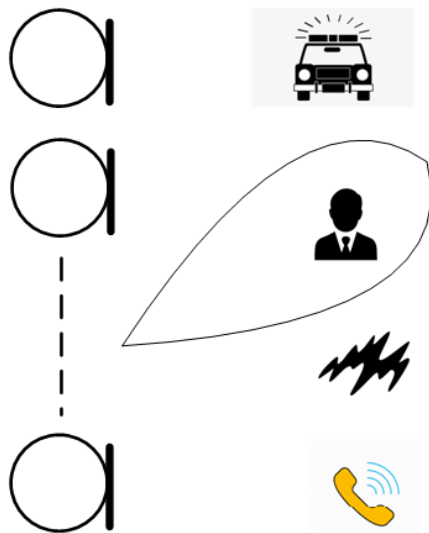


Figure 2: The significant benefit of using MA.

GSC beamformer is sufficient method for extracting target direction speech talker while eliminating background noise and immersing interference. This

beamformer has three main blocks: a fixed beamformer (FBF), a blocking matrix (BM) and an adaptive filter to extract the desired speech component and remove noise. The BM block play a major essential role in signal processing, BM’s task is blocking the desired speech target talker, passes the only noise. If there are exits a little amount of speech leakage, then the effectiveness of GSC beamformer will be deteriorated, the speech quality of the output signal decreased. In this article, the author suggested using a spectral mask for suppressing speech leakage to enhance the evaluation of GSC beamformer.

The quality and intelligibility of the output signal by MA in presence of interference and surrounding noise can be improved by signal processing algorithm.

The assumption of GSC beamformer is the BM block must retain the only noise component at the output and alleviate all desired useful signal. Herein, the control of coefficient of BM and ANC block is an important task in GSC beamformer. Usually, the BM is preferred to extract noise and not allowed pass through leakage signal, which often deteriorate performance. An estimation of DOA to the conventional GSC module, which improved the blocking matrix and decreased the leakage of useful signal (Li and Zhang, 2016). Khayeri et al. (Khayeri et al., 2011) suggested using the linear constrained minimum variance (LCMV) beamformer to suppress speech leakage and enhance noise reduction and overall performance. Utilizing the sound-source presence probability to combine with voice activity detection to enhance BM’s working (Yoon et al., 2007). In the frequency domain, a similar GGC was outperformed to Herbordt and Kellermann (Herbordt and Kellermann, 2021) to improve and increase the speech quality of the output signal. In (Hoshuyama et al., 1998), the estimation of signal-to-interference ratio (SIR) obtained by the output power of BM and FBF was used to control the coefficients of BM.

Dual-microphone system (DMA2) is one of the most widely implemented MA for almost acoustic device, hearing aid, teleconference, mobile telephone. In experiments, the author use DMA2 for illustrating advantage of the proposed method in speech enhancement. DMA2 with it’s compact, and easy to implement with low computational load for processing. Otherwise, a numerous of pre-processing and post-filtering technique can be applied on DMA2 to achieve high diversity and noise reduction.

The rest of this contribution is organized as follow. In the next section, a brief of the principle working of GSC beamformer are introduced. Section 3 introduce the spectral mask, which help blocking the speech

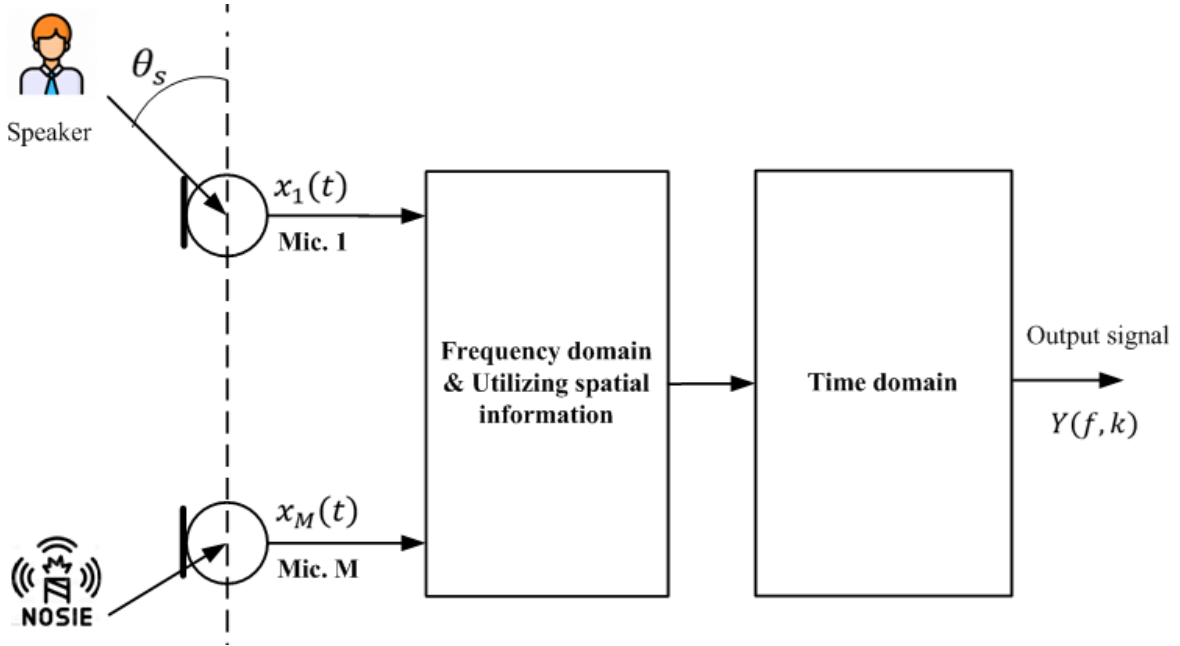


Figure 3: An implementation of MA in frequency domain.

leakage from the reference signal. Experiments with target talker in presence of interference, background noise and numerical results are expressed in section 4. Concluding remark, and the main ideal for further research are introduce in section 5.

2 GENERALIZED SIDELobe CANCELLER BEAMFORMER

Almost microphone array algorithm implemented in STFT domain. We denote some necessary parameters for signal processing as: $X_1(f, k), X_2(f, k)$ is the observed microphone array signals on two microphones; f, k is the index of frequency and temporal considered frame respectively. The scheme of GSC beamformer is illustrated in figure 4. Two noisy signals can be derived by the following equations:

$$X_1(f, k) = S(f, k)e^{j\Phi_s} + V_1(f, k) \quad (1)$$

$$X_2(f, k) = S(f, k)e^{-j\Phi_s} + V_2(f, k) \quad (2)$$

where $S(f, k)$ is desired target speech, $V_1(f, k), V_2(f, k)$ is additive unwanted noise in microphone 1, 2; $\Phi_s = \pi f \tau_0 \cos(\theta_s)$, $\tau_0 = d/c$, d is the inter-microphone distance, $c = 343(m/s)$ is speed of propagation sound in the air, θ_s is the assumed direction-of-arrival of interest useful speech.

The output of FBF beamformer $Y_s(f, k)$ and BM block $Y_r(f, k)$ is algorithm delay-and-sum and method

subtraction signal after compensation phase. The formulations of these signal can be expressed as:

$$Y_s(f, k) = \frac{X_1(f, k)e^{-j\Phi_s} + X_2(f, k)e^{j\Phi_s}}{2} \quad (3)$$

$$Y_r(f, k) = \frac{X_1(f, k)e^{-j\Phi_s} - X_2(f, k)e^{j\Phi_s}}{2} \quad (4)$$

The information of auto and cross power spectral density of $Y_s(f, k), Y_r(f, k)$ are very necessary for determining an adaptive filter.

$$P_{Y_s Y_r}(f, k) = (1 - \alpha) * P_{Y_s Y_r}(f, k - 1) + \alpha * Y_s(f, k) Y_r^*(f, k) \quad (5)$$

$$P_{Y_r Y_r}(f, k) = (1 - \alpha) * P_{Y_r Y_r}(f, k - 1) + \alpha * Y_r(f, k) Y_r^*(f, k) \quad (6)$$

where α is the smoothing parameter, in range of $\{0..1\}$.

The adaptive filter $H(f, k) = \frac{P_{Y_s Y_r}(f, k)}{P_{Y_r Y_r}(f, k)}$ help extracting the only desired target directional speech while eliminating all surrounding background noise, non-target signals. Due to the sensitivities of GSC beamformer with the phase error, the performance often corrupted when microphone mismatches, imprecise position MA, or inexactly the direction-of-arrival of useful signal. For increasing the robustness of GSC beamformer, the author proposed a method, which eliminate the component speech leakage to achieve the only noise at reference signal.

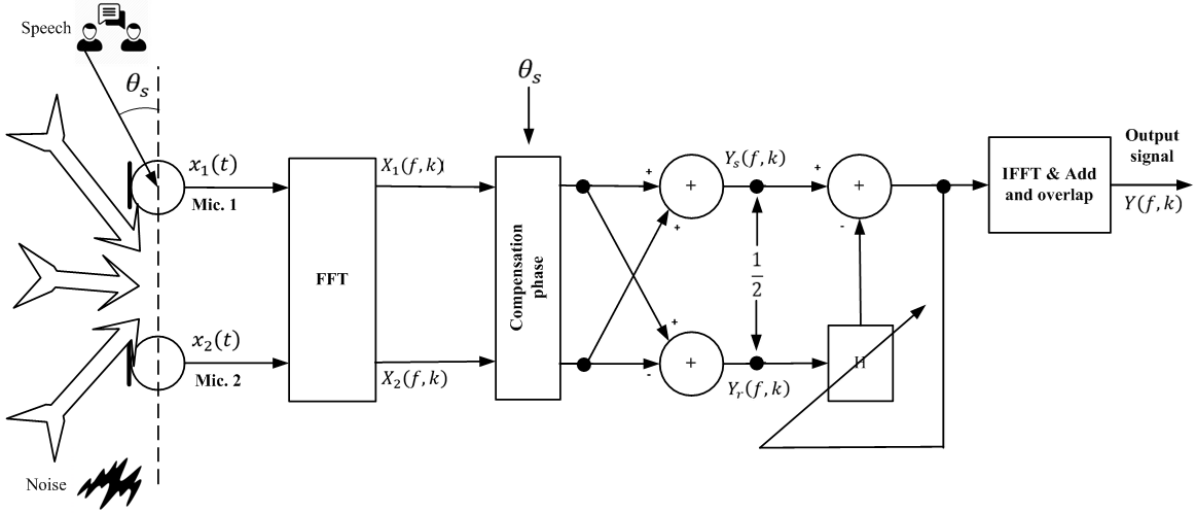


Figure 4: The scheme of GSC beamformer.

3 THE SPECTRAL MASK

The author's ideal is the using of a priori $SNR(f, k)$ to determine an appropriate spectral mask $SM(f, k)$ for alleviating the speech component in the reference signal.

The signal $Y_r(f, k)$ will be multiplied by $SM(f, k)$ to remove the retaining desired speech to enhance GSC's performance.

$$Y_r^n(f, k) = Y_r(f, k) * SM(f, k) \quad (7)$$

$SM(f, k)$ is a function, which exploits the coherence between two signals and an estimation of the signal-to-noise, is derived by:

$$SM(f, k) = |\Gamma_{X_1 X_2}(f, k)|^{SNR(f, k)} \quad (8)$$

where

$$\Gamma_{X_1 X_2}(f, k) = \frac{P_{X_1 X_2}(f, k)}{\sqrt{P_{X_1 X_1}(f, k) * P_{X_2 X_2}(f, k)}} \quad (9)$$

$P_{X_1 X_1}(f, k), P_{X_2 X_2}(f, k), P_{X_1 X_2}(f, k)$ are the auto-PSD, and cross-PSD of microphone signals $X_1(f, k), X_2(f, k)$ respectively.

With these assumptions, that the noise power is the same on two microphones and uncorrelated, the desired target talker and noise are uncorrelated. In (Zelinski, 1988), the covariance of speech $\sigma_s^2(f, k)$ is calculated by:

$$\sigma_s^2(f, k) = \frac{Re\{P_{X_1 X_2}(f, k) + P_{X_2 X_1}(f, k)\}}{2} \quad (10)$$

and noise covariance $\sigma_n^2(f, k)$ as:

$$\sigma_n^2(f, k) = \frac{P_{X_1 X_1}(f, k) + P_{X_2 X_2}(f, k)}{2} - \sigma_s^2(f, k) \quad (11)$$

The temporal $SNR(f, k)$:

$$SNR(f, k) = \frac{\sigma_s^2(f, k)}{\sigma_n^2(f, k)} \quad (12)$$

In coherence noise field, at the frame only noise, the value $\Gamma_{X_1 X_2}(f, k)=1$, so the spectral mask doesn't affect of these frames. But at the frame with presence of speech, $\Gamma_{X_1 X_2}(f, k) < 1$, so spectral mask $SM(f, k)$ always less than 1, and the advantage of spectral mask will suppress the remaining speech leakage. The result is the existing only noise component, without speech. The spectral mask $SM(f, k)$ is used to eliminate the existing speech component in the reference signal $Y_r(f, k)$, and thus is to improve the final of GSC beamformer.

In the next section, an experiment will be illustrated to verify the effectiveness of the additive spectral mask.

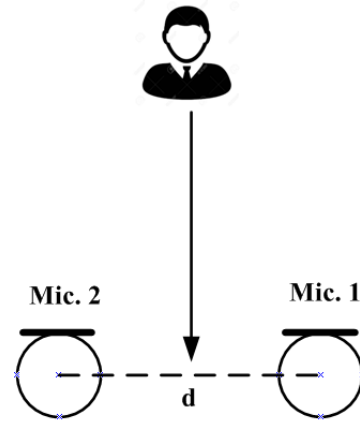


Figure 5: The recording situation with DMA2.

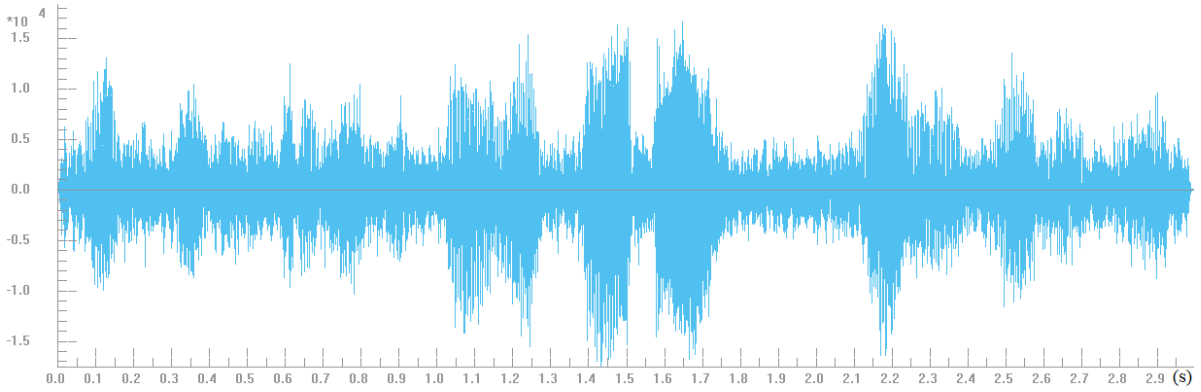


Figure 6: The waveform of microphone array signal.

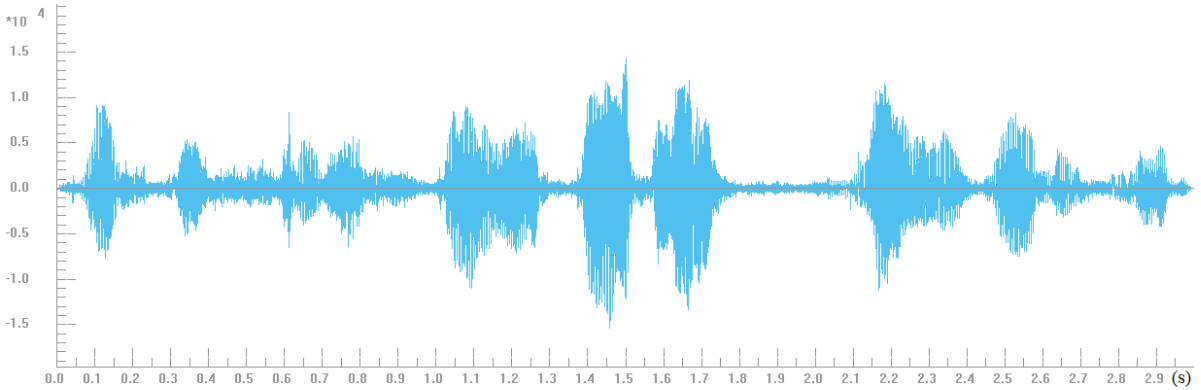


Figure 7: The processed signal by GSC-ctl.

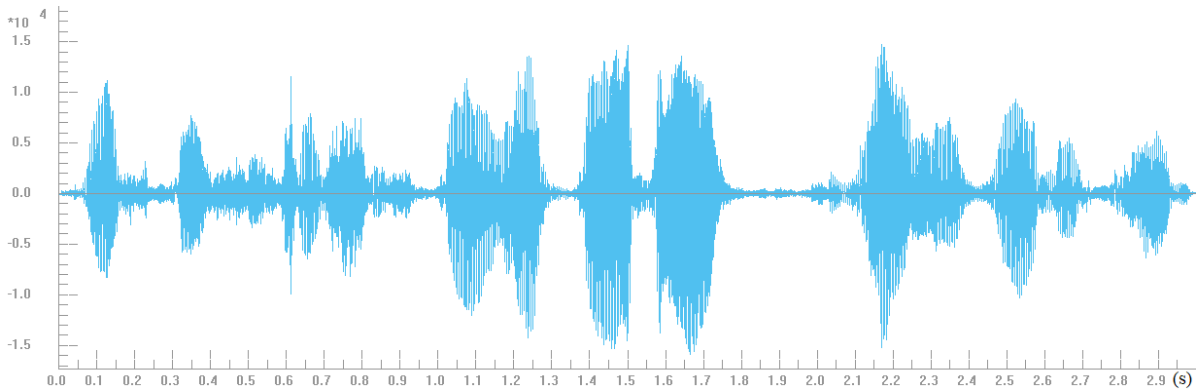


Figure 8: The processed signal by GSC-sp.

4 EXPERIMENTS AND DISCUSSION

The scheme of DMA2's performance was illustrated in figure 5. The distance between two microphones $d = 5(cm)$.

All microphone array signals were transformed into STFT domain by using NFFT=512, overlap 50%, Hamming window. For further signal processing,

smoothing parameter $\alpha = 0.1$ was used. The speaker is stand at distance $L = 2(m)$, the direction-of-arrival $\theta_s = 90(deg)$ relative to the axis of DMA2. This section is aiming to illustrate the effectiveness of the spectral mask for reducing speech distortion and enhancing the obtained speech quality of the processed signal. An objective measurement (Ellis, 2011) is used to estimate the signal-to-noise ratio (SNR). A comparison between the processed signal by the conventional GSC (GSC-ctl) and the proposed method

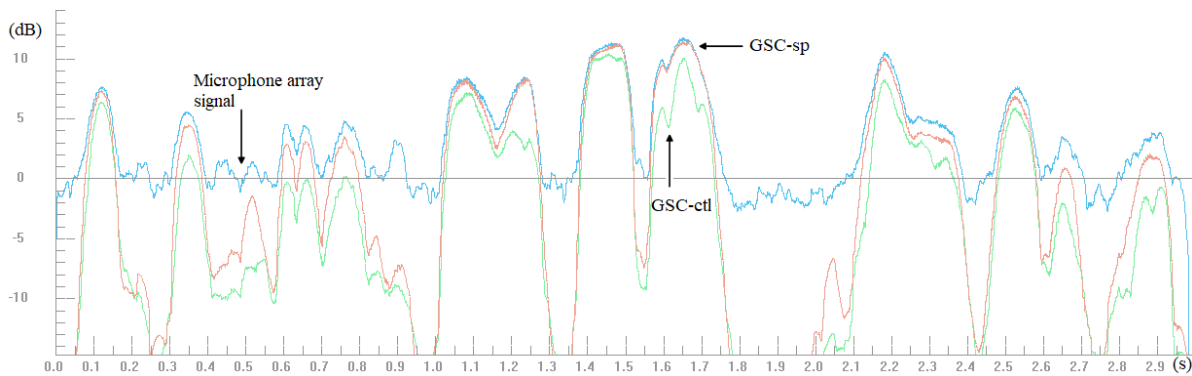


Figure 9: The energy of original microphone signal and signals, which processed by GSC-ctl, GSC-sp.

(GSC-sp) is derived for verifying the promising results.

The original signal, which captured by DMA2 is shown in figure 6.

The processed signals by GSC-ctl and GSC-sp are illustrated in figure 7, 8.

It was shown through the energy of original microphone signal and the results, which processed by GSC-ctl and GSC-sp. GSC-sp achieves a substantially higher speech quality by saving the original speech source and therefore reducing speech distortion than the conventional method. In the other side, in overall performance, the proposed method increased the speech intelligibility. In comparison with GSC-ctl, GSC-sp reduce speech distortion to 5.5 (dB) in figure 9. The signal-to-noise ratio (SNR) between two processed signals is depicted in table 1.

Table 1: The signal-to-noise ratio (dB).

Method Estimation	Microphone array signal	GSC-ctl	GSC-sp
WADA SNR	6.56	18.4	20.7

In this paper, the author exploited the properties of coherence between two microphones, the temporal SNR to form a precise spectral mask, which can remove the remaining in the reference signal. The speech quality was increased from 18.4 (dB) to 20.7 (dB). The effectiveness of a spectral mask for GSC beamformer was verified and confirmed in reducing the remaining component speech leakage in the reference signal of BM block, as a result, the speech quality of GSC beamformer was enhanced. This spectral mask can be used in other speech equipment for dealing the problem of suppressing background noise, interference.

In numerous speech applications, such as speech enhancement, automatic conferencing and speech recognition, the recorded speech signals always be

corrupted by surrounding unwanted noise. The author's approach requires less additive memories and fewer mathematical operations, which doesn't affect on overall GSC beamformer. The proposed method can be integrated in these applications for reducing speech distortion and increasing the speech intelligibility. The experimental results were verified the effectiveness of the author's technique in annoying complex recording environment.

5 CONCLUSION

Adaptive beamforming is a challenge task in digital signal processing by MA. However, the its evaluation is too sensitive to any mismatches of direction of arrival of interest signal, microphone sensitivities and the distribution of MA geometry. In this contribution, the author's suggested method is devoted to the task of increasing the performance of GSC beamformer by using spectral mask to mitigate speech leakage in the reference signal. This problem is inherent, which degrades overall speech quality and robustness of speech processing system. Simulation results show the capability of the proposed method to solve the problem existing of speech components due to phase error, microphone mismatches or different level amplitude microphone array. As a result, the developed model validates the advantages of proposed technique over the conventional GSC beamformer. The remained speech leakage in the reference signal was deal, and the improvement of speech enhancement in term of the signal-to-noise ratio shows us that the author's approach can be further integrated into other multi-channel for different speech applications. In the future, the properties of surrounding environment will be studied for increasing the performance of GSC beamformer.

ACKNOWLEDGEMENTS

This research was supported supported by Digital Agriculture Cooperative. The author thank our colleagues from Digital Agriculture Cooperative, who provided insight and expertise that greatly assisted the research.

REFERENCES

- Benesty, J., Chen, J., and Huang, Y. (2008). *Microphone Array Signal Processing*, volume 1 of *Springer Topics in Signal Processing*. Springer Berlin, Heidelberg. <https://doi.org/10.1007/978-3-540-78612-2>.
- Benesty, J., Cohen, I., and Chen, J. (2017). *Fundamentals of Signal Enhancement and Array Signal Processing*. John Wiley & Sons Singapore. <https://doi.org/10.1002/9781119293132>.
- Brandstein, M. and Ward, D., editors (2001). *Microphone Arrays: Signal Processing Techniques and Applications*. Digital Signal Processing. Springer Berlin, Heidelberg. <https://doi.org/10.1007/978-3-662-04619-7>.
- Elko, G. W. and Pong, A.-T. N. (1997). A steerable and variable first-order differential microphone array. In *1997 IEEE International Conference on Acoustics, Speech, and Signal Processing*, volume 1, pages 223–226. <https://doi.org/10.1109/ICASSP.1997.599609>.
- Ellis, D. (2011). Objective measures of speech quality/SNR. <https://labrosa.ee.columbia.edu/projects/snreval/>.
- Herbordt, W. and Kellermann, W. (2021). Computationally efficient frequency-domain robust generalized sidelobe canceller. In *Proceedings of the 7th International Workshop on Acoustic Echo and Noise Control (IWAENC), Darmstadt, Germany, 10–13 September 2001*. <https://www.iwaenc.org/proceedings/2001/main/data/herbordt.pdf>.
- Hoshuyama, O., Begasse, B., Sugiyama, A., and Hirano, A. (1998). A real time robust adaptive microphone array controlled by an SNR estimate. In *Proceedings of the 1998 IEEE International Conference on Acoustics, Speech and Signal Processing, ICASSP '98 (Cat. No.98CH36181)*, volume 6, pages 3605–3608. <https://doi.org/10.1109/ICASSP.1998.679659>.
- Khayeri, P., Abutalebi, H. R., and Abootalebi, V. (2011). A nested superdirective generalized sidelobe canceller for speech enhancement. In *2011 8th International Conference on Information, Communications & Signal Processing*, pages 1–5. <https://doi.org/10.1109/ICICS.2011.6174269>.
- Li, B. and Zhang, L.-H. (2016). An improved speech enhancement algorithm based on generalized sidelobe canceller. In *2016 International Conference on Audio, Language and Image Processing (ICALIP)*, pages 463–468. <https://doi.org/10.1109/ICALIP.2016.7846528>.
- Yoon, B.-J., Tashev, I., and Acero, A. (2007). Robust Adaptive Beamforming Algorithm using Instantaneous Direction of Arrival with Enhanced Noise Suppression Capability. In *2007 IEEE International Conference on Acoustics, Speech and Signal Processing - ICASSP '07*, volume 1, pages I–133–I–136. <https://doi.org/10.1109/ICASSP.2007.366634>.
- Zelinski, R. (1988). A microphone array with adaptive post-filtering for noise reduction in reverberant rooms. In *ICASSP-88., International Conference on Acoustics, Speech, and Signal Processing*, pages 2578–2581 vol.5. <https://doi.org/10.1109/ICASSP.1988.197172>.

A Different Phase-Based Improved Performance of Differential Microphone Array

Quan Trong The^a

Digital Agriculture Cooperative, No. 15 Lane 2, Tho Thap, Dich Vong, Cau Giay, Hanoi, Viet Nam
quantrongthe1984@gmail.com

Keywords: Microphone Array, Different Phase, Differential Microphone Array, Dual-System, Speech Enhancement, Noise Reduction, Background Noise.

Abstract: Various speech applications such as speech separation, speech recognition, communication, teleconference, hearing aids common use microphone array (MA) as front-end speech enhancement structure. By using the spatial information, geometry of MA, the characteristic of recording environment, MA help overcome of single-channel algorithm to suppress noise without speech distortion. A critical major component of MA system is the beamforming technique, which forms beampattern to a certain target directional sound source while alleviating different noise. Differential Microphone Array (DIF) is one of the most popular structure is used in several speech application. DIF has a lot of advantages which own the capability of null-steering beampattern to the noise source. In this article, the author proposes a method to enhance performance of DIF for separating speaker in real dialogue conference. Experiment was illustrated in real situation and obtained results show the effectiveness of the suggested method in comparison with the previous author's work.

1 INTRODUCTION

In several speech communication systems, separation target directional speaker of a mixture of interference, noise and third-party speaker is a challenging problem especially in situation with complex surrounding noise and low SNR (signal-to-noise ratio) values. In general, due to the above reason, the speech quality and speech intelligibility are often significant degraded. The necessary of communication is need to improve speech enhancement, even in scenario of low SNR is an importance research. Single-channel approach can't adapt all requirement, because of it uses spectral subtraction method, which lead to speech distortion of the final output. Therefore, MA technology has been developed for dealing this problem. Nowadays, MA is used in almost speech applications, such as speech recognition, mobile device, hearing aid, teleconference, human-machine interface in order to obtain an acceptable degree of speech quality from any algorithms trying to mitigate background noise and extracting desired speech. MA exploits the spatial diversity, the priori of knowledge of the direction-of-arrival (DOA), the properties of acoustic situation, the characteristic of noise field to achieve a beampat-



Figure 1: The complicated task of separating desired speech source.

tern, which toward speech source and remove all of noise.

Because of possibly changing recording scenario and varying position of the noise source relative to MA, DIF beamformer allows null-steering beampattern to noise. In the previous work, the author suggested an additive equalizer for enhancing separation

^a <https://orcid.org/0000-0002-2456-9598>

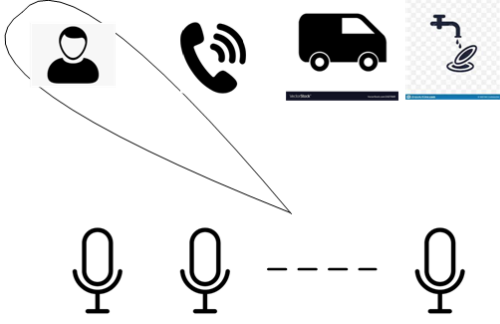


Figure 2: The advantage of utilizing the MA beamforming.

each talker when using DIF.

G. W. Elko (Elko, 1997, 2000; Teutsch and Elko, 2001) formed a cardioid beampattern when combined signal with compact spaced microphones. Therefore, the directivity index of MA was increased.

The designing with small arrays and an appropriate geometry and associated beamforming algorithms, which can pass all through bandpass speech signals still a challenging problem to the scholars (Barfuss et al., 2017a,b). Among different several types of MA, DMA is the most suitable architecture to measure differential of the sound target desired speech, and more appropriate for achieving high diversity, high noise reduction, high directivity index and invariant-frequency beampattern toward the direction of talker (De Sena et al., 2012; Buck, 2002). Recently, many efforts are successful with flexible differential beamforming and robustness of DIF's performance are enhanced (Huang et al., 2020; Benesty et al., 2019; Cohen et al., 2019).

An essential issue in differential beamforming is steering flexibility in any direction of signal or noise. Linear DMAs do not have much flexibility, due to the beampattern varies with steering angle and the optimum directivity factor occurs only in end-fire case DMA. A numerous works are attempted to improving the flexibility of steering DMA's beampattern. In (Elko and Pong, 1997; Derkx and Janse, 2009), a two-dimensions MA are utilized to steer the resulting beampattern in a certain number of directions. First-order steerable DMAs (Wu et al., 2014; Wu and Chen, 2016) are evaluated to construct a combination of monopole and dipoles using 4 microphones square array. In (Benesty et al., 2015), uniform circular DMAs were performed to steering beampattern to some wanted directions. Bernardini et al. (Bernardini et al., 2017) suggested using DMA to steer second-order with monopole and dipole. In (Huang et al., 2017), a beamforming technique was evaluated to design an approximately constant beampattern, and has capable to steer between two directions

of the reference beams. In (Parra, 2005, 2006), a designed method was suggested for forming invariant-frequency beampattern for spherical array. In (Lai et al., 2013), a broadband beampattern was presented with arbitrary geometry of microphones for spherical MA.

With a great obtained progress in designing steerable DMA's beampattern with high directivity index, good noise reduction, more robustness, and high capability of steering beampattern.

In this paper, the author continues to deal the problem of separating talker when using the subspace technique to reduce the remaining speech component non-target talker at the output DIF beamformer.

The rest of this paper is organized as follow. The next section presents model signal, advantage of DIF and the previous author's work. Section 3 introduce how to use the information about phase error between two microphones to form a post-filtering, which based on Wiener filter. Section 4 described experiments with two speakers, and a comparison between the proposed method and the previous work. Concluding remark and future work is presented in Section 5.

2 DIFFERENTIAL MICROPHONE ARRAY

We will consider the DMA2's working in STFT domain. DMA2 allows obtaining high diversity, noise reduction, directional beampattern to target speech. DMA2 have super directivity, small size and can null-steering beampattern to the direction of noise, which makes it possible to achieve high performance, even in reverberation, noisy environment, and suitable for almost acoustic equipment. The obtained effectiveness of DMA2 is suppressing complicated background noise and extracting the target speaker.

The representation of two noisy microphone arrays $X_1(f, k), X_2(f, k)$ in the STFT domain as:

$$X_1(f, k) = S(f, k)e^{j\Phi_s} \quad (1)$$

$$X_2(f, k) = S(f, k)e^{-j\Phi_s} \quad (2)$$

where f, k is the index of frequency and current considered frame, $\Phi_s = \pi f \tau_0 \cos(\theta_s)$, $\tau_0 = d/c$, d is the distance of two microphones, $c = 343(m/s)$ is the speech of sound propagation in the air, θ is the direction-of-arrival (DOA) of useful speech.

With a certain delay τ is added, we can obtain high directivity beampattern toward two speakers. The output signals, which are based on subtraction signal

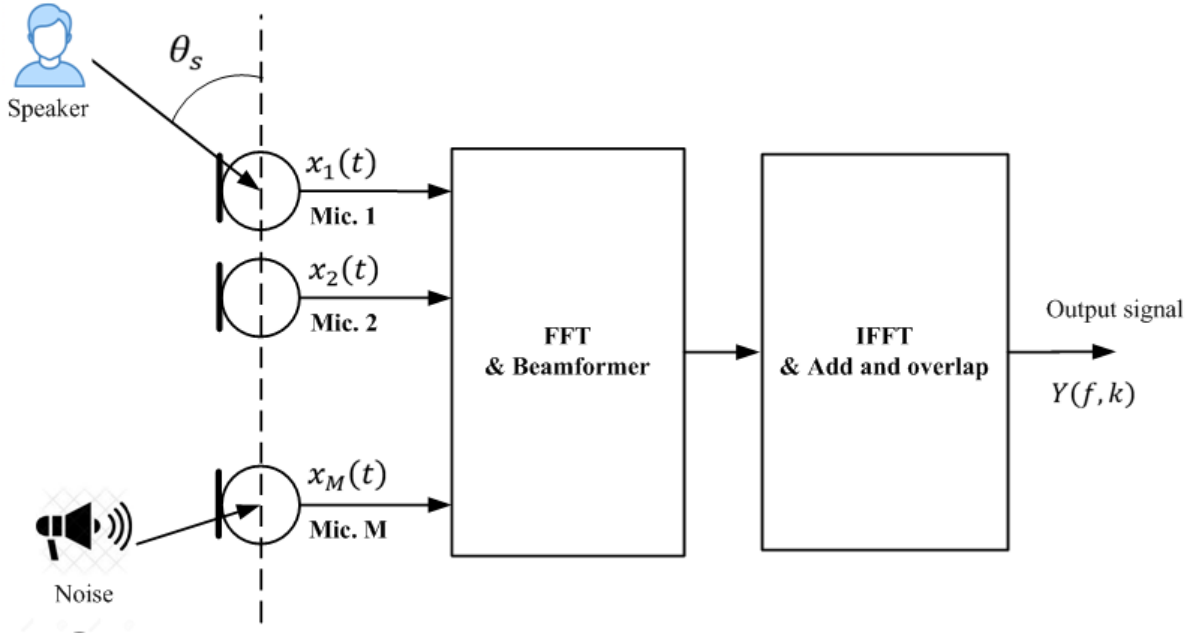


Figure 3: The MA signal processing in the frequency domain.

can be expressed as:

$$Y_{1DIF}(f, k) = \frac{X_1(f, k) - X_2(f, k)e^{-j\omega\tau}}{2} \quad (3)$$

$$= jS(f, k)\sin\left(\frac{\omega\tau_0}{2}\left(\cos\theta + \frac{\tau}{\tau_0}\right)\right) \quad (4)$$

$$Y_{2DIF}(f, k) = \frac{X_2(f, k) - X_1(f, k)e^{-j\omega\tau}}{2} \quad (5)$$

$$= -jS(f, k)\sin\left(\frac{\omega\tau_0}{2}\left(\cos\theta - \frac{\tau}{\tau_0}\right)\right) \quad (6)$$

The directional two beampatterns, which received from equation (3) - (6) are derived as:

$$B_1(f, \theta) = \left| \frac{Y_1(f, k)}{S(f, k)} \right| = \left| \sin\left(\frac{\omega\tau_0}{2}\left(\cos\theta + \frac{\tau}{\tau_0}\right)\right) \right| \quad (7)$$

$$B_2(f, \theta) = \left| \frac{Y_2(f, k)}{S(f, k)} \right| = \left| \sin\left(\frac{\omega\tau_0}{2}\left(\cos\theta - \frac{\tau}{\tau_0}\right)\right) \right| \quad (8)$$

Stolbov et al. (Stolbov et al., 2018) proposed utilizing an equalizer for preserving the useful signal at the low-frequency band. The equalizer can be expressed as the following equation:

$$H_{eq}(f) = \begin{cases} 6 & 0 \text{ Hz} < f \leq 200 \text{ (Hz)} \\ \frac{1}{\sin\left(\frac{f}{2F_c}\right)} & 200 \text{ Hz} < f \leq F_c \\ 1 & F_c < f \leq 2*F_c \\ 0 & 2*F_c < f \end{cases} \quad (9)$$

where $F_c = \frac{1}{4*\tau_0}$. A constant threshold 12(dB) is determined for $H_{eq}(f)$. The final output signals are:

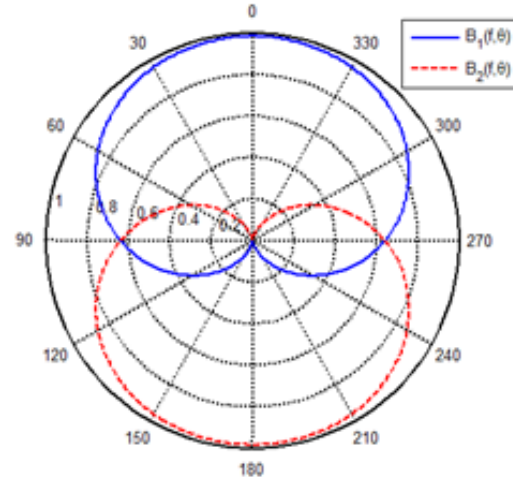


Figure 4: The beampatterns.

$$Y_1(f, k) = Y_{1DIF}(f, k) * H_{eq}(f) \quad (10)$$

$$Y_2(f, k) = Y_{2DIF}(f, k) * H_{eq}(f) \quad (11)$$

In many realistic scenario, the remaining noisy component at the output signal often deteriorate the speech quality of DIF beamformer. In the next section, the author show an additive post-filtering, which based on the priori information of DMA2.

3 THE POST-FILTERING

An additive post-filtering, which based on the subspace technique is presented in figure 5.

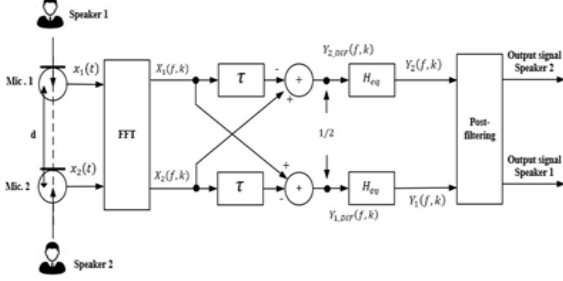


Figure 5: The suggested post-filtering for DMA2 to separate useful signal.

In the STFT-domain, with the assumption as the noise magnitudes are equal for two microphones. The different phase $\theta_k(f)$ is defined as:

$$\theta_k(f) = \arg(X_1(f, k)) - \arg(X_2(f, k)) - 2\pi f \tau_0 \quad (12)$$

A major information that the different phase is always in range $[-\pi, \pi]$. In the frames, which contain the speech component, $\theta_k(f)$ tends to 0 and in the noisy frame, $\theta_k(f)$ tends to π or π .

The author proposed a post-filtering, which use the a priori information $\theta_k(f)$ as:

$$PF(f) = \cos \frac{\theta_k(f)}{2} \quad (13)$$

At the frames, in which the desired target speaker exists, $PF(f)$ equal approximately 1 and will save the speech component. Thus in, at the other noisy frames, $PF(f)$ close to 0 and remove the interference or background noise.

At the final, the received output signal are determined as:

$$Y_{1out}(f, k) = Y_1(f, k) * PF(f) \quad (14)$$

$$Y_{2out}(f, k) = Y_2(f, k) * PF(f) \quad (15)$$

In the next section, the author illustrated and experiment to very the useful of the proposed post-filtering in compared with the previous author's work (Stolbov et al., 2018) by using a DMA2 to extract the desired target talker while suppressing the interference.

4 EXPERIMENTS AND DISCUSSION

The purpose of this experiment is enhancing the performance, which based on the DIF beamformer. The

derived problem is alleviating the second talker's component while preserving target directional first talker. A degree of suppression second speaker's speech component is calculated to confirm the promising results. The scheme of experiment is depicted in figure 6. DMA2 with the inter-microphone distance is $d = 5(cm)$. The desired speaker talk while the interference at the other opposite direction.

For calculating the spectral power density, some parameters were used for transformed into STFT domain: Hamming window, NFFT=512, overlap 50%, the sampling frequency $F_s = 16kHz$, smoothing parameter $\alpha = 0.1$. A DMA2 was used for recording speech from target talker at the direction $\theta_s = 0(deg)$ in presence of unwanted interference, which stand at the opposite direction $\theta_v = 180(deg)$.

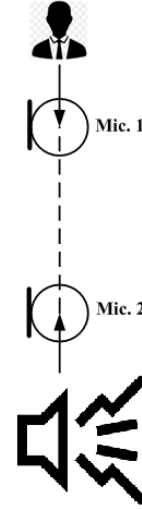


Figure 6: The evaluated recording scenarios with two speakers.

The waveform of the received signal was illustrated in figure 7.

In figure 8, the obtained processed signal by the previous author's work (Stolbov et al., 2018) and the proposed method are illustrated in figure 9.

From these figures, as we can see that, the remaining of speech component of the second talker is removed to 5(dB) in comparison with (Stolbov et al., 2018). The effectiveness of the proposed technique was confirmed in suppressing the remaining speech component of second talker while ensuring keep the first second's speech. This is the major advantage in comparison with the previous work (Stolbov et al., 2018).

So in this paper, the author exploits the different phase approach to forming an additive post-filtering to enhance the final desired target speaker. As can be observed, the enhancement of suggested method

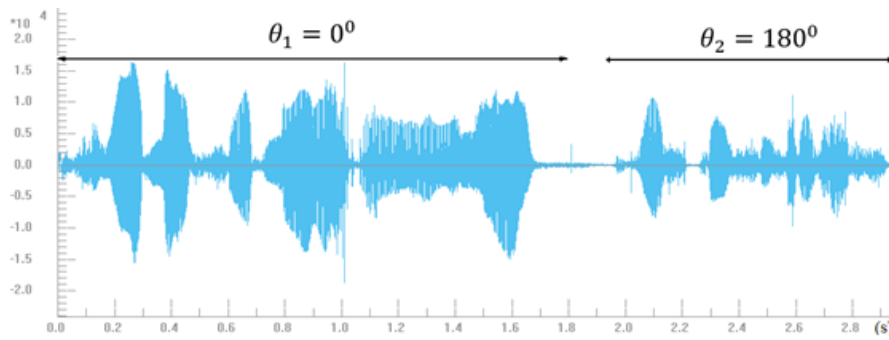


Figure 7: The waveform of the capture microphone array signal.

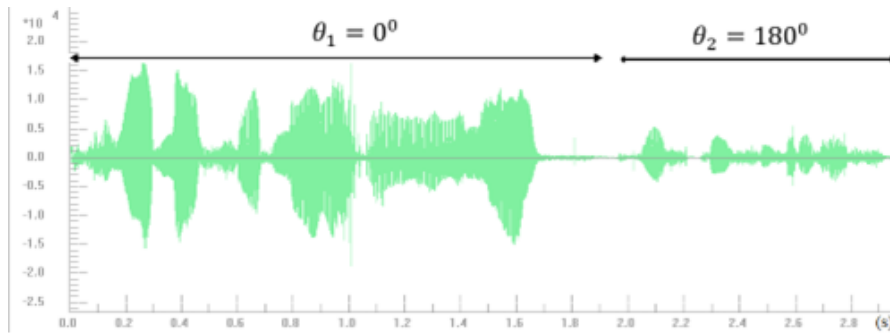


Figure 8: The processed signal by (Stolbov et al., 2018).

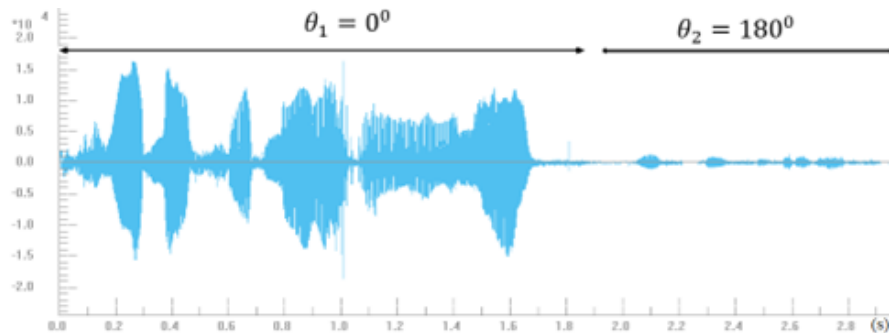


Figure 9: The obtained processed signal by additive post-filtering.

was more significant realized than the work (Stolbov et al., 2018). This technique can be applied into other acoustic system.

DMA2 has the capability of impact, low computation, easy implementation. These advantages make DMA2 is commonly installed in almost acoustic equipments; therefore the demand of enhancing of of high directivity, more robustness still exists. The author use the available information about difference phase to improve the previous work.

Separation of target speaker in complex environment, in which the third-party talker or background noise existed, still a challenge to all scholars. The use of the characteristics between two microphones

is the advantage of MA to improve the speech enhancement. Different phase is one of the most interesting object for studying to improve the performance of DMA2.

5 CONCLUSION

MA beamforming are now common installed in various range of acoustic applications such as cellular phones, teleconferencing, speech recognition, robotics, smart device, telephone hands-free. A challenging task is perfectly separating speech each speaker, which requires using model a suitable DMA.

In this paper, the author suggested exploit the characteristic subspace of microphone array signals to improve and increase the robustness of DMA system than the previous work. A knowledge of the power target speech source used for post-filtering to suppress the non-target different speaker without speech distortion of target source. Numerical result was verified in real scenario and confirm the ability of the proposed method. Phase error approach can be further studied in future for installing into multi-microphone system. In the future, the author will investigate the property of environment to enhance the performance of MA algorithms.

ACKNOWLEDGEMENTS





This research was supported supported by Digital Agriculture Cooperative. The author thank our colleagues from Digital Agriculture Cooperative, who provided insight and expertise that greatly assisted the research.

REFERENCES

- Barfuss, H., Bachmann, M., Buerger, M., Schneider, M., and Kellermann, W. (2017a). Design of robust two-dimensional polynomial beamformers as a convex optimization problem with application to robot audition. In *2017 IEEE Workshop on Applications of Signal Processing to Audio and Acoustics (WASPAA)*, pages 106–110. <https://doi.org/10.1109/WASPAA.2017.8170004>.
- Barfuss, H., Buerger, M., Podschus, J., and Kellermann, W. (2017b). HRTF-based two-dimensional robust least-squares frequency-invariant beamformer design for robot audition. In *2017 Hands-free Speech Communications and Microphone Arrays (HSCMA)*, pages 56–60. <https://doi.org/10.1109/HSCMA.2017.7895561>.
- Benesty, J., Chen, J., and Cohen, I. (2015). *Design of Circular Differential Microphone Arrays*, volume 12 of *Springer Topics in Signal Processing*. Springer Cham. <https://doi.org/10.1007/978-3-319-14842-7>.
- Benesty, J., Cohen, I., and Chen, J. (2019). *Array Processing: Kronecker Product Beamforming*, volume 18 of *Springer Topics in Signal Processing*. Springer Cham. <https://doi.org/10.1007/978-3-030-15600-8>.
- Bernardini, A., D'Aria, M., Sannino, R., and Sarti, A. (2017). Efficient Continuous Beam Steering for Planar Arrays of Differential Microphones. *IEEE Signal Processing Letters*, 24(6):794–798. <https://doi.org/10.1109/LSP.2017.2695082>.
- Buck, M. (2002). Aspects of first-order differential microphone arrays in the presence of sensor imperfections. *European Transactions on Telecommunications*, 13(2):115–122. <https://doi.org/10.1002/ett.4460130206>.
- Cohen, I., Benesty, J., and Chen, J. (2019). Differential Kronecker Product Beamforming. *IEEE/ACM Transactions on Audio, Speech, and Language Processing*, 27(5):892–902. <https://doi.org/10.1109/TASLP.2019.2895241>.
- De Sena, E., Hacıhabiboglu, H., and Cvetkovic, Z. (2012). On the Design and Implementation of Higher Order Differential Microphones. *IEEE Transactions on Audio, Speech, and Language Processing*, 20(1):162–174. <https://doi.org/10.1109/TASL.2011.2159204>.
- Derkx, R. M. M. and Janse, K. (2009). Theoretical Analysis of a First-Order Azimuth-Steerable Superdirective Microphone Array. *IEEE Transactions on Audio, Speech, and Language Processing*, 17(1):150–162. <https://doi.org/10.1109/TASL.2008.2006583>.
- Elko, G. W. (1997). Adaptive noise cancellation with directional microphones. In *Proceedings of 1997 Workshop on Applications of Signal Processing to Audio and Acoustics*, pages 4 pp.–. <https://doi.org/10.1109/ASPAA.1997.625628>.
- Elko, G. W. (2000). Superdirectional Microphone Arrays. In Gay, S. L. and Benesty, J., editors, *Acoustic Signal Processing for Telecommunication*, volume 551 of *The Springer International Series in Engineering and Computer Science*, pages 181–237. Springer US, Boston, MA. https://doi.org/10.1007/978-1-4419-8644-3_10.
- Elko, G. W. and Pong, A.-T. N. (1997). A steerable and variable first-order differential microphone array. In *1997 IEEE International Conference on Acoustics, Speech, and Signal Processing*, volume 1, pages 223–226. <https://doi.org/10.1109/ICASSP.1997.599609>.
- Huang, G., Benesty, J., and Chen, J. (2017). On the Design of Frequency-Invariant Beampatterns With Uniform Circular Microphone Arrays. *IEEE/ACM Transactions on Audio, Speech, and Language Processing*, 25(5):1140–1153. <https://doi.org/10.1109/TASLP.2017.2689681>.
- Huang, G., Chen, J., and Benesty, J. (2020). Design of planar differential microphone arrays with fractional orders. *IEEE/ACM Transactions on Audio, Speech, and Language Processing*, 28:116–130. <https://doi.org/10.1109/TASLP.2019.2949219>.
- Lai, C. C., Nordholm, S., and Leung, Y. H. (2013). Design of Steerable Spherical Broadband Beamformers With Flexible Sensor Configurations. *IEEE Transactions on Audio, Speech, and Language Processing*, 21(2):427–438. <https://doi.org/10.1109/TASL.2012.2219527>.
- Parra, L. C. (2005). Least squares frequency-invariant beamforming. In *IEEE Workshop on Applications of Signal Processing to Audio and Acoustics, 2005.*, pages 102–105. <https://doi.org/10.1109/ASPAA.2005.1540179>.
- Parra, L. C. (2006). Steerable frequency-invariant beamforming for arbitrary arrays. *The Journal of the Acoustical Society of America*, 119(6):3839–3847. <https://doi.org/10.1121/1.2197606>.
- Stolbov, M., Tatarnikova, M., and The, Q. T. (2018).

- Using Dual-Element Microphone Arrays for Automatic Keyword Recognition. In Karpov, A., Jokisch, O., and Potapova, R., editors, *Speech and Computer*, volume 11096 of *Lecture Notes in Computer Science book series*, pages 667–675, Cham. Springer International Publishing. https://doi.org/10.1007/978-3-319-99579-3_68.
- Teutsch, H. and Elko, G. W. (2001). First- and second order adaptive differential microphone arrays. In *Seventh International Workshop on Acoustic Echo and Noise Control, IWAENC 2001*, Darmstadt. <https://www.iwaenc.org/proceedings/2001/main/data/teutsch.pdf>.
- Wu, X. and Chen, H. (2016). Directivity Factors of the First-Order Steerable Differential Array With Microphone Mismatches: Deterministic and Worst-Case Analysis. *IEEE/ACM Transactions on Audio, Speech, and Language Processing*, 24(2):300–315. <https://doi.org/10.1109/TASLP.2015.2506269>.
- Wu, X., Chen, H., Zhou, J., and Guo, T. (2014). Study of the Mainlobe Misorientation of the First-Order Steerable Differential Array in the Presence of Microphone Gain and Phase Errors. *IEEE Signal Processing Letters*, 21(6):667–671. <https://doi.org/10.1109/LSP.2014.2312729>.

The System of Automated Diabetes Control

Vitalii L. Levkivskiy¹^a, Galyna V. Marchuk¹^b, Oleksandr V. Kuzmenko¹^c
and Anton Yu. Levchenko²^d

¹Zhytomyr Polytechnic State University, Department of Computer Science, 103 Chudnivska Str., Zhytomyr, 10003, Ukraine

²Zhytomyr Polytechnic State University, Department of Software Engineering, 103 Chudnivska Str., Zhytomyr, 10003, Ukraine
{levkivskyy, pzs_mgv, kkn_kov, levchenko}@ztu.edu.ua

Keywords: Diabetes, Disease, Glucose, Insulin, Glycemia, Data Analysis, Insulin/Glucose Balance.

Abstract: Modern information technology creates new opportunities for quickly obtaining information about the status and trends of diseases such as diabetes. This paper considers the task of automating the collection and analysis of data on the condition of a patient. The object of the research is information technology for creating mobile applications and mathematical models for calculating the optimal insulin therapy. The aim of the work is to analyze the incidence of diabetes and the development of a software product for man-aging blood glucose levels. We developed a self-control diary which is the main functional feature of the system. It allows users to quickly obtain information about the state and trends of the disease. Based on the accumulated daily data, it is possible to take the necessary actions on time to improve the disease course. In the process of development, the database was designed and mathematical methods were used to analyze the data. The module of the analysis of the collected data for the specific period is developed. The results of the analysis can be obtained by the following indicators: the average glucose blood level, the number of glucose measurements, glucose deviations, the number of basal insulin injections, the number of hypo/hyperglycemia, the amount of bolus insulin. In our work we used object-oriented design techniques, document-oriented databases, modern web technology stacks for mobile application development and design of interfaces. The result of solving the given task is a system of accumulation and systematization of statistical data on the course of the disease. An automated diabetes control system has been designed and developed. Mathematical models were used to calculate the glucose/insulin balance. The developed software can significantly improve the living standards of people with this disease. The system was tested by patients with diabetes.


1 INTRODUCTION


Diabetes mellitus, commonly known as diabetes, is a chronic disease characterized by high blood glucose level over a prolonged period of time. This leads to serious problems in various systems of the human body, especially nerve endings and blood vessels. Diabetes is a dangerous complication that leads to disability. In low- and middle-income countries, the prevalence of diabetes is growing faster than in high-income countries.


Diabetes is one of the leading causes of blindness, kidney failure, heart attacks, strokes and lower extremity amputations. From 2000 to 2016, premature


mortality from diabetes increased by 5%. In 2019, diabetes became the ninth leading cause of death in the world and is estimated to be the direct cause of 1.5 million deaths. According to the World Health Organization (WHO), the disease increases mortality by 2-3 times and significantly reduces life expectancy. At the same time, the number of patients increases annually in all countries by 5-7%, and doubles every 12-15 years (World Health Organization, 2022).

Diabetes is treatable. A healthy diet, regular physical activity, maintaining a healthy weight and abstaining from tobacco use can prevent or delay the onset of diabetes. The implementation of the mobile application "Automated Diabetes Control System" will allow for more effective treatment, thereby improving the course of the disease. Users will be able to keep a diary of self-control, particularly to enter and edit data of physical activity, taking medication and food; view disease-based analytics based on input and sync

^a <https://orcid.org/0000-0002-1643-0895>

^b <https://orcid.org/0000-0003-2954-1057>

^c <https://orcid.org/0000-0002-4937-3284>

^d <https://orcid.org/0000-0002-4411-6465>

data with an application server.

2 PROBLEM STATEMENT

Diabetes is a disease whose main symptom is a constant rise of blood sugar level. In the human body, the pancreas is responsible for stabilizing blood glucose levels, producing the hormones insulin and glucagon, which increase or decrease glucose levels. However, patients with diabetes have pancreas malfunction in combination with low insulin sensitivity. This leads to fluctuations in blood glucose levels, in particular to the appearance of both hyperglycemia (high glucose concentration) and hypoglycemia (low glucose concentration). Therefore, there is a need to find treatments that can improve the living standards of people with this disease.

The main purpose of our research is to analyze the problem of diabetes and to develop an automated control system. The defined purpose determines the following tasks:

- to define the basic metrics and ways of their reception for the development of the mathematical module of the system;
- to design the structural components and algorithms of the system;
- to develop an automated disease control application.

3 REVIEW OF THE LITERATURE

The article “Global and regional diabetes prevalence estimates for 2019 and projections for 2030 and 2045: results from the International Diabetes Federation Diabetes Atlas, 9th edition” evaluates the prevalence of diabetes in 2019 and forecasts for 2030 and 2045. The study was conducted on 255 qualitative data sources from 138 countries. Data was taken from adults aged 20-79 years for the period from 1990 to 2018, the forecasts are not comforting (Saeedi et al., 2019). According to the IDF diabetes Atlas, the global prevalence of diabetes in 2021 is estimated at 10.5% (536.6 million people) and may increase to 12.2% (783.2 million people) in 2045 (Sun et al., 2022).

Saeedi et al. (Saeedi et al., 2020) estimated the number of deaths related to diabetes among adults aged 20–79. Diabetes is estimated to cause 11.3% of deaths worldwide. Using a model that has only one glucose compartment in its structure, the authors conducted a number of simulations: taking into account the peculiarities of glucose absorption from the

intestine, they improved the procedure for detecting latent forms of diabetes and analyzed the optimal insulin therapy for an automated dispenser (Lapta et al., 2014).

Levkivskiy et al. (Levkivskiy et al., 2020) investigated the algorithms of data mining, which on the basis of rules and calculations allow the creation of a model that analyzes data by searching for certain patterns and trends. Through the study of data mining algorithms, models and methods have been developed to determine the impact of some chronic diseases on others. The developed methods were implemented in the system of intelligent data processing. The conducted research testifies to the prospects of using methods of data mining to improve the quality of medical care for patients.

The research conducted by Bolodurina et al. (Bolodurina et al., 2020) aims to develop and numerically solve the problem of optimal glycemic control in patients with type 1 diabetes mellitus by insulin therapy based on the conditions of optimality for non-smooth systems with constant delay in the phase variable.

In the article by Karpel’ev et al. (Karpel’ev et al., 2015) the basic mathematical models of the biological control system of plasma glucose concentration are presented.

Palumbo et al. (Palumbo et al., 2013) offers a method focused on the most important clinical / experimental tests conducted to understand the mechanism of glucose homeostasis.

The dynamic behavior of a mathematical model, confirmed by experimental data, is studied by Trobia et al. (Trobia et al., 2022) which takes into account the relationship between glucose and insulin concentrations.

Shabestari et al. (Shabestari et al., 2018) presented a new mathematical model to describe the interaction between glucose, insulin and β -cells. The results showed that the system shows different behaviors under different conditions and is able to explain the interaction between glucose, insulin and β -cells.

4 MATERIALS AND METHODS

4.1 Methods and Metrics for Modeling an Automated Diabetes Control System

To develop a system of automated control of diabetes, it is necessary to define and implement methods for collecting input data on the patient’s condition in real

time. These data can be divided into two groups: streaming and constant. Streaming data require regular input and include blood glucose, alcohol, carbohydrates, weight, insulin, time and date, place of administration, physical activity, stress and illness. The constant data include such indicators as age, gender, type of diabetes.

Some of these data can only be obtained by manually entering it by a patient, others can be obtained automatically. Information about blood glucose can be obtained in two ways:

- after measuring blood glucose with a glucometer. A patient can either enter data manually or synchronize data with the system using Bluetooth technology (if supported by the meter);
- with a continuous glucose monitoring system. The monitor measures blood sugar every 10 seconds and records the average value every 5 minutes.

After measuring the weight, the patient can either enter the data or synchronize the data with the system using Bluetooth technology (if supported by the scale).

Information about physical activity has a different nature of collection, one of which is the synchronization of data from an external device such as a fitness tracker – a gadget that, in most cases, is worn on the hand and has built-in sensors that monitor activity during the day, including: number of steps, heart rate, sleep, calories burned, etc. An analogue of a fitness tracker is data collection using an application installed on the user's smartphone, or the user can simply enter data about daily activity manually.

If the data is entered manually, also the time and date are required to be entered. If the data comes from other devices or applications, it already contains time and date information.

For developing the mathematical module of the system metrics and methods for obtaining them were determined.

Sokol et al. (Sokol et al., 2014) proposed the principle of applying mathematical modeling to calculate optimal insulin therapy. Bhonsle and Saxena (Bhonsle and Saxena, 2020) analyze various mathematical models – despite the large number of mathematical models, they are all based on one of two original basic models: the model of the oral glucose tolerance test (OGTT) developed by Beaulieu in 1961 and the model of the intravenous glucose tolerance test (IGTT) by Bergman-Kobelli (Bergman et al., 1979). The Beaulieu model is narrow in use, in particular, it is generally unsuitable for describing the exponential decline of the glycemic curve of IGTT. The main

disadvantage of the IGTT model, in contrast to the Beaulieu model, is that insulin is an input variable, the value of which is determined clinically.

The mathematical model proposed by Shirokova and Shirokov (Shirokova and Shirokov, 2006) is based on the ratio of glucose balance and insulin concentration in human blood over a certain period of time and improved by Bolodurina et al. (Bolodurina et al., 2020).

Therefore, the experimental determination of glycemic characteristics of insulin is as follows: knowing the initial level of glucose in the blood, as well as its integral characteristics, it is possible to choose the right amount of insulin.

4.2 Design and Developing the Algorithms of the System

For design and developing the automated diabetes control system functional requirements were defined:

- User registration and authentication must be provided in the system;
- Data storage: the system must store information and allow the user to manage it;
- Keeping a diary of self-control: entering and editing data of physical activity, medication and food;
- Analytics review: the system should provide the ability to review analytics for the selected period.

The algorithm of the automated diabetes control system is presented in figure 1. First, the user gets to the authorization screen, if he is registered, he can immediately pass it and get to the main screen. Otherwise, it is necessary to go through the registration process by filling out a standard form, the entered data are checked for validity and entered into the appropriate collection in the database.

Once on the home screen, the user can immediately view the statistics. The user can also go to the screen with analytics, where the information for a specified period is displayed. To work with entries, the diary screen with the functions of viewing, adding, deleting and editing entries is available. It is possible to set user settings, medication and glucose level. The data entered by the user when making changes to the settings or when working with diary entries are entered into the database.

On the main screen it is possible to add a new diary entry by clicking on the correspondent button. On the opened modal window with a form current time and date are passed. After the user enters the data, validation and synchronization with the database are performed and the user is redirected to the home screen

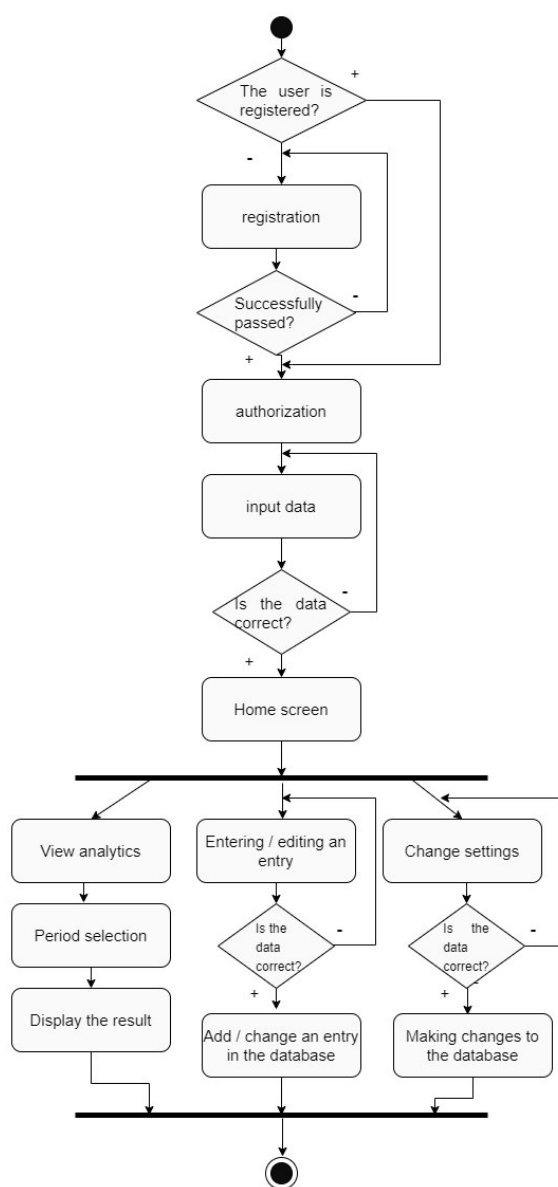


Figure 1: Activity diagram.

and methods are called to update the statistics based on the entered data.

The analysis of functional requirements allowed us to identify the following entities of the developing process. Figure 2 shows a class diagram.

Some classes shown on the diagram are described below.

- Home – a class of the main screen of the application. It has the following methods: `ionViewDidLoad` – this method starts after loading the screen and initializes the methods for updating statistics, `updateStats` – updating statistics for the week, `dailyStats` – updating statistics for the day, `prepareStats` – preparing statistics for the week, `filter-`

`ByDate` – filtering diary entries by date, `newNote` – create a new diary entry, `getFormattedDate`, `getTime` – get the date and time, `showHelp` – display help information.

- Diary – a class for work with the screen of the system. It has the following methods: `ionViewDidLoad` – this method is started after loading the screen and initializes the methods for updating the list of entries, `editNote` – editing the entry.
- `NewNotePage` – a class for work with the modal window of adding and editing entries. Its methods – `showDatePicker`, `showTimePicker` – display forms for selecting the date and time, `add`, `edit` and `delete` for making corresponding operations with entries.
- Analytics – a class for work with the analytics screen. It has the following methods: `ionViewDidLoad` – it is called after loading the screen and initializes methods for analytics update, `updateAnalytics`, `prepareReport` (analytics data preparation), `filterByDate` (filtering entries by date), `getFormattedDate`, `setFormattedDate`, `showDatePicker` (getting and setting dates, date selection form correspondingly).
- Settings – a class for work with settings.
- `Insulin-settings` and `Glucose-settings` are classes for work with medicine and glucose settings. They have the following methods: `ionViewDidLoad` – the method is called after loading the screen and loads the settings, `ionViewWillLeave` – the method is called before closing the screen and saves the changes in the settings.
- `Personal-settings` – a class for work with personal settings. The class has the following methods: `ionViewDidLoad`, `ionViewWillLeave`, `showDatePicker`.
- Login is a class for the user authentication screen. It has a method `login` for user authentication.
- Register is a class for the user registration screen. It has a method `register` for new user registration.
- `SettingsProvider` – a class for working with user settings in the database. Its methods: `getSettings` – to get settings from the database, `updateSettings` – to update the settings in the database, `addNewUserSettings` – to create a document with the settings of a new user.
- `NotesProvider` – a class for working with user diary entries in the database. Its methods are `getNotes` – to load all user entries from the database, `addNewNote` – to add a new entry to the database, `editNote` – to update the entry in the database, `deleteNote` – to delete the entry from the database.

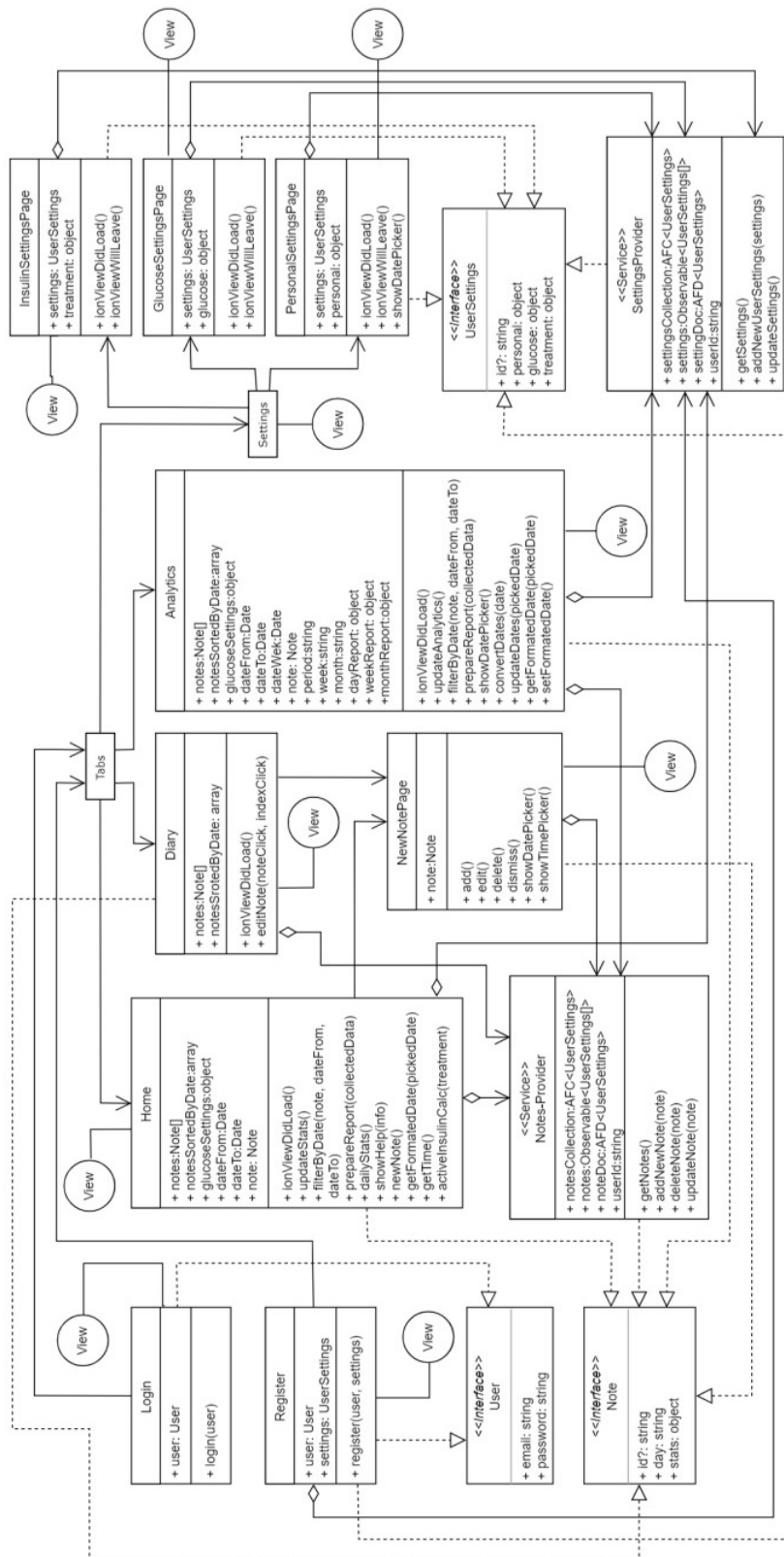


Figure 2: Class diagram.

Thus, the developed application has the functionality of making and editing entries in the system, medicine selection, obtaining analytics, data synchronization between devices, provided by the methods of the components Home, Diary, NewNotePage, Analytics, Settings, Login, Register, Personal-settings, Insulin-settings, Glucose-settings, SettingsProvider, NotesProvider.

Functions in the class Analytics are used to perform analytics. The code snippet is below:

```
updateAnalytics() {
  this.notesForAnalytics =
  this.notesSortedByDate.filter(note =>
  this.filterByDate(note, this.dateFrom,
  this.dateTo));
  let report;
  let collectedData = {
    noteCounter: 0,
    glucoseCounter: 0,
    glucoseSum: 0,
    hiLowCounter: 0,
    bolusInjectionCounter: 0,
    basalUCounter: 0,
    bolusUCounter: 0
  }
  this.notesForAnalytics.forEach(function
  (noteScope, i, notes) {
    noteScope.stats.forEach(function(note, i,
    notesFromScope){
      collectedData.noteCounter++;
      if(note.stats.glucose){
        collectedData.glucoseCounter++;
        collectedData.glucoseSum +=
        parseFloat(note.stats.glucose);
        if(note.stats.glucose <
        this.glucoseSettings.lowLevel
        || note.stats.glucose >
        this.glucoseSettings.hiLevel){
          collectedData.hiLowCounter++;
        }
      }
    }
  )
  if(note.stats.bolus){
    collectedData.bolusInjectionCounter++;
    collectedData.bolusUCounter +=
    parseFloat(note.stats.bolus);
  }
  if(note.stats.basal){
    collectedData.basalUCounter +=
    parseFloat(note.stats.basal);
  }
  }.bind(this));
  report = this.prepareReport(collectedData);
  if (i === 0){
    if (noteScope.day === this.day) {
      this.dayReport = report;
    }
    this.weekReport = report;
    this.monthReport = report;
  } else if ( i <= 6){
    this.weekReport = report;
    this.monthReport = report;
  }
}
```

```
} else {
  this.monthReport = report;
}
}.bind(this)); }
```

To store and access system information a database was designed. It consists of three main collections (User, UserSettings, UserNotes) (figure 3).

5 RESULTS

After starting the automated diabetes control system, the login screen is shown, where the user must login or register by clicking on the registration button. After successful authentication the main screen is displayed (figure 4) with statistics of the main indicators for the week and for the current day, namely: bolus insulin per day, the amount of active bolus insulin at the moment, the number of hypo/hyperglycemia for the current day, average sugar level in seven days, mean deviation of sugar in seven days and the amount of hypo/hyperglycemia in seven days in percent. By clicking on these indicators, the user can get reference information (figure 4).

On the main screen there is a button to create a new diary entry. By clicking on it a modal window with a form is opened. Navigation is carried out through four tabs: Home screen, Diary, Analytics, Settings. On the screen of a diary (figure 5), all entries sorted and grouped by date and time are displayed as rows of cards with entered metrics.

By clicking on any entry, a modal window is opened to edit or delete the entry (figure 6). This window has a form with all the necessary fields for filling: medicine, food, activity, sugar level. The user can also choose the time and date of the entry. In editing mode of an entry, a button for deleting an entry appears in the navigation bar with a dialog box to confirm the deletion of the record.

On the screen of analytics the user can choose the desired period of a report, namely: one day, seven days and thirty days. Also, the date can be specified from which the data will be calculated (figure 7).

The screen with settings displays the user's email and a list of settings groups: personal settings, glucose settings for adjusting glucose levels for hypo/hyperglycemia, medication settings for choosing medications. There is also a login button in the navigation bar.

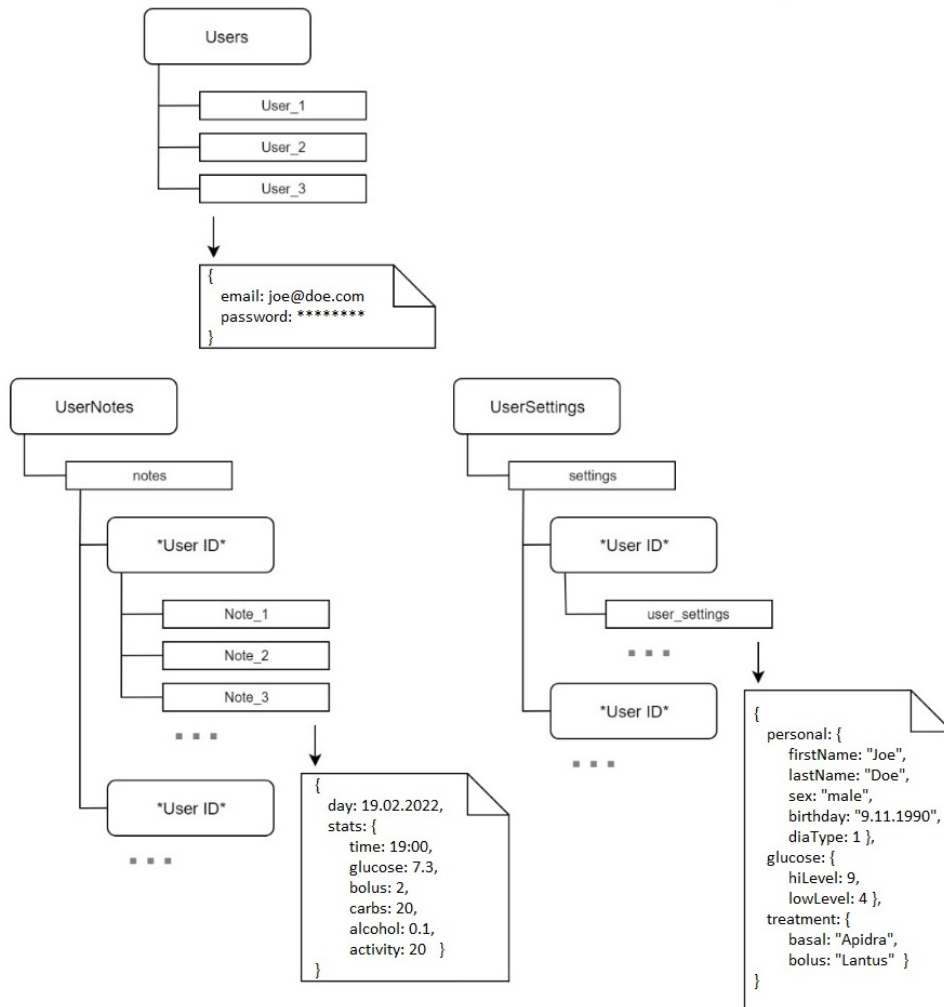


Figure 3: Database schema.

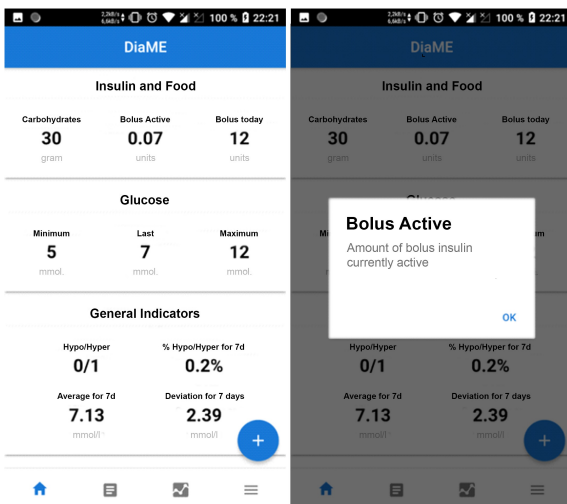


Figure 4: Home screen. Reference information.

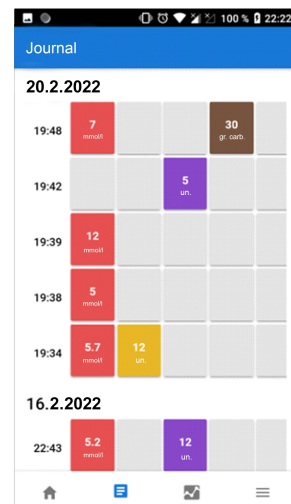


Figure 5: The screen of a diary.

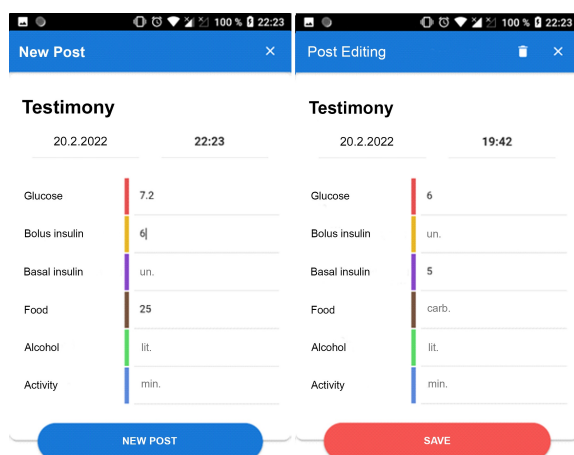


Figure 6: The forms for creating and editing entries.

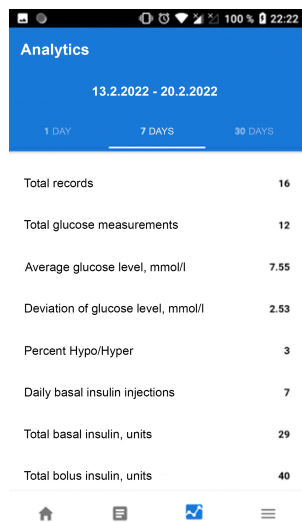


Figure 7: The screen of analytics.

6 CONCLUSIONS

It is estimated that diabetes is the cause of one in nine deaths among adults aged 20-79. Prevention of diabetes and its complications is important, especially in middle-income countries, where the current impact is estimated to be greatest (Saeedi et al., 2020).

As a result of the research, an analysis of the problem of diabetes was conducted. The basic metrics and methods of production of these metrics for the mathematical module of the system are determined. The functional requirements for the automated disease control system were analyzed. Algorithms of the system functions were defined and described, the order of interaction of classes during the execution of the programing code was determined and the system

of automated control of diabetes mellitus was developed.

In the process of development and testing, we consulted with doctors and took into account their recommendations. The system has received positive feedback from diabetes patients who continue to use it. The developed software product is ready for use.

REFERENCES

- Bergman, R. N., Ider, Y. Z., Bowden, C. R., and Cobelli, C. (1979). Quantitative estimation of insulin sensitivity. *American Journal of Physiology-Endocrinology and Metabolism*, 236(6):E667. <https://doi.org/10.1152/ajpendo.1979.236.6.E667>.
- Bhonsle, S. and Saxena, S. (2020). A review on control-relevant glucose–insulin dynamics models and regulation strategies. *Proceedings of the Institution of Mechanical Engineers, Part I: Journal of Systems and Control Engineering*, 234(5):596–608. <https://doi.org/10.1177/0959651819870328>.
- Bolodurina, I. P., Ivanova (Lugovskova), Y. P., and Antsiferova, L. M. (2020). Optimal Control of Glycemia Regulation Dynamics in Patients with Type I Diabetes Mellitus. *Bulletin of the South Ural State University. Ser. Computer Technologies, Automatic Control, Radio Electronics*, 20(4):144–154. <https://doi.org/10.14529/ctcr200415>.
- Karpel’ev, V. A., Filippov, Y. I., Tarasov, Y. V., Boyarsky, M. D., Mayorov, A. Y., Shestakova, M. V., and Dedov, I. I. (2015). Mathematical Modeling of the Blood Glucose Regulation System in Diabetes Mellitus Patients. *Annals of the Russian academy of medical sciences*, 70(5):549–560. <https://doi.org/10.15690/vramn.v70.i5.1441>.
- Lapta, S. S., Pospelov, L. A., and Solovieva, O. (2014). Computerized early diagnosis of diabetes mellitus by methods of mathematical modeling. *Vestnik NTU KHPI*, 36(1079):55–61. <http://repository.kpi.kharkov.ua/handle/KhPI-Press/9388>.
- Levkivskiy, V., Lobanchykova, N., and Marchuk, D. (2020). Research of algorithms of Data Mining. *E3S Web of Conferences*, 166:05007. <https://doi.org/10.1051/e3sconf/202016605007>.
- Palumbo, P., Ditlevsen, S., Bertuzzi, A., and De Gaetano, A. (2013). Mathematical modeling of the glucose–insulin system: A review. *Mathematical Biosciences*, 244(2):69–81. <https://doi.org/10.1016/j.mbs.2013.05.006>.
- Saeedi, P., Petersohn, I., Salpea, P., Malanda, B., Karuranga, S., Unwin, N., Colagiuri, S., Guariguata, L., Motala, A. A., Ogurtsova, K., Shaw, J. E., Bright, D., and Williams, R. (2019). Global and regional diabetes prevalence estimates for 2019 and projections for 2030 and 2045: Results from the International Diabetes Federation Diabetes Atlas, 9th edition. *Diabetes Research and Clinical Practice*, 157:107843. <https://doi.org/10.1016/j.diabres.2019.107843>.

- Saeedi, P., Salpea, P., Karuranga, S., Petersohn, I., Malanda, B., Gregg, E. W., Unwin, N., Wild, S. H., and Williams, R. (2020). Mortality attributable to diabetes in 20–79 years old adults, 2019 estimates: Results from the International Diabetes Federation Diabetes Atlas, 9th edition. *Diabetes Research and Clinical Practice*, 162:108086. <https://doi.org/10.1016/j.diabres.2020.108086>.
- Shabestari, P. S., Panahi, S., Hatf, B., Jafari, S., and Sprott, J. C. (2018). A new chaotic model for glucose-insulin regulatory system. *Chaos, Solitons & Fractals*, 112:44–51. <https://doi.org/10.1016/j.chaos.2021.111753>.
- Shirokova, N. A. and Shirokov, I. V. (2006). Mathematical model of the balance “glucose – insulin – glucagon” in human blood. *Bulletin of Omsk University*, (3):51–53. <https://tinyurl.com/5dsampk5>.
- Sokol, E. I., Lapta, S. S., Pospelov, L. A., and Solovieva, O. I. (2014). Raschet rezhimov insulinoterapii na osnove ma-tematicheskogo komp’juternogo modelirovanija. *Visnik NTU ”HPI”*, 36(1079):61–66. <http://repository.kpi.kharkov.ua/handle/KhPI-Press/9389>.
- Sun, H., Saeedi, P., Karuranga, S., Pinkepank, M., Ogurtsova, K., Duncan, B. B., Stein, C., Basit, A., Chan, J. C., Mbanya, J. C., Pavkov, M. E., Ramachandran, A., Wild, S. H., James, S., Herman, W. H., Zhang, P., Bommer, C., Kuo, S., Boyko, E. J., and Magliano, D. J. (2022). IDF Diabetes Atlas: Global, regional and country-level diabetes prevalence estimates for 2021 and projections for 2045. *Diabetes Research and Clinical Practice*, 183:109119. <https://doi.org/10.1016/j.diabres.2021.109119>.
- Trobia, J., de Souza, S. L. T., dos Santos, M. A., Szezech, J. D., Batista, A. M., Borges, R. R., da S. Pereira, L., Protachevich, P. R., Caldas, I. L., and Iarosz, K. C. (2022). On the dynamical behaviour of a glucose-insulin model. *Chaos, Solitons & Fractals*, 155:111753. <https://doi.org/10.1016/j.chaos.2021.111753>.
- World Health Organization (2022). Diabetes. <https://www.who.int/news-room/fact-sheets/detail/diabetes>.

An Intelligent Robotic Platform for Conducting Geodetic and Ecological Surveys of Water Bodies

Andrii Tkachuk¹^a, Mariia Hrynevych¹^b, Tetiana A. Vakaliuk^{1,2,3}^c, Oksana A. Chernysh¹^d
and Mykhailo G. Medvediev⁴^e

¹Zhytomyr Polytechnic State University, 103 Chudnivsyka Str., Zhytomyr, 10005, Ukraine

²Institute for Digitalisation of Education of the NAES of Ukraine, 9 M. Berlynskoho Str., Kyiv, 04060, Ukraine

³Kryvyi Rih State Pedagogical University, 54 Gagarin Ave., Kryvyi Rih, 50086, Ukraine

⁴ADA University, School of Information Technologies and Engineering, Baku, AZ1008, Azerbaijan
andru.tkachuk@ukr.net, {mariia.skyless, tetianavakaliuk, chernyshoxana}@gmail.com, miserablewisdom@ukr.net

Keywords: Robotics, Geodesy, Measurement, Acidity, Temperature.

Abstract: The article considers the relevance of using a new intelligent robotic platform to quickly conduct basic research on water quality assessment in reservoirs and analyze the relief of the reservoir bottom, preserving all the data. The paper proves that using an intelligent platform for water analysis significantly facilitates the research. Moreover, it increases the studied area of the reservoir. It simplifies the process of establishing the correspondence of data to a particular place on the reservoir compared to classical methods of water quality analysis in the reservoir. It describes the platform's advanced design, which consists of a housing, a control board, sensors, actuators such as servo motors and a brushless motor, a radio module, a GPS module, and a motor speed controller. In addition, it illustrates the cutting-edge platform control panel. The article analyzes a functional diagram of an intelligent robotic platform for water quality assessment and bottom topography. It presents the study of the developed system carried out on the reservoir, the main idea of which was to study the correctness of the system's operation, evaluate the effectiveness of the conducted studies, and display water quality sensors. The paper studies an ultrasonic sensor for measuring depth and sensors for water acidity and temperature. It presents the outcomes of the developed monitoring system experiments that resulted in a map of the reservoir's bottom area and certain conclusions on water quality.

1 INTRODUCTION

Modern realities signify a rapid increase in consumption and the amount of waste. Therefore the question arises whether new digital technologies can compensate for these changes. The answer is obvious: it is necessary to look for new solutions that will help solve the problem of climate change and contribute to preserving the well-being of the entire planet.


Water pollution is the negative change in the physical, chemical, and bacteriological water properties caused by an excess of inorganic substances (solid, liquid, gaseous), organic, radioactive, or heat, which limit or prevent the use of water resources for drink-


ing and economic purposes.


Natural reservoirs, such as oceans, rivers, and lakes, can self-purify. However, getting too many pollutants into their system can cause irreversible damage. Therefore, it all depends on the number of pollutants.


Too many chemicals, bacteria, and other microorganisms cause severe water pollution. Chemical, organic, and mineral substances form colloidal solutions and suspensions. Natural factors determine the chemical composition of pollutants, for example, the decomposition of substances in soil and rocks, the development and death of aquatic organisms, and anthropogenic factors.


Consequently, a robotic platform enables remote analysis of water in the reservoir to measure the acidity of water, its temperature, and the depth of the reservoir. In case of acidity increase and water pollution detection, it will be possible to take a water sample from a particular reservoir area and carry out a de-

^a <https://orcid.org/0000-0003-2466-6299>

^b <https://orcid.org/0000-0001-9183-5211>

^c <https://orcid.org/0000-0001-6825-4697>

^d <https://orcid.org/0000-0002-2010-200X>

^e <https://orcid.org/0000-0002-3884-1118>

tailed water analysis in the ground laboratory. Moreover, the floating platform takes real-time readings from sensors and follows the executive mechanisms. Thus, it detects the source of pollution and marks the exact location by dropping a beacon in the highest pollution concentration for further investigation of the nature and pollution level.

Furthermore, the platform is a helpful tool for training qualified economists and promoting the development of environmental consciousness and motivation for transforming knowledge in behavioral models.

2 THEORETICAL BACKGROUND

The problem of water pollution is becoming more significant. Some “mobile” laboratories allow conducting research in field conditions. However, it is a long-term process that requires detailed preparation and preliminary water sampling.

There are no absolute analogs of the system presented.

The automated surface platforms that are fully autonomous or controlled are reviewed in (Dimitropoulos, 2019; Brans, 2021; Rivero, 2022; Niiler, 2020; Drăgan, 2021). Therefore, they are suitable for extreme conditions to research in the ocean or transport cargo along a specific, established route.

Sea Machines (Sea Machines, 2023) highlight an autonomous self-piloting system, which allows remote control of the vessel, receives information from sensors on the user interface, and has a complete picture of the vessel’s state.

Li et al. (Li et al., 2020) suggested a spectral processing method for analyzing the reflectivity of water samples and applied machine learning methods to estimate water quality parameters.

Therefore, the investigation aims to develop an intelligent robotic platform for conducting geodetic and environmental research, which will be easy to manage, “mobile”, and fast compared to similar systems. Moreover, it will also allow us to quickly make sets of water samples for more accurate and detailed analysis in the laboratory. In addition, it contributes to an actual experiment to assess the robotic platform’s effectiveness and the system’s correctness.

Koval’ (Koval’, 2015), Bezvesilna et al. (Bezvesilna et al., 2017) describe modern sensors for measuring acceleration and gravity anomalies. However, they do not indicate the feasibility of using them in the design of intelligent robotic platforms.

Various ways to control intelligent robotic platforms are suggested in (Chung et al., 2018; Tedeschi

and Carbone, 2014). An example of a fuzzy neural network and a Kalman filter to control a mobile robot is provided. A stabilization algorithm with the applied close-loop control system, including an inertial measuring unit as a feedback sensor, is delivered. A Control system is applied to calculate the engine angles to achieve stability on the inclined surface.

3 RESULTS

3.1 The Structure of the Intelligent Robotic Platform

Zhytomyr Polytechnic State University scholars have developed an intelligent robotic platform for geodetic and environmental research. According to the criteria of “cost-effectiveness” and mobility, the new system will be the best among its known analogs. The design of the robotic platform (figure 1) consists of the following main elements: body; control unit (1), which includes a microcontroller based on an Arduino Nano board (2), a radio module (3), a JSN-SR04T-2.0 sensor control board (4), a PH-4502C module to which a water acidity sensor is connected (5); collectorless engine (6), its cooling jacket (7), engine regulator (9) connecting clutch (24) for transferring rotation from the engine shaft to the deadwood shaft (23), which in turn is connected to the propeller (22)); the system is powered by a battery (8); servomotors (10), (11), (12) and (13) are used as cargo compartment drives (25) and (26), steering wheel drive (21) and water intake mechanism drive; sensors for temperature (14), acidity level (15), ultrasonic for measuring the distance from the bottom of the platform to the bottom of the reservoir (16), distance sensor (27); navigation of the platform is provided by the GPS module (28) and the antenna (29); overall emitters (17) – (20) help in driving in the dark.

The platform equipment is powered by a Turnigy Li-Po 7.4V 5300mAh 2S2P 25C battery, which allows you to use the robotic intelligent platform for a long time and provides the necessary power supply voltage for the correct operation of the system. An Arduino Nano board built on an ATmega328 microcontroller was chosen as the control device. It is compact and enables all the tasks set in this project. For remote data transmission and platform control, the NRF 24L01P+ radio module is used, ensuring good signal reception and transmission quality at a distance of up to 1 kilometer. Furthermore, the following sensors receive data about the environment: ultrasonic distance sensor JSN-SR04T-2.0, which provides mea-

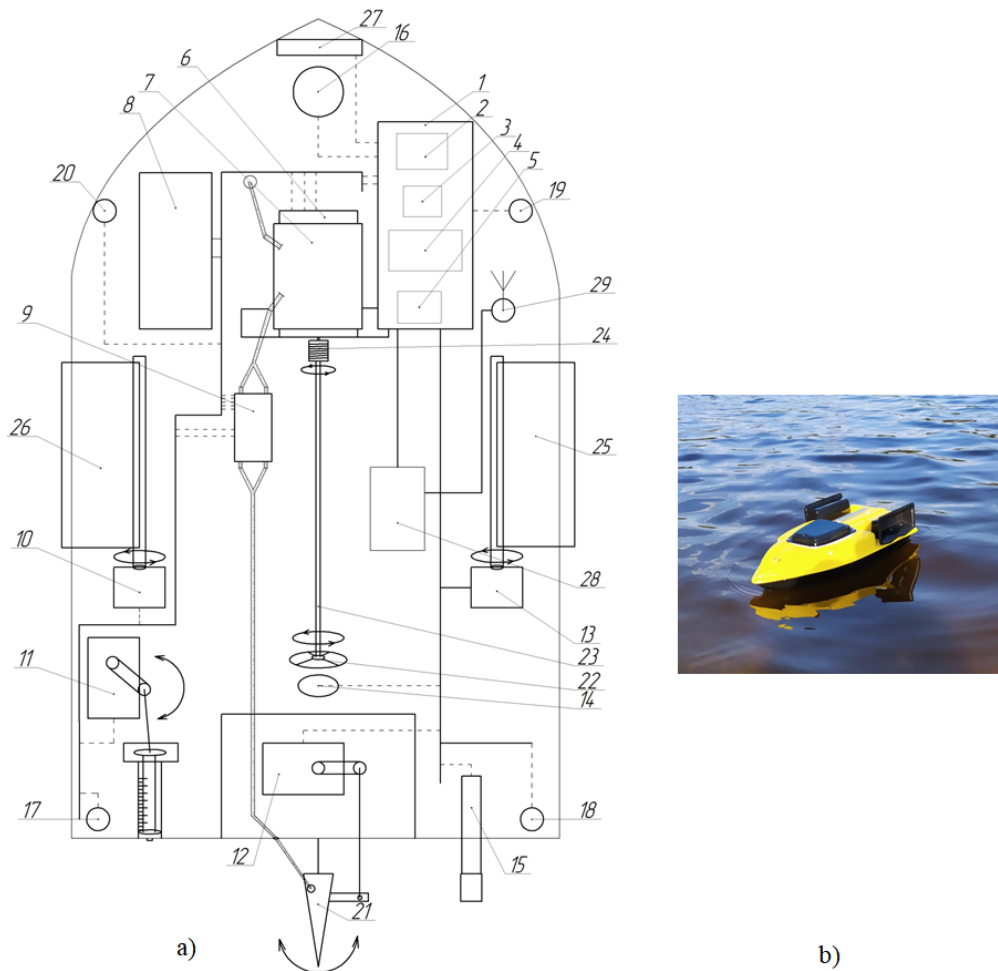


Figure 1: Structural elements of the robotic intelligent platform (a) the robotic platform (b).

surement of the distance from the swimming platform to the bottom of the reservoir and thereby allows displaying a map of the topography of the bottom by constructing a graph based on the data received from the sensor, as well as measuring depth in a specific place of the reservoir and make a preliminary calculation of the water volume of the reservoir; the DFRobot ADC151 water acidity sensor is used to analyse water quality, which helps to explore and determine the acidity of water almost instantly; to measure the water temperature, a DS18B20 digital sensor is used with the function of an alarm signal for monitoring the temperature and the range of the measured temperature from 55 to +125 °C; the Sharp GP2Y0A21YK0F infrared distance sensor was used to determine floating obstacles that may appear in the path of the platform; to determine the exact location of this system and further build a map of the bottom and link the received data to exact coordinates, the GPS module GPS NEO-6M SMA + IPEX

and the active antenna ANT GPS BY-GPS-07 SMA-M were used to increase sensitivity and increase the ratio “signal-to-noise” and reducing the impact of interference. The executive mechanisms are in the form of MG995 Tower Pro and MG996R-180 servomotors, which are necessary to implement the water collection mechanism for its further in-depth analysis, as well as to ensure the movement of the swimming platform in the required direction and to unload the cargo placed in two cargo compartments on top of the platform.

3.2 Control Panel

We developed the control panel for the platform by modernizing the existing panel, the structural diagram of which you can see below.

Control is carried out by the Arduino Nano board, which provides data processing. Moreover, it performs the control device function and ensures data processing from the GPS module and their recording

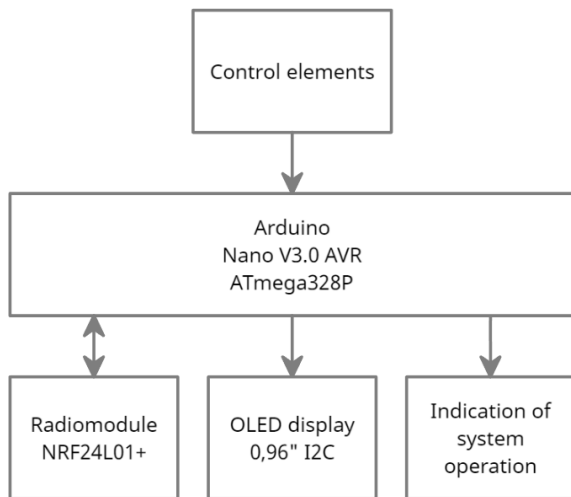


Figure 2: Structural diagram of the remote control panel.

on a flash drive.

Sticks are employed to control the platform remotely; buttons are used to drive the cargo compartments and activate the water sampling system. LEDs are used to display the status of the system.

The control panel receives and transmits data via the NRF 24L01+ radio module. The received sensor data from the radio module are processed by the control board and displayed on the OLED display of the control panel.

3.3 Algorithms of System Operation

For the operation of the robotic intelligent platform, it is necessary to organize the synchronous operation of the swimming platform and the remote control (data reception and transmission). First, according to the system's algorithm (figure 3), the controller ports are configured, and the input data is zeroed. In this case, the transmitter considers the robotic intelligent platform, i.e., the initiator of the data exchange. Then a request is sent to the air to connect to the control panel. If there is no response, a cyclical request to connect to the control panel is sent again. If there is a connection and a signal is received, a response occurs to work on exchanging data with the remote control and checking the necessity of continuing work. If the work is finished, the cycle ends. If the system continues, cyclical work with the remote control takes place until the work with the remote control is finished.

The control panel operations algorithm (figure 4) begins with initialization. Then, the remote control acts as a receiver. Therefore, there is a wait for a free request on the air to connect to the robotic intelligent platform. In the absence of active requests, there is a cyclic wait for a connection request. In the case of

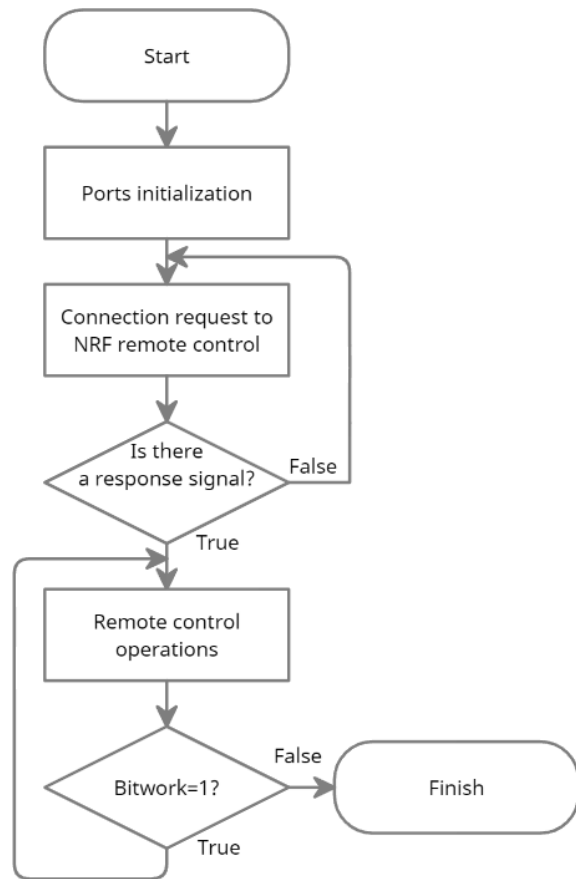


Figure 3: The basic algorithm of the robotic intelligent platform.

a connection and receiving a signal, it is essential to exchange data with the platform and check the need to continue work. If the work is finished, the cycle ends.

3.4 Features of the System

When activating the data recording system for building a three-dimensional model of the reservoir bottom, the system activation is checked, the GPS module and the SD module are launched, and their settings for operation are performed. The GPS module needs time to connect to satellites and determine its coordinates. Therefore, determining the coordinates of the robotic platform location takes time. Then a file is created to make further recordings of the depth sensor data and the corresponding coordinates. In addition, a timer is started, which is set to 10 minutes by default. During this time, the data will be recorded in the created file. Next, the coordinates and depth are cyclically read. Finally, this data is written to a file with an interval of 30 seconds during the time set by the timer. This data file is the basis for construct-

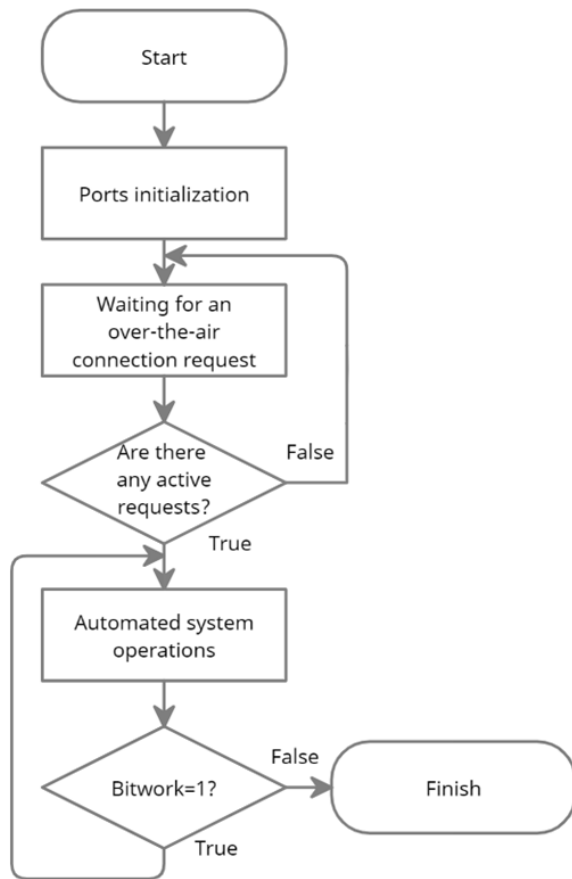


Figure 4: The basic algorithms of the control panel.

ing a wavelet diagram of the reservoir bottom section. If the data recording system is activated again, it is checked whether the coordinates of the module are determined, and the work continues in the cycle. Otherwise, the reactivation of the system is expected.

With the help of radio modules, such data as control signals from the remote control are transmitted. They are responsible for the movement of the platform, turning on/off the dimensions, and collecting a water sample for deeper analysis. In addition, there is a data transfer received from sensors, namely water acidity level, temperature, depth, coordinates of the platform location, and battery charge level.

To create a map of the bottom relief, first of all, it is necessary to collect data on the depth of the reservoir using an ultrasonic distance sensor JSN-SR04T-2.0. Then, two more parameters are needed to build a three-dimensional model. One of them is time, and the other is coordinates, the determination of which is performed using GPS data of the mobile platform location on the reservoir. Finally, when conducting research, it is necessary to choose a site on the reservoir and, moving through the reservoir step by step, receive data from the depth sensor and coordinates

at these points, respectively, and write this data to a file on the platform of the RPi 3B+ mini computer installed on the mobile platform.

3.5 Data Processing

The MATLAB system was used to process the data and build a three-dimensional relief model of the bottom of the reservoir, namely the Wavelet Toolbox, which provides functions and applications for analyzing and synthesizing signals and images. The toolbox includes algorithms for continuous wavelet analysis, wavelet coherence, synchrosqueezing, and data-adaptive time-frequency analysis. Using continuous wavelet analysis, it is possible to study how spectral functions evolve with time, identify common time-varying patterns in two signals, and perform time-localized filtering. Discrete wavelet analysis helps to analyze signals and images in different extensions to detect discontinuities and other defects that are not easily visible in the raw data. In addition, it is possible to compare signal statistics on multiple scales and perform a fractal analysis of the data to reveal hidden patterns. Finally, with the Wavelet Toolbox, you can obtain a sparse representation of data valid for denoising or compressing data while preserving important features. Many toolbox functions support C/C++ code generation.

A1		fx 9:42:34						
	A	B	C	D	E	F	G	
1	9:42:34	50.236396	28.611356	155	24	6	5	5
2	9:42:37	50.236400	28.611360	146	24	6	5	
3	9:42:40	50.236412	28.611358	140	30	6	4	
4	9:42:43	50.236412	28.611354	134	29	6	4	
5	9:42:46	50.236415	28.611351	145	29	6	4	
6	9:42:49	50.236412	28.611351	132	30	6	4	
7	9:42:52	50.236396	28.611356	144	30	6	4	
8	9:42:55	50.236385	28.611362	144	30	6	4	
9	9:42:58	50.236381	28.611370	135	30	6	4	
10	9:43:01	50.236377	28.611373	151	30	6	4	
11	9:43:04	50.236373	28.611377	136	30	6	4	
12	9:43:07	50.236370	28.611379	147	30	6	4	
13	9:43:10	50.236362	28.611383	156	29	6	4	
14	9:43:13	50.236358	28.611383	131	29	6	4	
15	9:43:16	50.236354	28.611383	138	29	6	4	
16	9:43:19	50.236354	28.611381	147	29	6	4	
17	9:43:22	50.236354	28.611377	149	29	6	4	
18	9:43:25	50.236354	28.611375	99	29	6	4	
19	9:43:28	50.236354	28.611371	89	29	6	4	
20	9:43:31	50.236354	28.611370	96	29	7	4	
21	9:43:34	50.236358	28.611366	105	30	6	4	

Figure 5: Recorded data from a flash drive.

The investigation results prove that using wavelet transformations at the given stage of work is not entirely appropriate. Undoubtedly, it is necessary to follow a clear route to use wavelet transformations. For instance, it is crucial to select the coordinates of

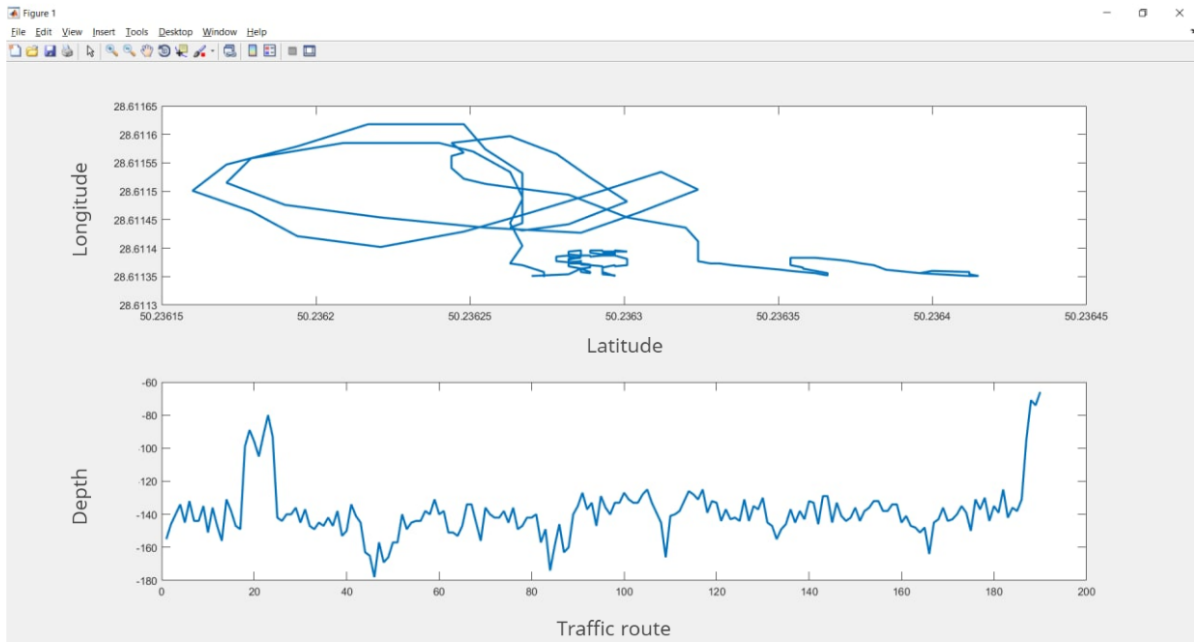


Figure 6: Intelligent robotic platform movement route and two-dimensional depth plot.

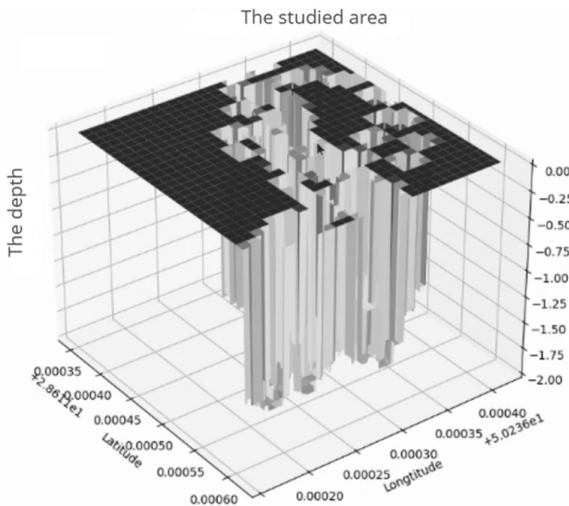


Figure 7: Three-dimensional model of the bottom of the reservoir.

a specific section, which are autonomously traversed robotically by the platform at the same speed, the same passes, and exclude measurement errors due to the influence of external factors.

4 CONDUCTING AN EXPERIMENT

Before the experiment, the platform and all elements' efficiency were thoroughly checked. Then, a shallow

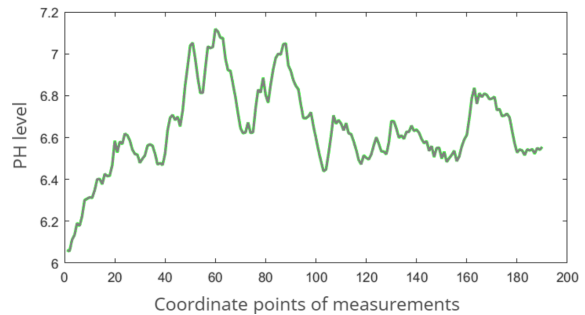


Figure 8: Changes in water acidity in the reservoir.

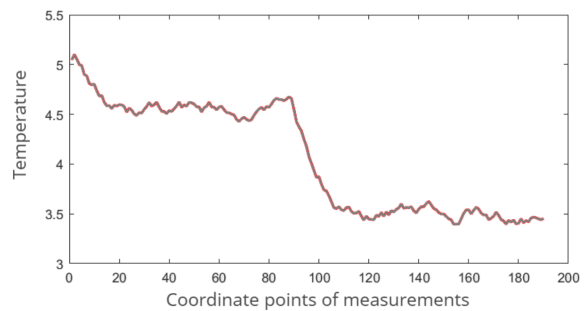


Figure 9: Water temperature changes in the reservoir.

water body was chosen for the test launch of the intelligent robotic platform and the necessary data collection. Finally, a route with different trajectories was traversed, and sensor data were recorded, which was the primary aim of the research.

All the research data is recorded in a file stored on a flash drive. It is convenient for further processing

and analysis. Some recorded data is shown in figure 5.

The GPS module determines the current location and indicates the exact time regarding the location in specific coordinates. The data analysis makes it possible to build a map of the intelligent robotic platform's route and a two-dimensional depth graph (figure 6).

Furthermore, a three-dimensional model of the reservoir bottom was built based on the platform's route data and measured data at specific points along the route. However, it is not highly detailed, as it considers only the specified points of the route. Thus, to increase its informativity, all intermediate points must be filled with relevant data (figure 7).

According to the readings of the temperature and acidity sensor at each determined point of the robotic platform route, graphs of changes in these values were built (figure 8, 9).

5 CONCLUSIONS


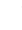




The research introduces a new intelligent robotic platform for geodetic and ecological studies of water bodies. It helps assess water quality and measure a water body's depth. It provides a detailed layout of all structural elements, describes the methodology, and clarifies further data processing. Sensitive system elements such as temperature, water acidity, and distance sensor were chosen, which meet all platform installation requirements. Finally, it investigates the effectiveness and correctness of the system performance on a natural reservoir (a river and a lake). Furthermore, all necessary measurements were taken, including a water sample. Based on the results, conclusions were made about the water quality in the reservoir. Moreover, three-dimensional models of the studied bottom area and graphs of changes in the values (temperature and acidity) were constructed. In addition, the research highlights the problem of using a wavelet diagram to describe the area of the reservoir bottom.

The installation has a set of functions, which can be increased in the future, for example, adding the function of work autonomy at specified points, which contributes to building a full-fledged detailed map of the reservoir bottom. In addition, the article considers the possibility of a more detailed analysis of water locally.

REFERENCES

- Bezvesilna, O., Tkachuk, A., Chepyuk, L., Nechai, S., and Khylychenko, T. (2017). Introducing the principle of constructing an aviation gravimetric system with any type of gravimeter. *Eastern-European Journal of Enterprise Technologies*, 1(7(85)):45–56. <https://doi.org/10.15587/1729-4061.2017.92941>.
- Brans, P. (2021). What Norwegians are learning as they pioneer autonomous ships. <https://tinyurl.com/4pcatcdt>.
- Chung, H.-Y., Chung, Y.-L., and Hung, Y.-J. (2018). An Effective Hexapod Robot Control Design Based on a Fuzzy Neural Network and a Kalman Filter. In *2018 IEEE Region Ten Symposium (Tensymp)*, pages 248–253. <https://doi.org/10.1109/TENCONSpring.2018.8691947>.
- Dimitropoulos, S. (2019). The New Ocean Explorers. <https://www.popularmechanics.com/technology/infrastructure/a29849406/unmanned-ocean-drones-antarctic-voyage/>.
- Drăgan, O. (2021). This Solar-Powered Electric Ferry Is the First Maritime Robotaxi in Europe. <https://tinyurl.com/4bf65wut>.
- Koval', A. V. (2015). Simulation of gravimetric measurements by gyroscopic integrator of linear accelerations. *Gyroscopy and Navigation*, 6:344–347. <https://doi.org/10.1134/S2075108715040070>.
- Li, Y., Wang, X., Zhao, Z., Han, S., and Liu, Z. (2020). Lagoon water quality monitoring based on digital image analysis and machine learning estimators. *Water Research*, 172:115471. <https://doi.org/10.1016/j.watres.2020.115471>.
- Niiler, E. (2020). The Robot Ships Are Coming ... Eventually. <https://www.wired.com/story/mayflower-autonomous-ships>.
- Rivero, N. (2022). Japan is home to the world's first autonomous container ships. <https://tinyurl.com/bdfpdf7e>.
- Sea Machines (2023). SM300 Autonomous Command & Control.
- Tedeschi, F. and Carbone, G. (2014). Design Issues for Hexapod Walking Robots. *Robotics*, 3:181–206. <https://doi.org/10.3390/robotics3020181>.

Drill String Vibration Monitoring as an Element of Automatic Control of Drilling

Vladimir Morkun¹^a, Natalia Morkun¹^b, Vitalii Tron²^c, Alona Haponenko³^d,
Iryna Haponenko³^e and Evhen Bobrov³^f

¹Faculty of Engineering Sciences, Bayreuth University, Universitätsstraße, 30, Bayreuth, 95447, Germany

²Department of Automation, Computer Science and Technology, Kryvyi Rih National University,
11 Vitalii Matusevych Str., Kryvyi Rih, 50027, Ukraine

³Research Department, Kryvyi Rih National University,

11 Vitalii Matusevych Str., Kryvyi Rih, 50027, Ukraine

{morkunv, nmorkun}@gmail.com, vtron@knu.edu.ua, {a.haponenko, haponenko}@protonmail.com,
evhenbobrov@tutanota.com

Keywords: Drilling, Vibration, Monitoring, Automatization, Ore, Mining.

Abstract: The research is aimed at monitoring drill string vibrations as an element of automatic control of the drilling process. To reduce negative impacts of vibrations occurring in the drill string at deep drilling of hard rocks, a mathematical model is proposed to consider parameters of the drilling process and predict the penetration rate. The following parameters are used as input variables when studying drilling data: weight-on-bit, rotations per minute, torque, mechanical specific energy, longitudinal, transverse and torsional vibrations. In this study, the rate of penetration is used as a resulting variable. Considering these parameters, a mathematical model of the drilling process is formed on the basis of adaptive neural-fuzzy inference structures. The accuracy of this model is 95.56 %.

1 INTRODUCTION


Deep drilling of hard rocks causes strong vibrations in the drill string associated with a reduced rate of penetration (ROP) and early failure of equipment (Cobern, 2003; Morkun et al., 2015c). The only available method of limiting vibrations during drilling is to change the rotary speed or weight-on-bit (WOB). Yet, these changes often reduce drilling efficiency.


There are a number of vibration sources in a drilling rig that can potentially reduce the mechanical rate of penetration and cause vibrations damaging sensors and clamps. These include, in particular, shock vibrations from bit cones and blades (Morkun et al., 2015c; Golik et al., 2015). There are several cones on the bit which make the string vibrate when moving. Vibration frequency is a multiple of


the speed of the bit blades.


Besides, in drilling there is a direct precession – lateral vibration – caused by imbalance in the drill string (Cobern, 2003; Morkun et al., 2015b). The imbalance can occur due to peculiarities of machining drill collars or due to their curvature, these causing lateral vibrations along the drill string. The reverse precession is caused by friction between the drill string and the borehole. If there is a sufficient contact effort and rotary speed, couplings begin to rotate around the borehole counterclockwise with the frequency that depends on the external diameter of the couplings and that of the borehole. This creates an imbalance effort on the drill string. Excitation is a multiple of the motor speed multiplied by the number of rotor blades.


In addition, the stabilizers have blades in contact with the borehole (Cobern, 2003; Deng et al., 2021). The resulting excitation is a multiple of the rotary speed multiplied by the number of blades. Straight blades cause greater vibration than inclined ones. The stick-slip phenomenon is another source of vibration caused by friction between couplings or stabilizers and the borehole as a result of gravity along the drill


^a <https://orcid.org/0000-0003-1506-9759>

^b <https://orcid.org/0000-0002-1261-1170>

^c <https://orcid.org/0000-0002-6149-5794>

^d <https://orcid.org/0000-0003-1128-5163>

^e <https://orcid.org/0000-0002-0339-4581>

^f <https://orcid.org/0000-0002-9275-3768>

string (Cobern, 2003; Moharrami et al., 2021). This phenomenon can make the element bit jammed. After accumulating enough effort to release the drill string, it resumes its rotation at a high angular speed.

The roller-cone bit is a kind of mechanism that, when interacting with the borehole bottom, converts rotation of the drill string or the borehole motor shaft in longitudinal, torsional, and under certain conditions, transverse vibrations (Novikov and Serikov, 2020; Bogomolov and Serikov, 2018). Strong vibrations during machine operation can cause destruction of drill collars and derrick elements, damage to borehole motors and equipment, an increase in the borehole diameter, early wear of the bit, reduction of the mechanical penetration rate. With intensified vibrations and no control of their level, the phenomenon of resonance can occur, which in most cases results in severe destruction of elements of drill collars and the bit (Bogomolov and Serikov, 2018; Morkun et al., 2015a).

Longitudinal and torsional vibrations are essentially connected with specific design of roller-cone bits and the principle of their operation (Novikov and Serikov, 2020; Liu et al., 2021). Vibrations are of a wavelike nature. They are classified into longitudinal, transverse and torsional. They occur simultaneously and depend on wavelike characteristics of the drill string and devices included in its assembly (calibrators, centrators, dampers, shock absorbers), bit size, properties of drilled rocks, and drilling mode parameters.

The causes of vibrations include a stick-slip nature of rock destruction, rough borehole bottom (Serikov and Ginzburg, 2015; Morkun and Tron, 2014), inhomogeneity, fracturing and sharp intermittency in hardness of drilled rocks, pressure differences under different support teeth of the bit (Novikov and Serikov, 2020; Serikov et al., 2016), uneven wear of teeth leading to formation of different contact areas with the rock; the toothed working surface of the bit, pressure pulsation in the discharge system (Vasiliev et al., 2015; Morkun et al., 2014) and discrete tool feed.

2 MATERIALS AND METHODS

In paper (Sharma et al., 2021) a lumped mass drill rod model that consists of two degrees of freedom was suggested. The drill rod is represented by the equivalent mass and rigidity for axial and torsional motions (figure 1).

Equations of for axial and torsional motions the drill string are as follows:

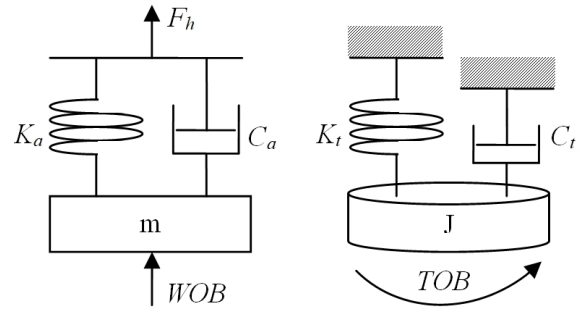


Figure 1: Simplified lumped model for axial and torsional motion: a – axial motion; b – torsional motion (Sharma et al., 2021).

$$m\ddot{x} + c_a\dot{x} + k_a(x - v_0 * t) = -WOB \quad (1)$$

$$J\ddot{\theta} + c_t\dot{\theta} + k_t(\theta - \Omega * t) = -TOB \quad (2)$$

where m is the effective mass of the drill rod, x is the axial displacement, J is the effective polar inertia moment, c_a is the damping coefficient during the axial motion, c_t is the damping coefficient during torsional motion, k_a is the axial rigidity, k_t is the torsional rigidity, v_0 is the initial axial velocity, θ is the angular displacement of the bit and Ω is the surface rotation rate in radians per second (RPS). Axial and torsional motion equations (1) and (2) are related due to interaction forces of the bit.

A method of direct quantitative determination of various vibration forms with parameters that can be easily transmitted to the surface was substantiated in (Cobern, 2003). The system uses four accelerometers and a magnetometer mounted on the drill string. By using various combinations of accelerometer output signals, it is possible to distinguish a whirl, a stick slip, a rebound of the bit, and lateral vibrations from each other. Three accelerometers are mounted in the cuff at the angle of 120 degrees from each other and oriented radially to be measured. The fourth accelerometer is installed axially. The magnetometer is also installed in one of the pockets. The pockets can also accommodate WOB and TOB (time on bottom) strain gauges providing a complete toolkit for borehole diagnostics. Installing accelerometers radially (figure 2) enables direct calculation of various vibration modes.

Radial accelerometers measure the centrifugal force, which is directly related to the rotary speed (Cobern, 2003). As a result, the rotary speed, the stick-slip and the swirl can be directly calculated. The magnetometer is used as a backup for measuring the rotary speed. To measure axial vibration, only a single-axis accelerometer is required. These parameters are calculated as follows.

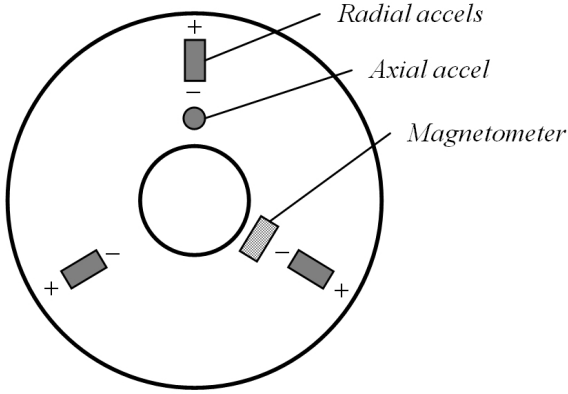


Figure 2: Drill collar sensors.

3 RESULTS AND DISCUSSION

Analysis of frequency characteristics of vibrations during drill string operation indicates different frequency ranges for individual technical components. In particular, Cobern (Cobern, 2003) reveals that vibrations of components cause vibrations of the following frequency: bit rotation – 1000 Hz, stick-slip motion of the bit – 10 Hz, direct precession – 10 Hz, reverse precession – 100 Hz. Also, the vibrations produced by these sources differ significantly in amplitude.

Transfer functions in a closed form associating deformation of the drill string with displacement on the bit in the dimensionless form are described by the following expressions:

$$\frac{\bar{X}_b}{\bar{W}_b}(\bar{s}) = \Psi_a h_a(\bar{s}) = -\frac{\Psi_a}{\bar{s}} \frac{1}{Z_{c,a} Z_{L,a} + Z_{c,a} \tanh \Gamma_a} \frac{Z_{c,a} + Z_{L,a} \tanh \Gamma_a}{Z_{c,a} Z_{L,a} + Z_{c,a} \tanh \Gamma_a}$$

$$\frac{\bar{\Phi}_b}{\bar{T}_b}(\bar{s}) = \Psi_t h_t(\bar{s}) = -\frac{\Psi_t}{\bar{s}} \frac{1}{Z_{c,t} Z_{L,t} + Z_{c,t} \tanh \Gamma_t} \frac{Z_{c,t} + Z_{L,t} \tanh \Gamma_t}{Z_{c,t} Z_{L,t} + Z_{c,t} \tanh \Gamma_t}$$

Graphical results of modelling the above transfer functions are obtained via software solutions described in (Aarsnes and Aamo, 2016) and shown in figure 3.

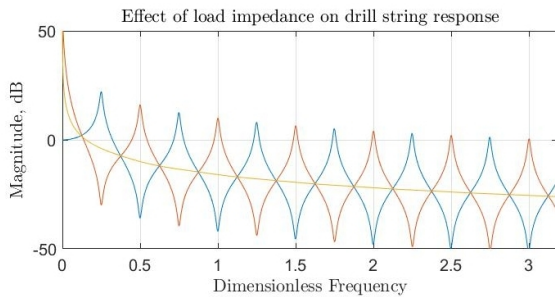
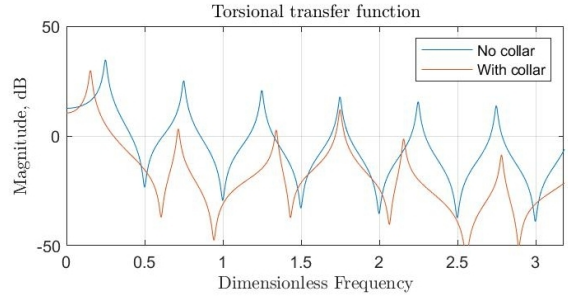


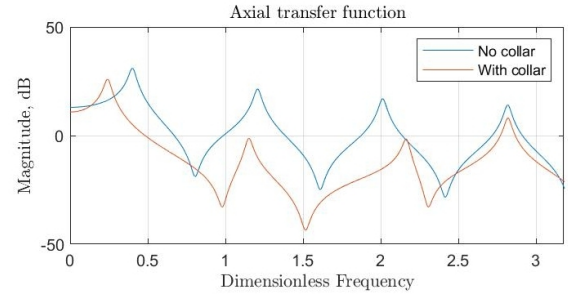
Figure 3: Drill collar sensors.

The bottom section of the drill string usually consists of weighted drill collars, which can have a great impact on dynamics of the drill string due to their extra inertia. In particular, transition from collars to couplings in the drill string causes reflections in traveling waves due to a change in the characteristic impedance of the line.

The length of sections is included in propagation operators, so they determine basic frequencies of an individual section. Figure 4 demonstrates the impact of a 200m drill collar on a 1200m drill string on transfer functions.



(a)



(b)

Figure 4: Transfer function with and without drill collars: a – torsional, b – axial.

To determine the rotary speed, we calculate the centripetal acceleration $A_c(t)$ (Cobern, 2003):

$$A_c(t) = (A_1(t) + A_2(t) + A_3(t))/3 \quad (3)$$

As $A_c(t) = \omega^2(t) - r$, where r is the sensor radius, ω is the angular rotary speed, radian/sec. From here:

$$\omega(t) = \sqrt{\frac{A_c(t)}{r}} \quad (4)$$

the instantaneous speed is determined by the expression:

$$RPM = \left(\frac{60}{2\pi}\right) \cdot \omega(t) \quad (5)$$

The stick-slip effect is set by the maximum rotary speed (Cobern, 2003):

$$\omega_{ss} = \max(\omega(t)) \quad (6)$$

The reverse precession is determined by the peak of the following expression (Cobern, 2003):

$$A_w(t) = A_1(t) + A_2(t) \cos(120 \text{ deg}) + A_3(t) \cos(240 \text{ deg})$$

Lateral vibration has two components. The x-axis acceleration is equal to:

$$A_x(t) = \frac{1}{2} \left(\frac{A_2(t) - A_c(t)}{\cos(30)} - \frac{A_3(t) - A_c(t)}{\cos(30)} \right) \quad (7)$$

The y-axis acceleration is determined by the formula:

$$A_y(t) = \frac{1}{3} (A_1(t) - A_c(t) + \frac{-A_2(t) + A_c(t)}{\sin(30)} - \frac{-A_3(t) + A_c(t)}{\sin(30)})$$

Thus, the value of lateral vibration is determined by the vector sum (Cobern, 2003):

$$A_{Lat}(t) = \sqrt{A_x(t)^2 + A_y(t)^2} \quad (8)$$

Axial vibration can be directly measured with an axial accelerometer.

To verify the mathematical model, the data on drill string operation published in (Tunkiel et al., 2021) is used. On figure 5 shows the results of measuring the weight-on-bit depending on the depth of the borehole.

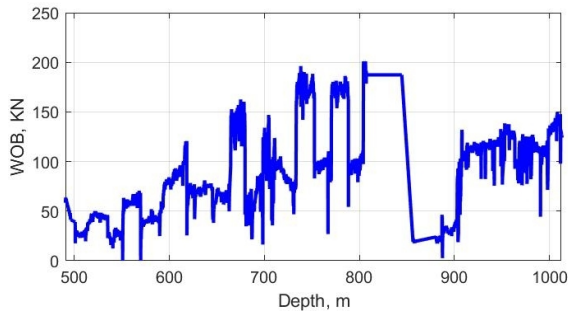
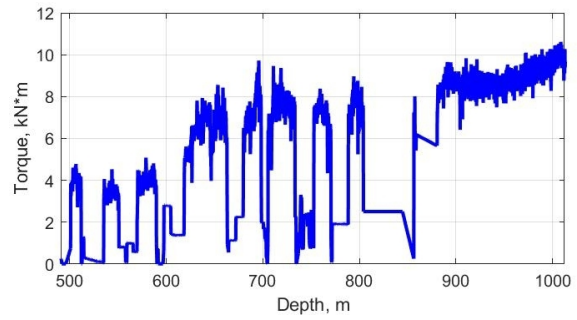


Figure 5: Dependence of the weight-on-bit on the borehole depth.

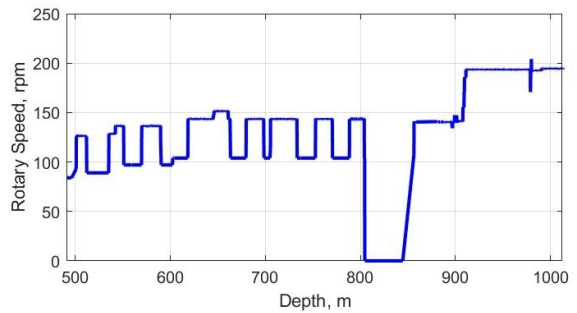
The graph of a dependence of the weight-on-bit on the borehole depth demonstrates characteristic stick-slip changes in the weight indicator which may be associated with alternation of various types of drilled rocks. On figure 6 revealed a dependence of the torque and the rotary speed on the borehole depth. These dependences are also characterized by areas with a stick-slip change in the indicator as in the case with the WOB indicator.

On figure 7 it is shown the change of the resulting indicator value (the ROP of the borehole) depending on the depth.

When studying the data on the drilling process, the above parameters are used as input variables: WOB,



(a)



(b)

Figure 6: Dependence of the torque and the rotary speed on the borehole depth: a – torque, b – rotary speed.

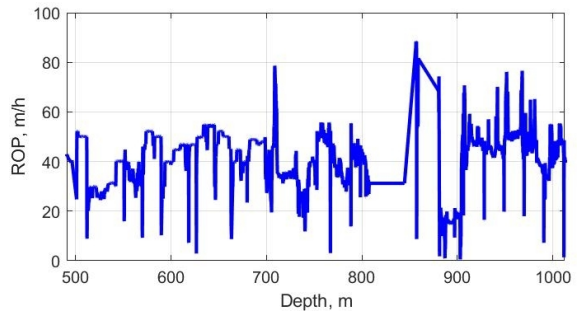


Figure 7: Drilling parameters.

RPM, torque, MSE, longitudinal, transverse and torsional vibrations. The resulting variable in this study is the ROP of the borehole.

Considering the above parameters, a mathematical model of the drilling process is formed on the basis of adaptive neural-fuzzy inference structures (ANFIS). There are three input terms of membership functions. The type of input membership functions is bell-shaped. On figure 8 it is shown the results of verification of the resulted model.

The verification results of the developed model on the test sample (figure 8) confirm its applicability to practical use. The accuracy of this model is 95.56 %.

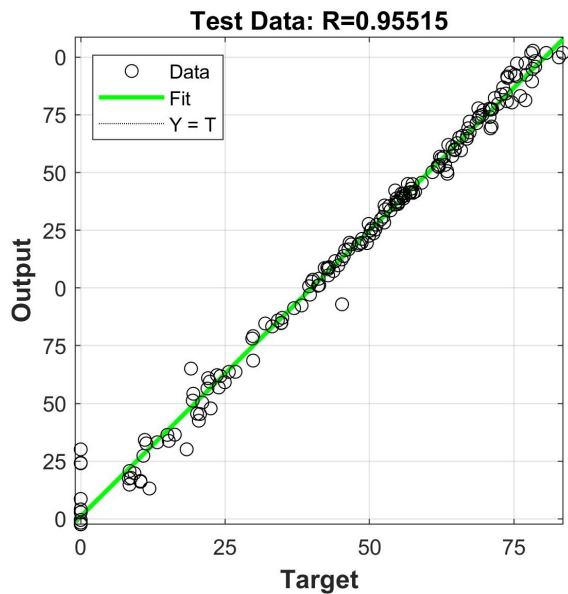


Figure 8: Modelling results.

4 CONCLUSIONS

To reduce negative impacts of vibrations occurring in the drill string at deep drilling of hard rocks, a mathematical model is proposed to consider parameters of the drilling process and predict the penetration rate. When studying the data on the drilling process, the above parameters are used as input variables: WOB, RPM, torque, MSE, longitudinal, transverse and torsional vibrations. The resulting variable is the ROP of the borehole. Considering the above parameters, a mathematical model of the drilling process is formed on the basis of adaptive neural-fuzzy inference structures (ANFIS). The accuracy of the given model makes 95.56 %.

REFERENCES

- Aarsnes, U. J. F. and Aamo, O. M. (2016). Linear stability analysis of self-excited vibrations in drilling using an infinite dimensional model. *Journal of Sound and Vibration*, 360:239–259. <https://doi.org/10.1016/j.jsv.2015.09.017>.
- Bogomolov, R. M. and Serikov, D. Y. (2018). Vibration damper-calibrator. *Equipment and Technologies for Oil and Gas Complex*, 3:39–43. <https://doi.org/10.30713/1999-6934-2018-3-39-43>.
- Coburn, M. E. (2003). Downhole vibration monitoring & control system. Final report, APS Technology. <https://doi.org/10.2172/831129>.
- Deng, P., Zhang, A., Fu, K., and Li, H. (2021). Nonlinear Vibration of a Time-Space Coupled Drill String System Based on the Surface Morphology of Rock. *Journal of Sound and Vibration*, 506:116153. <https://doi.org/10.1016/j.jsv.2021.116153>.
- Golik, V., Komashchenko, V., Morkun, V., and Zaalishvili, V. (2015). Enhancement of lost ore production efficiency by usage of canopies. *Metallurgical and Mining Industry*, 7(4):325–329. https://www.metaljournal.com.ua/assets/MMI_2014_6/MMI_2015_4/047-GolikKomashchenkoMorkunZaalishvili.pdf.
- Liu, Y., Li, Q., Qi, Z., and Chen, W. (2021). Defect suppression mechanism and experimental study on longitudinal torsional coupled rotary ultrasonic assisted drilling of CFRPs. *Journal of Manufacturing Processes*, 70:177–192. <https://doi.org/10.1016/j.jmapro.2021.08.042>.
- Moharrami, M. J., de Arruda Martins, C., and Shiri, H. (2021). Nonlinear integrated dynamic analysis of drill strings under stick-slip vibration. *Applied Ocean Research*, 108:102521. <https://doi.org/10.1016/j.apor.2020.102521>.
- Morkun, V., Morkun, N., and Pikilnyak, A. (2014). Modeling of ultrasonic waves propagation in inhomogeneous medium using fibered spaces method (k-space). *Metallurgical and Mining Industry*, 6(2):43–48. <https://www.metaljournal.com.ua/assets/Journal/a8.pdf>.
- Morkun, V., Morkun, N., and Tron, V. (2015a). Distributed control of ore beneficiation interrelated processes under parametric uncertainty. *Metallurgical and Mining Industry*, 7(8):18–21. https://www.metaljournal.com.ua/assets/Journal/english-edition/MMI_2015_8/004Morkun.pdf.
- Morkun, V., Morkun, N., and Tron, V. (2015b). Identification of control systems for ore-processing industry aggregates based on nonparametric kernel estimators. *Metallurgical and Mining Industry*, 7(1):14–17. https://www.metaljournal.com.ua/assets/Journal/english-edition/MMI_2015_1/3%20Morkun,%20Tron.pdf.
- Morkun, V., Morkun, N., and Tron, V. (2015c). Model synthesis of nonlinear nonstationary dynamical systems in concentrating production using Volterra kernel transformation. *Metallurgical and Mining Industry*, 7(10):6–9. https://www.metaljournal.com.ua/assets/Journal/english-edition/MMI_2015_10/001Morkun.pdf.
- Morkun, V. and Tron, V. (2014). Automation of iron ore raw materials beneficiation with the operational recognition of its varieties in process streams. *Metallurgical and Mining Industry*, 6(6):4–7. https://www.metaljournal.com.ua/assets/MMI_2014_6/1-MorkunTron.pdf.
- Novikov, A. S. and Serikov, D. Y. (2020). Some features of the work of drill bits and practical techniques for their use [Nekotorye osobennosti raboty burovkykh dolot i prakticheskie priemy pri ikh ispolzovanii]. *Sphere. Oil and Gas*, 2:44–49. https://xn--80aaigboe2bzaiqsf7i.xn--p1ai/upload/journal/sphereoilandgas_2020-2.pdf.
- Serikov, D. Y. and Ginzburg, E. S. (2015). Increasing the efficiency of destruction of medium and hard rocks

- through the use of helical cones [Povyshenie effektivnosti razrusheniia srednikh i tverdykh porod putem ispolzovaniia kosozubogo vooruzheniia sharoshek]. *Equipment and Technologies for Oil and Gas Complex*, 4:18–22. <https://www.elibrary.ru/item.asp?id=23868184>.
- Serikov, D. Y., Panin, N. M., and Ageeva, V. N. (2016). Improvement of sealing systems for bearing assemblies of cone bits [Sovershenstvovanie sistem germetizatsii podshipnikovykh uzlov sharoshechnykh dolot]. *Construction of oil and gas wells on land and at sea*, 4:16–19. <https://www.elibrary.ru/item.asp?id=25849083>.
- Sharma, A., Al Dushaishi, M., and Nygaard, R. (2021). Fixed Bit Rotary Drilling Failure Criteria Effect on Drilling Vibration. In *U.S. Rock Mechanics/Geomechanics Symposium*, volume All Days, page 116–121. <https://onepetro.org/ARMAUSRMS/proceedings-pdf/ARMA21/All-ARMA21/ARMA-2021-2083/2480289/arma-2021-2083.pdf>.
- Tunkiel, A. T., Sui, D., and Wiktorski, T. (2021). Reference dataset for rate of penetration benchmarking. *Journal of Petroleum Science and Engineering*, 196:108069. <https://doi.org/10.1016/j.petrol.2020.108069>.
- Vasiliev, A. A., Vyshegorodtseva, G. I., and Serikov, D. Y. (2015). Study of the influence of the flushing scheme of a roller-cone drill bit on the bottom hole cleaning [Issledovanie vliianiia skhemy promyvki sharoshechnogo burovogo dolota na ochistku zaboia skvazhiny]. *Construction of oil and gas wells on land and at sea*, 5:25–28. <https://www.elibrary.ru/item.asp?id=23702308>.

Simulator of Computer Networks and Basic Network Protocols

Tetiana A. Vakaliuk^{1,2,3}^a, Oleksii V. Chyzhmotria¹^b, Olena H. Chyzhmotria¹^c,
Dmytro S. Antoniuk¹^d, Valerii V. Kontsedailo⁴^e and Viacheslav Kryvohyzha¹^f

¹Zhytomyr Polytechnic State University, 103 Chudnivska Str., Zhytomyr, 10005, Ukraine

²Institute for Digitalisation of Education of the National Academy of Educational Sciences of Ukraine,
9 M. Berlynskoho Str., Kyiv, 04060, Ukraine

³Kryvyi Rih State Pedagogical University, 54 Gagarin Ave., Kryvyi Rih, 50086, Ukraine

⁴Inner Circle, Nieuwendijk 40, 1012 MB Amsterdam, Netherlands

tetianavakaliuk@gmail.com, {chov, ch-o-g}@ztu.edu.ua, dmitry.antonyuk@yahoo.com, valerakontsedailo@gmail.com,
vkryvohyzha@gmail.com

Keywords: Simulator, Computer Networks, Network Protocols, Development.

Abstract: Currently, computer networks are characterized by the complexity of the topology, so the question often arises of preliminary modeling of computer networks. Through modeling, the optimal topology of the future network, the necessary network equipment, as well as the possibility of future development is determined. In addition, modeling a computer network avoids the costs that result from actually building a network in the future. The analysis of software analogs made it possible to present their advantages and disadvantages. The given theoretical information about the network properties of devices and protocols made it possible to formulate the requirements that the designed simulator must meet. Designed and developed the structure of the program code and the main architecture of the system. Classes for interaction with the user and classes for the operation of the application, for communication between applications, are described. The methodology for using the created application is described. The processes of creating a project, creating devices, connecting them to a network, creating traffic between devices, viewing a log, and communicating between devices were described and shown. The designed software meets the requirements and is sufficiently fast, without taking up large resources of the computer on which it is running.

1 INTRODUCTION


We live in a century of information and communication systems and technologies, where it is impossible to imagine any organization without modern computing technology. Today, one enterprise can have about a hundred or even more computers. Consequently, the entire set of equipment, connected by communication lines and exchanging data with each other by certain rules, is a local area network.


Currently, computer networks are characterized by the complexity of the topology, so the question often arises of preliminary modeling of computer networks. Through modeling, the optimal topology of


the future network, the necessary network equipment, as well as the possibility of future development is determined. In addition, modeling a computer network avoids the costs that result from actually building a network in the future.


Also, for the correct interaction of computers operating in networks of different structures and using different software, it is necessary to have certain standards. These standards currently exist in quite a large number. Standards and protocols strictly define the norms and rules for the technical organization of computer networks and programs that implement network interaction.


Since the specific number of personal computers connected in a network is steadily growing, consideration of such problems as network protocols and standards is of particular relevance. This problem also plays an important role in the aspect of choosing one method of building a computer network that meets a given set of requirements.


^a <https://orcid.org/0000-0001-6825-4697>

^b <https://orcid.org/0000-0002-5515-6550>

^c <https://orcid.org/0000-0001-8597-1292>

^d <https://orcid.org/0000-0001-7496-3553>

^e <https://orcid.org/0000-0002-6463-370X>

^f <https://orcid.org/0000-0002-1038-4621>

For a developing country, this highlights the challenge for training and educational institutions as the demand for IT professionals continues to grow. Understanding how computer networks are designed, how they function, and how they can be managed is a necessary skill that an IT professional must acquire.

Students studying in the field of “Information Technology” have a list of compulsory disciplines for study. One of these disciplines is “Computer Networks”, as a result of which students should be able to explain the basics of the functioning of computer networks. To achieve this learning goal, students will have to spend many hours on hands-on design, configuration, and implementation of a computer network. Efficiency in this direction is achieved only when there is enough quality equipment to allow the individual practice of customizing software and hardware.

An alternative approach is to provide students with network simulation software, although this is not intended to completely replace the hardware. However, “it presents a useful and cost-effective approach for understanding computer network concepts, protocols, and applications better than traditional tools” (Lee, 2013).

For this, so-called simulators are often used in the educational process. Network simulators are widely used in solving a variety of problems – both educational in the study of the operation of protocols, and workers in the design of a real network.

The work aims to design and develop a software application for designing and simulating computer networks and protocols.

2 THEORETICAL BACKGROUND

Questions of computer networks and their modeling or development of simulators are considered by Adeniji et al. (Adeniji et al., 2023), Vakaliuk et al. (Vakaliuk et al., 2020), Sun et al. (Sun et al., 2022), Wei et al. (Wei et al., 2022).

In particular, Adeniji et al. (Adeniji et al., 2023) developed an IPv6 experimental stand modeled using the Mininet network. The authors took into account the use of different protocols for individual actions. So, they considered the flow-visor protocol specifically for creating network segments in the topology, and the Floodlight protocol for creating a controller in the Mininet network emulator, as well as virtual switches and virtual hosts.

Vakaliuk et al. (Vakaliuk et al., 2020) considered the possibility of using simulators in the educational process when studying computer networks, and also

substantiated the feasibility of using massive open online courses in teaching the discipline “Computer Networks” to future IT specialists using the Cisco PacketTracer simulator.

Sun et al. (Sun et al., 2022) proposed a CloudSimSFC simulator that simulates server failure/restore events in an MDSN environment. At the same time, other scientists were studying the characteristics of dynamic routing by combining the characteristics of the FANETs themselves.

Wei et al. (Wei et al., 2022) propose to compare and study traditional methods of dynamic routing MANET AODV and DSR using the NS3 simulator.

2.1 Analysis of Analogs of a Software Product

Cisco Packet Tracer is a network simulator that can be used by students as well as teachers and network administrators. This software offers a wide range of Cisco switches and routers running on IOS 12 and IOS 15, Linksys wireless devices, and multiple-end devices such as PCs and command line servers (Jesin, 2014).

Packet Tracer has two workspaces – logical and physical (figure 1). The logical workspace allows users to build a logical network topology by placing, connecting, and clustering virtual network devices. The physical workspace provides a graphical physical dimension of the logical network, giving a sense of the scale and placement of how network devices such as routers, switches, and hosts would look in a real environment.

Packet Tracer has a well-realized simulation of working with hardware settings. For virtual computers, all basic network settings are available, as well as access to the command line emulator and the necessary network utilities. Virtual routers support terminal settings with the ability to use all the necessary commands. Many commands and options are also duplicated in the graphical interface. This is useful when you have to deal with a large amount of virtual hardware, as it saves time on repetitive operations.

Packet Tracer supports all major protocols. You can check the designed network both in the “real-time” mode and by turning on the step-by-step mode. Both general demonstration (indicators on communication channels) and more subtle tests of the lower level are supported, for example, specifically configured packages between virtual devices. As a result, complex network configurations can be modeled and tested relatively quickly.

The disadvantages include focusing exclusively on Cisco equipment – only images of Cisco equip-

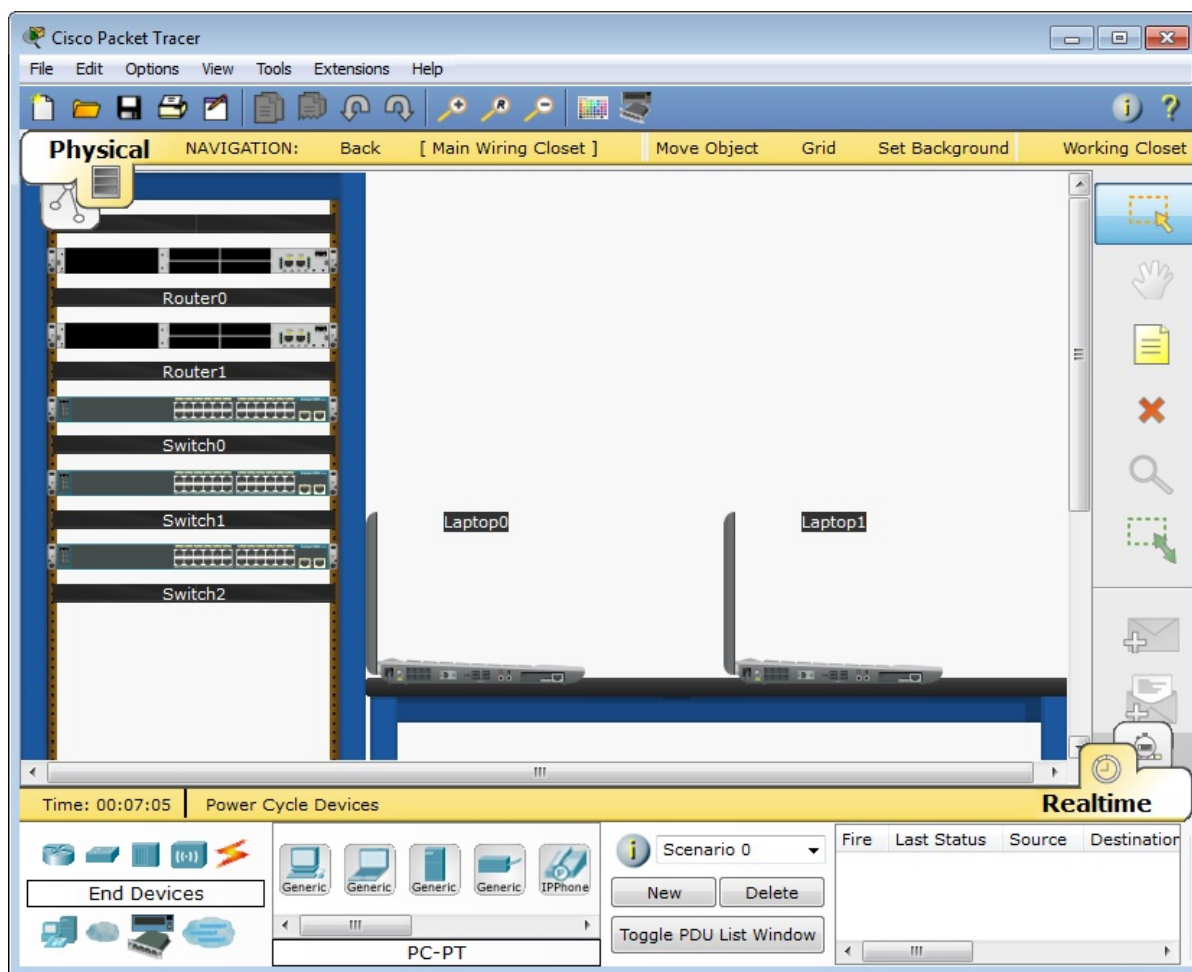


Figure 1: Physical workspace in Cisco Packet Tracer.

ment are included in the application. There is no way out to the real world, projects can be transferred between programs only in the form of internal format files (Čabarkapa, 2015).

Graphical Network Simulator (GNS3) is used by hundreds of thousands of network engineers around the world to emulate, configure, test, and troubleshoot virtual and real networks (04, 2023). This was confirmed by the results of the crowdfunding campaign, during which the GNS3 developer quickly collected quite a substantial amount for the development of the software package.

This package consists of a set of separate independent programs, the composition of which can be changed during installation (figure 2). Individual applications are responsible for their feature blocks. For example, Dynamips is used to simulate virtual routers, and VirtualBox is used to emulate host computers. GNS3 plays the role of a platform that allows you to conveniently link them into a seamless visual

environment. Plugins, extensions, and other options are available (TracerouteNG, PortScanner, Network-Configuration, Real-TimeNetFlowAnalyzer). The latest versions of required components are downloaded from the network automatically during the installation of the GNS3 package.

By default, the GNS3 delivery includes models of only the simplest network devices and conditional ones that are not tied to specific brands. This is due to the fact that GNS3 developers are not directly related to network equipment manufacturers, and therefore they do not have the right to include physical device software images in their package. Therefore, you will have to search and install images of genuine routers separately and independently. However, this approach improves the accuracy of modeling through the use of real images, rather than conditional simulations.

One of the features of GNS3 is the ability to link virtual devices with real ones. For example, the package base includes Wireshark and WinPcap applica-

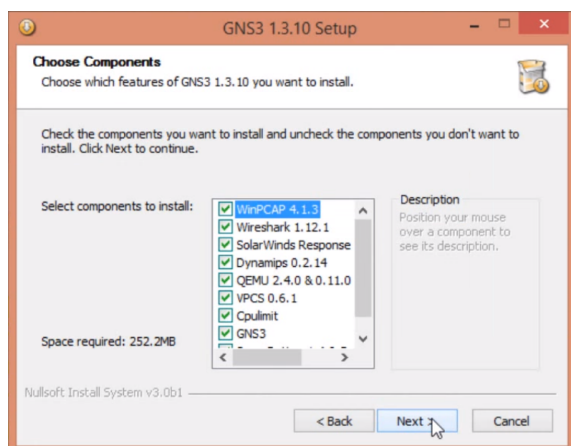


Figure 2: List of programs that will be installed from GNS3.

tions that allow you to manipulate data transmitted in real networks. It becomes possible to work not only in a local virtual sandbox but also in a real network with real devices.

As a result, GNS3 can be used not only for modeling but also for analyzing the operation of existing real computer networks. Moreover, you can mix virtual and physical devices in one project. In other words, a real computer will be able to receive real traffic and process it using a virtual network device, sending an imitation response to the network.

GNS3 has some drawbacks to be aware of. Although theoretically, it is not so important what hardware images will be used, in reality, it is easiest to find, install and get advice on how to use Cisco device images. In addition, we should not forget that GNS3 has high system requirements. Since GNS3 builds full-fledged virtual models without fakes and imitations, the package on more or fewer complex projects has serious system requirements for the computer on which the simulation is being carried out.

Another tool that allows you to simulate the activity of computer networks is EVE-NG (figure 3). Its work and possibilities of use were investigated by Balyk et al. (Balyk et al., 2019).

The most important advantages of this emulator include free of charge, wide user functionality, undemanding requirements for PC resources, support for CISCO equipment, etc.

2.2 Description of the Properties of Computer Networks, and Protocol Devices

The Open System Interconnection (OSI) reference model has served as a set of the most basic elements of computer networks since its inception in 1984. The

OSI model is based on a proposal developed by the International Standards Organization (ISO). The original goal of the OSI model was to create a set of design standards for hardware manufacturers to communicate with each other. The OSI model defines a hierarchical architecture that logically separates the functions necessary to maintain communication between systems.

The OSI model has seven layers, each with a different level of abstraction and performing a well-defined function. The following principles are applied to reach the seven levels (Feig, 1994):

- the level should be created where a different level of abstraction is needed;
- each level must perform a clearly defined function;
- the function of each level should be chosen to take into account the definition of international standardized protocols;
- level limits should be chosen to minimize the flow of information through interfaces;
- the number of levels should be large enough so that different functions do not need to be transferred to the same level from the necessary ones, and small enough so that the architecture does not become unwieldy.

The seven OSI levels, starting with the lowest (El-naggar, 2015):

1. Physical layer – responsible for the transmission and reception of bit streams through the physical medium.
2. Link layer – responsible for the reliable transmission of data frames between two nodes connected at the physical layer.
3. Network layer – responsible for structuring and managing a multi-node network, including addressing, routing, and traffic control.
4. Transport layer – responsible for the reliable transmission of data segments between points in the network, including segmentation, acknowledgment, and multiplexing.
5. Session layer – responsible for establishing communication, maintaining sessions, authentication, and also provides security.
6. Presentation layer – responsible for moving data between the network service and the application; includes character encoding, data compression, encryption, and decryption.
7. Application layer – provides a set of interfaces for applications to access network services.

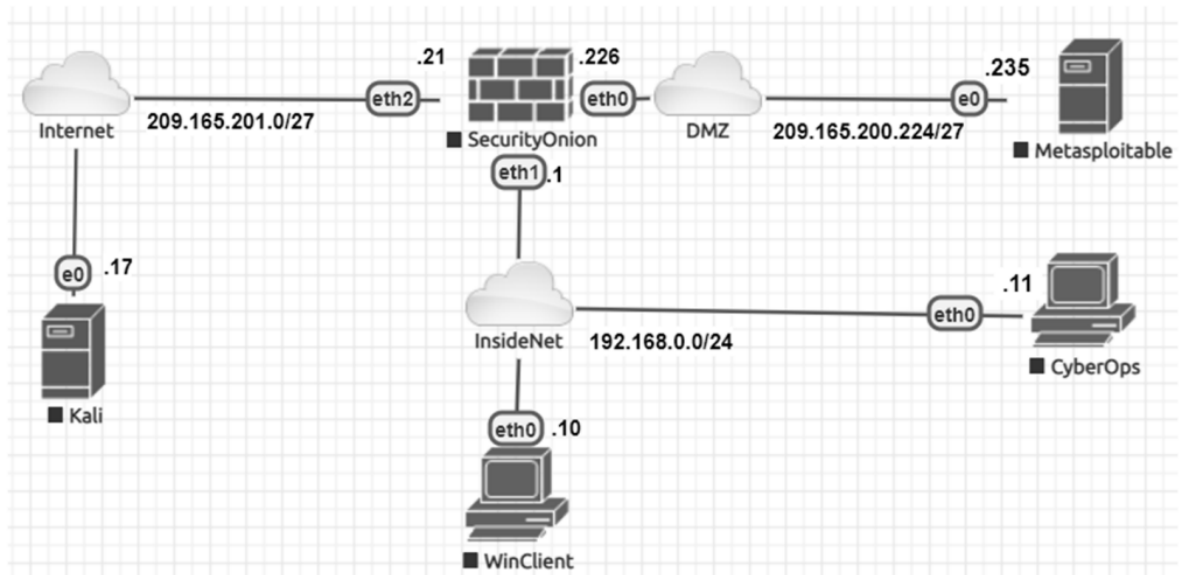


Figure 3: The network topology for labs in EVE-NG.

The Network Interface Controller (NIC) is the primary hardware used to connect to the network. Although traditionally associated with PCs, laptops, and servers, NICs can exist on almost any network device, including printers, phones, and scanners. Some networking hardware, such as switches used for network storage arrays, has plug-in modules that allow for different connection types. These modules are also technically NICs.

The NIC converts data packets between two different data transfer technologies. The end device uses parallel communication technology to transfer data between its internal parts, while the media that enables the communication between different devices uses serial communication technology.

Typically, modern network devices have built-in NICs. If additional NICs are needed, they are also available separately as additional devices. Desktop or server systems, are available in the form of an adapter plugged into the available slots.

There are two types of NICs:

1. Based on the media, NICs are used according to the media type. Different types of NICs are used to connect different types of environments. To connect a particular type of media, we must use a NIC specially designed for this type of media.
2. Based on network design – specific network design requires a special NIC. For example, FDDI, Token Ring, and Ethernet have their characteristic type of NIC cards. They cannot use other types of NIC cards.

The TCP/IP protocol stack is a set of Internet pro-

ocols. The name comes from the core protocols of the Internet – IP (Internet Protocol) and TCP (Transmission Control Protocol). This is a systematized protocol stack, divided into four layers, correlated with the OSI reference model.

TCP/IP levels: application, transport, internetwork, channel. The data link layer describes the data encoding method for transmitting a data packet at the physical layer (i.e., special bit sequences that determine the beginning and end of the data packet and also provide noise immunity). Link layer protocol examples include Ethernet, IEEE 802.11 WLAN, SLIP, Token Ring, ATM, and MPLS. The internetwork layer defines the protocols responsible for the logical transfer of data throughout the network. The main protocols found on this layer are:

1. IP (Internet Protocol) – responsible for delivering packets from the output host to the target host by looking at the IP addresses in the packet headers. IP has 2 versions – IPv4 and IPv6.
2. ICMP (Internet Control Message Protocol) – encapsulated within IP datagrams and is responsible for providing hosts with information about network problems.
3. ARP (Address Resolution Protocol) is responsible for finding the hardware address of the host from a known IP address. ARP has several types: Reverse ARP, Proxy ARP, Gratuitous ARP, and Inverse ARP.

The transport layer is responsible for continuous communication and delivery of data. It keeps top-level applications safe from data complexity.

The two main protocols present in this layer are:

1. TCP (Transmission Control Protocol) provides reliable and trouble-free communication between end systems. It is responsible for sequencing and data segmentation. It also has an acknowledged function and controls the flow of data through a flow control mechanism.
2. UDP (User Datagram Protocol) is a protocol for transmitting datagrams without establishing a connection. UDP does not allow you to verify the delivery of the message to the recipient, as well as the possible mixing of packets. Applications that require guaranteed data transmission use the TCP protocol. UDP is commonly used in applications such as video streaming and gaming, where packet loss is tolerated and retrying is difficult or unjustified, or in challenge-response applications (such as DNS queries) where establishing a connection takes more resources than retrying sending.

The application layer includes the protocols used by most applications to provide user services or exchange application data over network connections established by lower-layer protocols.

Examples of application layer protocols include Hypertext Transfer Protocol (HTTP), File Transfer Protocol (FTP), Simple Mail Transfer Protocol (SMTP), and Dynamic Host Configuration Protocol (DHCP).

3 RESULTS

3.1 Designing a Computer Network Simulator System

A simulator of computer and basic network protocols must provide certain capabilities. Namely, the design of computer networks and the study of their work.

The computer network simulator should provide the ability to add devices to the network. Each device can have network cards containing ports for different communication channels. Each device has parameters such as name, IP address, and others. Devices must be connected via communication channels. Devices can communicate with each other via communication channels. In a computer network simulator, the functionality should be implemented that allows you to track the processes of communication between devices. The main function of a computer network simulator is to enable users to connect to each other's networks. The user can open access to the network with the ability to view or edit in real-time.

After analyzing the requirements of users, we highlight the following use cases:

1. Create a network project.
2. Selection and creation of network devices.
3. Select and create connections between devices.
4. Set up an IP address for the created devices.
5. Viewing the network log of devices.
6. Create and send traffic between devices.
7. Ability to open access to your project.
8. Opportunity to join another project.

Let's define the functional requirements for the simulator:

1. Building a computer network: the system must have a set of programmed devices and connections with which you can create and expand a computer network.
2. The work of several people on one project: the user has the opportunity to open access to his project.

The analysis of functional requirements made it possible to single out the following entities through which we implement the software product. Model-View-ViewModel (MVVM) is an architectural pattern to separate application logic from GUI.

The Model describes the data used in the application. Models can contain logic related to this data, such as logic for validating model properties. At the same time, the model should not contain any logic related to displaying data and interacting with visual controls.

It is not uncommon for a model to implement the `INotifyPropertyChanged` or `INotifyCollectionChanged` interfaces to notify the system of model property changes. This makes it easier to bind to the view, although there is no direct interaction between the model and the view.

The View defines the visual interface through which the user interacts with the application. Concerning WPF views, this is XAML code that defines the interface in the form of buttons, text fields, and other visual elements.

Although a window (the `Window` class) in WPF can contain both an interface in XAML and C# code bound to it, ideally the C# code should not contain any logic other than a constructor that calls the `InitializeComponent` method and performs the initialization of the window. However, there may be some logic in the code file that is difficult to implement within the MVVM pattern in the `ViewModel`.

The `ViewModel` binds the model and the view through a data-binding mechanism. If parameter values change in the model, when the model implements the `INotifyPropertyChanged` interface, the displayed data in the view automatically changes, although the model and views are not specifically connected.

The view model also contains the logic for getting data from the model, which is then passed to the view. The view model also defines the logic for updating the data in the model.

Since view elements, that is, visual components such as buttons, do not use events, the view interacts with the view model using commands.

For example, the user wants to save the data entered in a text field. It presses the button and thereby sends a command to the view model. And the view model already receives the transferred data and updates the model accordingly.

The result of applying the MVVM pattern is the functional distribution of the program into three components that are easier to develop and test, as well as further modify and maintain.

In the diagram shown in figure 4, you can see 4 classes of windows and 2 classes of graphic elements – `MainWindow`, `LogWindow`, `ConfigurationWindow`, `TrafficWindow`, `OpenSystemUserControl`, and `PhysicalMediaUserControl`.

The `MainWindow` class is responsible for displaying the main user interaction elements. The `MainWindow` class also displays devices and connections added by the user. The `LogWindow` class is responsible for displaying the device log, with which you can trace what is happening on the device. The `ConfigurationWindow` class is responsible for displaying device information and editing its IP address. The `TrafficWindows` class is responsible for creating and sending artificial traffic from one device to another. The `OpenSystemUserControl` and `PhysicalMediaUserControl` classes are responsible for the graphical display of devices and connections, as well as user interaction on the `MainWindow` window.

The diagram also shows 4 classes of view models (`MainWindowVm`, `TrafficWindowVm`, `PhysicalMediaVm`, `OpenSystemVm`), which contain the user interaction logic, and 2 models (`OpenSystemModel`, `PhysicalMediaModel`), which store information about devices and connections.

In the diagram shown in figure 5, you can see the classes for communicating an application with another application of this type. The classes are implemented using the WCF framework. They are designed and implemented in such a way that the application can work in client-server mode.

The `SharingService` class contains the functional-

ity responsible for running the application in server mode. The `SharingServiceClient` class contains the functionality responsible for running the application in client mode. The `SharingServiceCallback` class contains functionality that helps the server communicate with the client.

In the diagram shown in figure 6, classes representing network devices are visible: `BaseOpenSystem`, `Computer`, `Router`, and `Switch`.

The `BaseOpenSystem` class is the parent of the `Computer`, `Router`, and `Switch` classes. It includes the functionality and data basic to all network devices.

The `Computer`, `Router`, and `Switch` classes override the functionality implemented in the base class.

The diagram shows the `BaseNetworkInterfaceController` and `NetworkInterface` classes for working with network cards and network interfaces. These classes implement functionality for sending, receiving, and processing data.

The diagram also shows the `PhysicalMedia`, `Cable`, and `Connector` classes, which implement functionality for connecting network devices and transferring data.

In addition, on the diagram you can see 3 classes for creating network equipment `OpenSystemBuilder`, `NetworkInterfaceControllerBuilder`, `PhysicalMediaBuilder`, and `PhysicalMediaManager` for managing network connections, namely connection to network devices.

In the diagram shown in figure 7, classes are shown in work with the link layer, and the ARP protocol is implemented.

The `DataLinkLayerService` class implements functionality for working with link layer protocols. The `HandleArpPdu` method contains the core functionality for handling ARP packets.

The `ArpProtocolService` class contains functionality for working with the ARP protocol. The `_arpCache` field has been created in the class, which stores IP addresses cached to a pair of MAC addresses.

Methods implemented in this class:

- `AddValueToCache` – adds a pair to the cache if there is no such pair;
- `DecapsulateFrameToArpPdu` – decapsulates the received frame into an ARP packet;
- `EncapsulateArpPduToFrame` – encapsulates an ARP packet into a frame;
- `GenerateArpReply` – generates an ARP packet based on the input parameters, and automatically fills the `OperationCode` field with the `Reply` value, which is responsible for determining the packet type (`Request`, `Reply`);

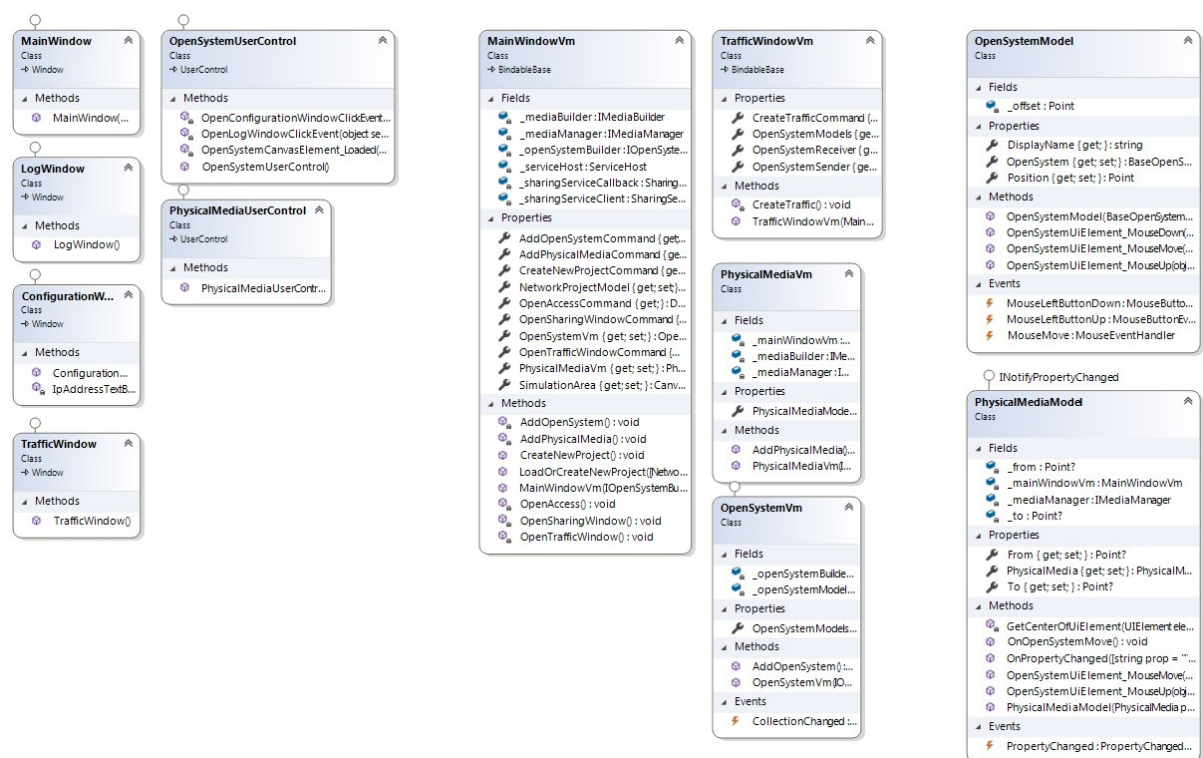


Figure 4: Diagram of classes responsible for working with a graphical interface using the MVVM pattern.

- **GenerateArpRequest** – generates an ARP packet based on the input parameters, and automatically fills the `OperationCode` field, which is responsible for determining the packet type (Request, Reply), with the Request value;
- **GenerateGratuitousArpPdu** – creates an ARP packet based on the input parameters, the packet is created in such a way as to get a GratuitousARP packet as a result;
- **GetCachedMacAddress** – looks up the value of the cached MAC address using the IP address. If no cached value is added, null is returned for further processing;
- **UpdateMacAddressToCache** – looks up the value of the cached MAC address using the IP address and updates its value.

The `EthernetType2Frame` class represents an Ethernet frame used for communication between devices. Looking at figure 8, you can map the fields of the class to the fields of the Ethernet frame.

The `ArpPdu` class represents an ARP packet that, when passed down to the layer, is encapsulated in an Ethernet frame. Looking at figure 9, you can map the fields of the class to the fields of the ARP packet.

The `EtherType` class and the `OperationCode`, `ProtocolType`, `HardwareType` enumeration are part of the

`EthernetType2Frame` and `ArpPdu` classes.

3.2 Design and Implementation of System Operation Algorithms

After launching the program (figure 10) of the computer network simulator, the user can create a new project, add devices to it, add a connection between devices, create traffic from one device to another, open access to the project, or connect to another project. Also, after creating a device, when you right-click on the device, an auxiliary list appears with a choice - open the settings window or the log window of this device.

When choosing the option to create a new project, a command is created that clears all the fields that were previously filled in and initializes them with new values for the new project.

The add device to project option creates a command that initializes a new device and adds it to the collection of created devices. This collection is associated with the view of the main window, that is, when updating (adding or deleting) the collection, graphic elements will appear on the main window with which you can interact.

Adding a connection works in a similar way to add a device. A project must have at least two devices to

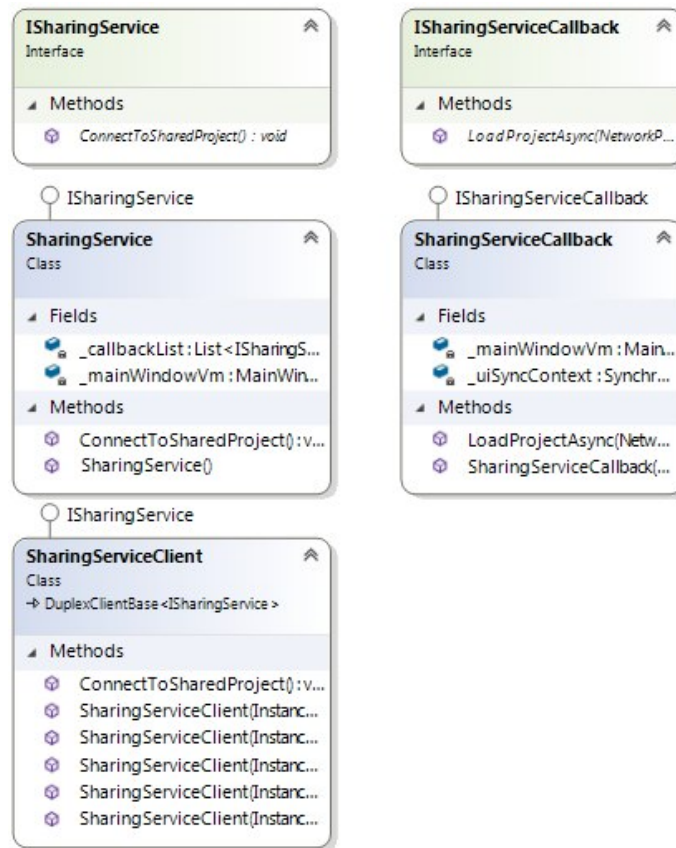


Figure 5: Class diagram for communicating applications with each other.

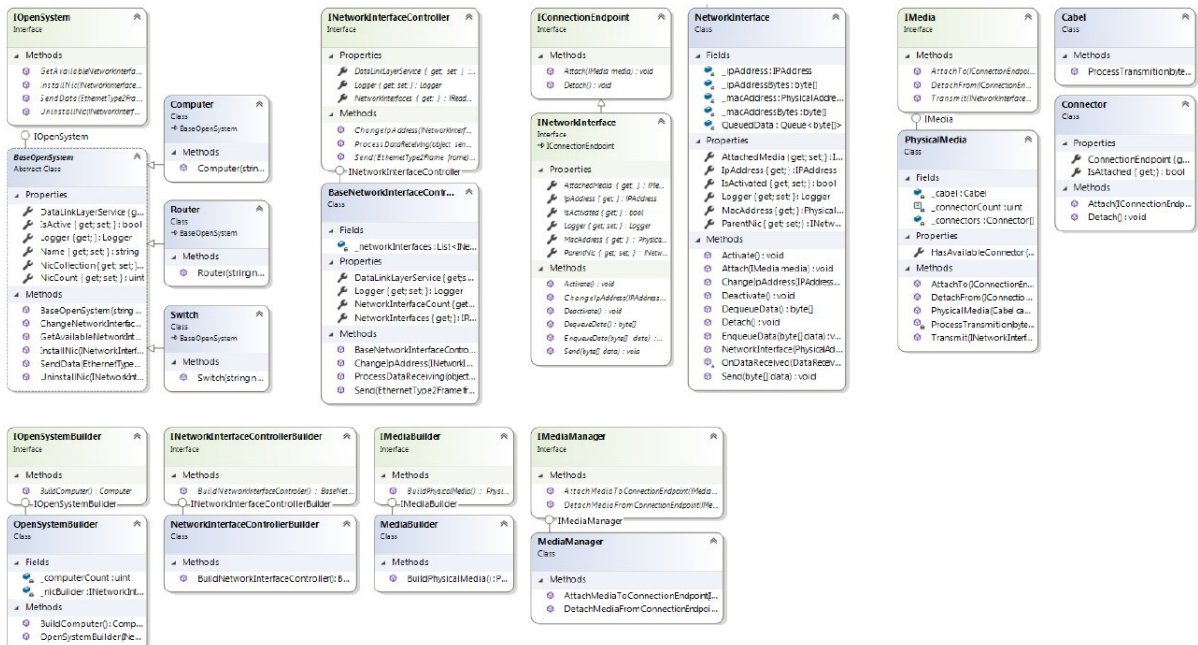


Figure 6: Diagram of classes representing network equipment.

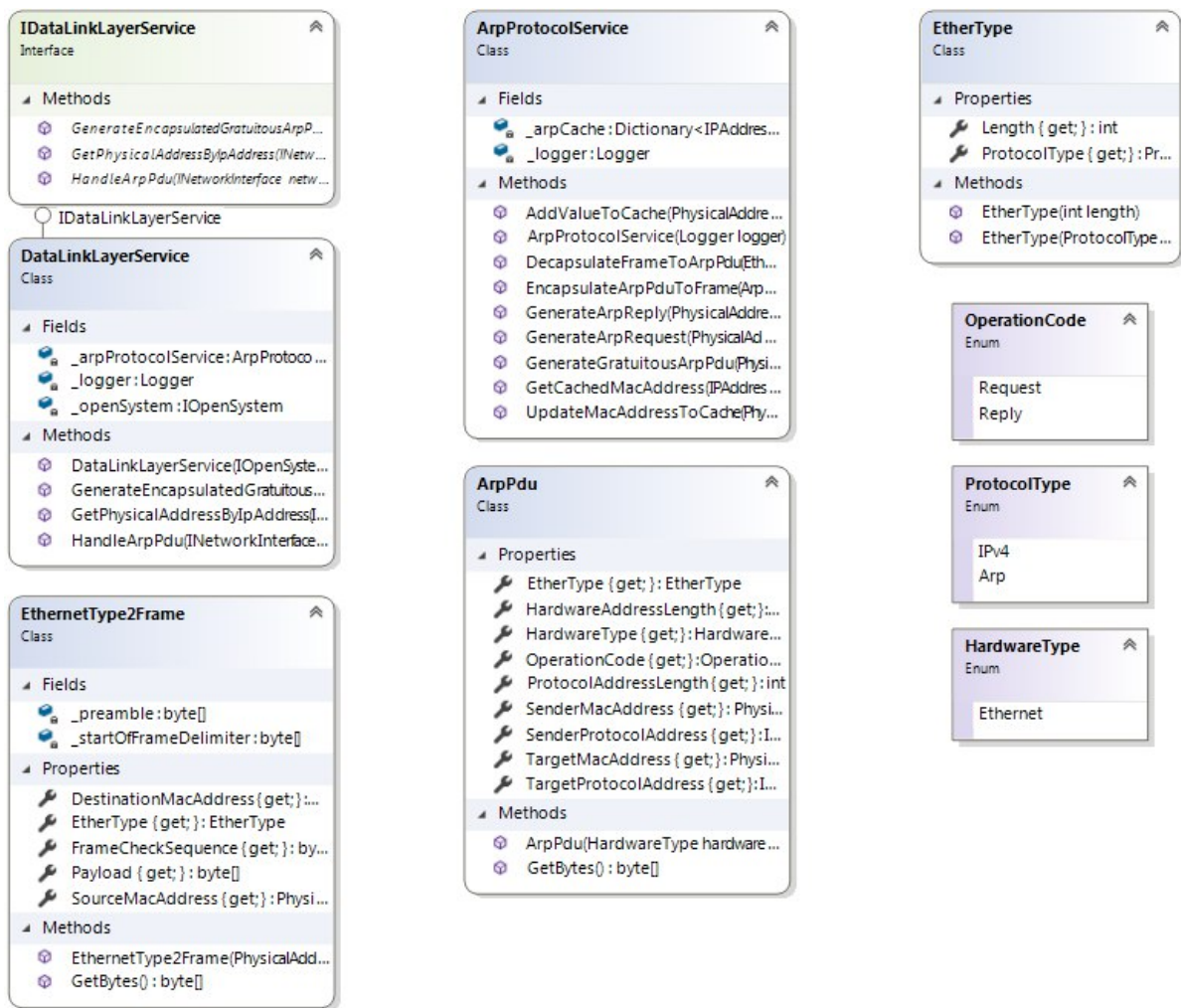


Figure 7: Class diagram for working with Ethernet frames and link layer protocols.

802.3 Ethernet packet and frame structure

Layer	Preamble	Start of frame delimiter	MAC destination	MAC source	802.1Q tag (optional)	Ethertype (Ethernet II) or length (IEEE 802.3)	Payload	Frame check sequence (32-bit CRC)	Interpacket gap
	7 octets	1 octet	6 octets	6 octets	(4 octets)	2 octets	46-1500 octets	4 octets	12 octets
Layer 2 Ethernet frame	← 64–1522 octets →								
Layer 1 Ethernet packet & IPG	← 72–1530 octets →								← 12 octets →

Figure 8: Ethernet frame format at the physical and link layers

be able to connect them.

When you select the traffic creation option, a new window opens in which you can select which device the traffic will be sent from, which device this traffic should come to, and which protocol packets should be sent. After filling in all the fields, the user presses the send button, which generates a command to start the process of sending traffic.

After creating a device, the user can open the

configuration window of this device, which displays its basic information and the network interface table, where you can see the MAC address and IP address of each interface. You can also change the IP address for each interface.

After creating a device and doing some work, such as connecting it to another device or sending traffic, you can open a log window that displays a list of device actions.

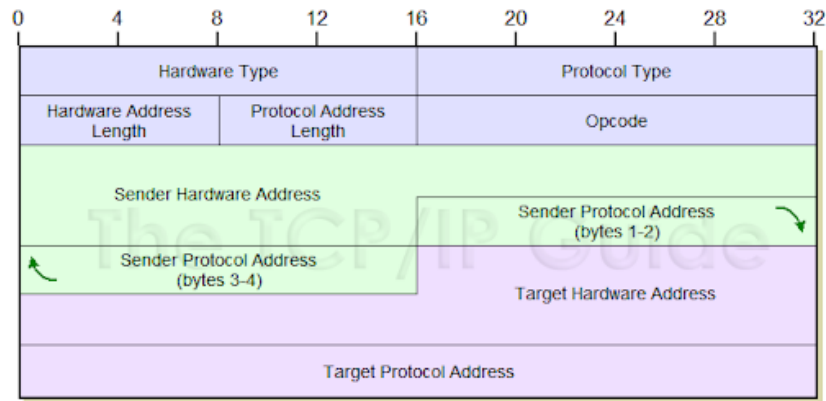


Figure 9: ARP Packet Format

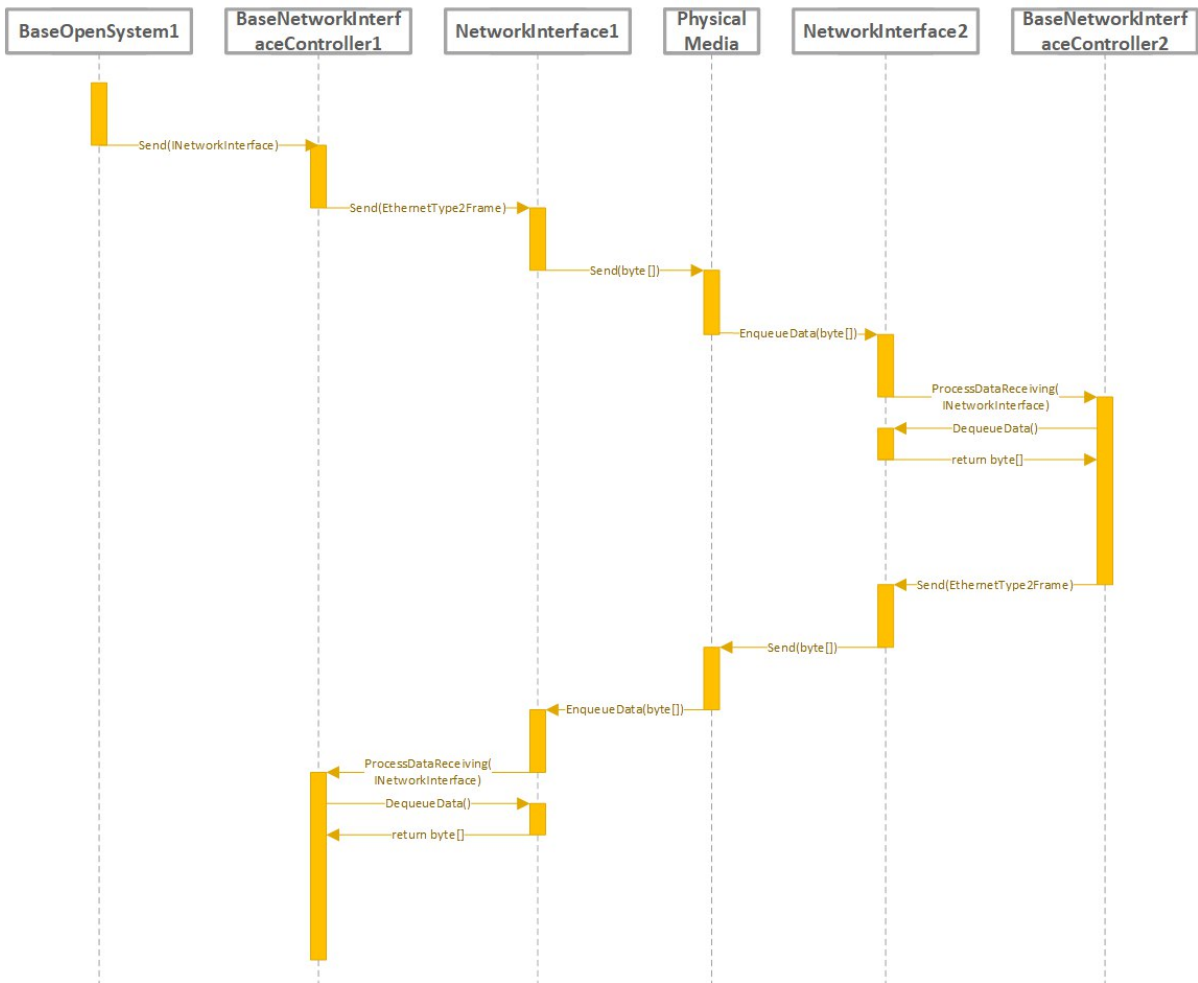


Figure 10: UML Sequence diagram of the process of sending data and receiving a response.

One of the main processes of a computer network simulator is sending data from one device to another (figure 10), provided that they are connected. The process of sending data begins in the BaseOpenSystem class in the SendData method. This method takes

an instance of the EthernetType2Frame class as parameters and knowing from which MAC address the data should be sent, selects the network interface with the corresponding MAC address and calls the Send method of this interface. The Send method of the net-

work interface, having received the data, turns it into a set of bytes, and then sends the data further down the chain to an instance of the PhysicalMedia class, where it simulates the passage of data through a communication channel, after which this data is sent to the next receiving device, and then processes the input data.

Having received the data, the network interface sends them to the network card (BaseNetworkInterfaceController class) to which it belongs. The network card, having received the data, turns it from a set of bytes into an instance of the EthernetType2Frame class, based on which the processing takes place. A special service (DataLinkLayerService class) is responsible for processing the received frame, which, based on the EtherType field, selects the service that will process the data.

Having received a frame, the network card decapsulates it and passes it to the HandlePdu method of the DataLinkLayerService class, which in turn processes the packet using the ArpProtocolService helper service, as shown in figure 11.

3.3 Design and Implementation of Inter-Additional Communication

The key class that hosts and communicates with the application is ServiceHost. It is part of the System.ServiceModel namespace. When an instance of the ServiceHost class is initialized, a service is created with the help of which communication is carried out at lower levels. An instance of the ServiceHost class is initialized with information about the type of service, one or more service endpoints, optional base addresses, and services that govern how the platform handles requests to the service.

Communication between applications occurs through the WCF platform. The main requirements fulfilled by WCF are the implementation of application communication in both client and server mode, that is, the application does not require third-party programs for communication. The first limitation that comes with this architecture is that applications can only communicate if they are on the same network and have access to each other. For communication, 3 classes were designed and implemented (figure 4):

1. Class SharingService – responsible for the communication of the server side. Contains a list of instances of the SharingServiceCallback class, that is, a list of connected clients through which the server can send updates to clients. The class implements the ConnectToSharedProject method, which collects all the data necessary to create a project and sends it to the client. The client, in

turn, creates and fills out a project based on the data received.

2. Class SharingServiceClient – responsible for the communication of the client side. Used to remotely call server methods.
3. Class SharingServiceCallback – encapsulates data about the client. Contains server-side callback methods. Contains the LoadProjectAsync method, which sends a project update to all connected clients.

3.4 The Structure of the Interface and the Procedure for Working with the System

After loading the application, a window appears with a menu for user interaction with the application and a space for building a computer network and interacting with it (figure 12).

To create a network project in which you can build a network, you need to click the item “File” – “Create project”. Once the project is created, the user can add devices by clicking “Devices” and selecting one of the options “Computer”, “Router” or “Switch”.

After creating at least 2 devices, the user can connect them using Connections - PhysicalMedia. By clicking on the item PhysicalMedia, the user must click on the 2 devices that he wants to connect (figure 12).

To create traffic, you need to open the traffic creation window using “Traffic” - “Send data” (figure 13). In the window that opens, you need to select the device from which the data will be sent, the device to which they will have to reach, and what type of protocol will be encapsulated (figure 14).

To communicate with other applications, the user can open access to the project using “Sharing” – “Open Access”, so that other users can join his project. To join someone else project, the user must select “Sharing” – “Connect” to a shared project.

In addition to the menu, the user can interact with devices in the main window. The user can call the context menu of a device by right-clicking on it. In the context menu, there are two options for selection - “Configuration”, which opens the device settings window, and “Log”, which opens the device network log window (figure 15).

By opening the device installation window, the user can see the static settings of the device and its network interfaces. The user can edit the IP address of the network interface (figure 16).

The device network log window that opens shows the actions that took place in the device context (fig-

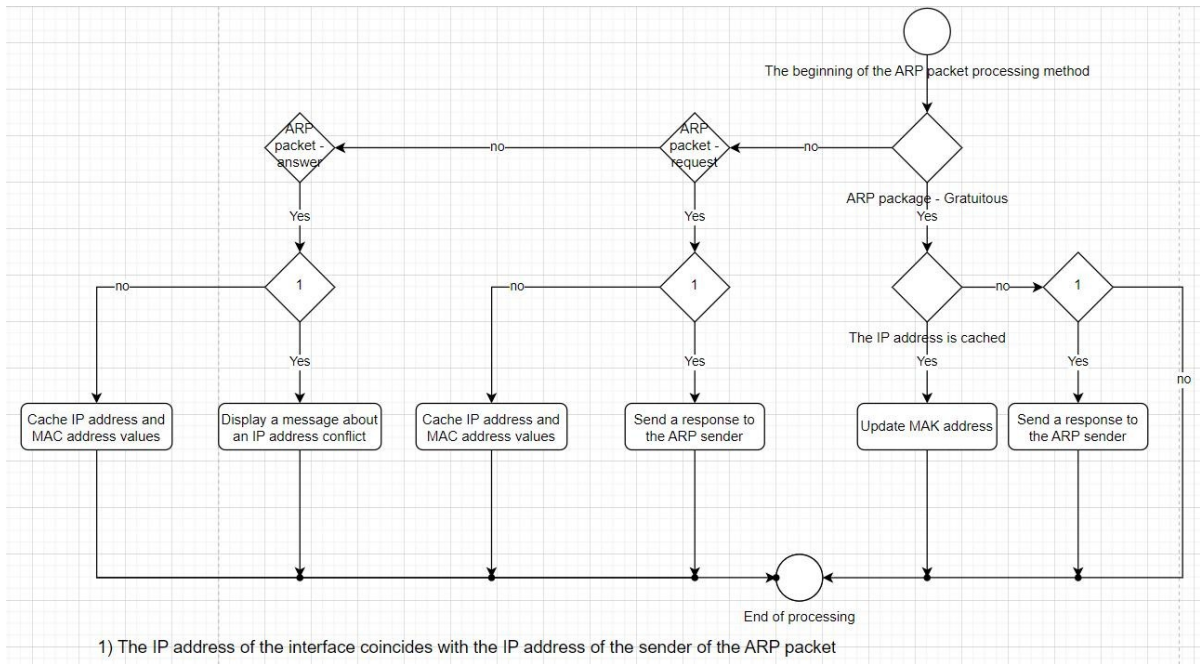


Figure 11: UML activity diagram that shows the process of processing an ARP packet.

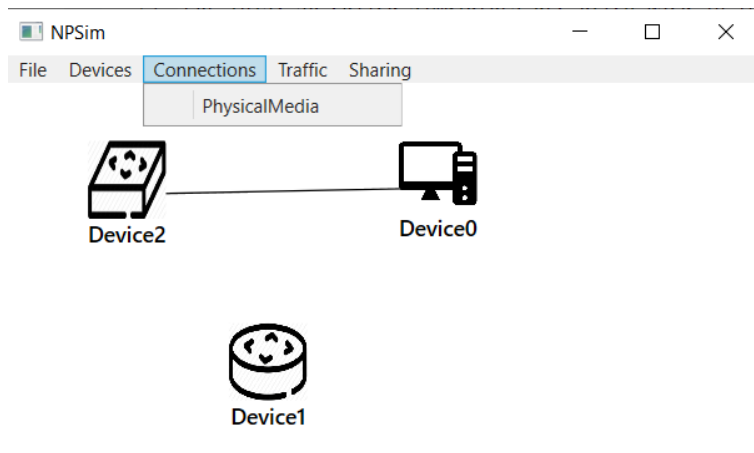


Figure 12: Connecting devices.

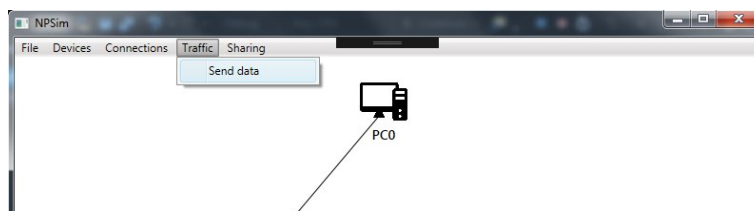


Figure 13: Menu item "Traffic" – "Send data" to open the window for creating traffic.

ure 17, 18). After creating the devices, connecting them to the network, and configuring them so that they have the same IP addresses, ARP Gratuitous packets are sent, with the help of which they learn about the conflict of the IP address (figure 17, 18).

On figure 18 shows an application acting as a

server. A project was created in the application and 2 computers were added, which were connected to the network. On figure 17 shows an application that acts as a client and has been attached to the application shown in figure 18. After connecting to the server application, the client application receives the

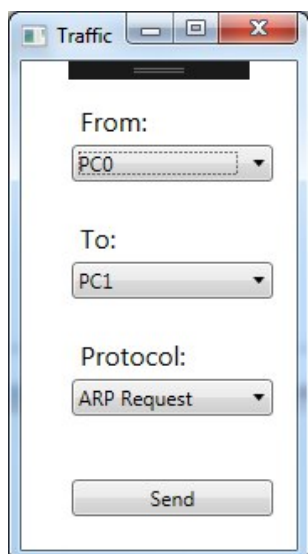


Figure 14: Traffic generation window.

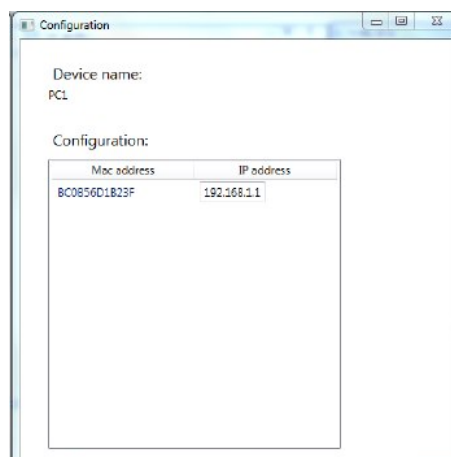


Figure 16: Device settings window.

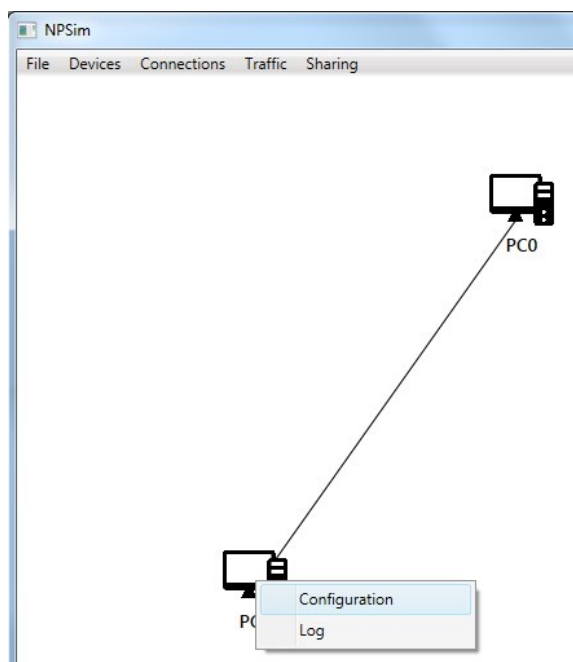


Figure 15: Device context menu.

project data and reproduces this project in the network building space. Also, the client application, having received the data, can trace the actions that took place in the server application using the log.

4 CONCLUSIONS

The analysis of software analogs made it possible to present their advantages and disadvantages. The given theoretical information about the network prop-

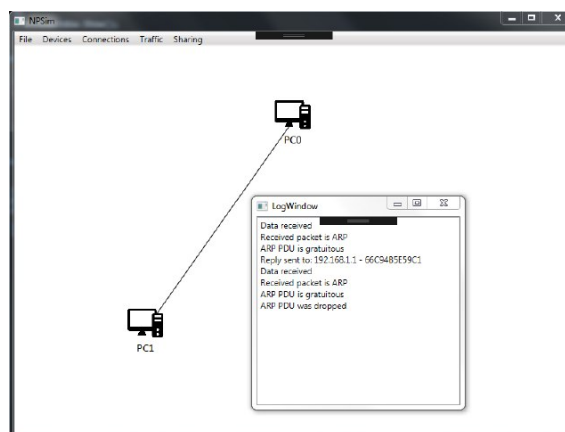


Figure 17: Application that acts as a client.

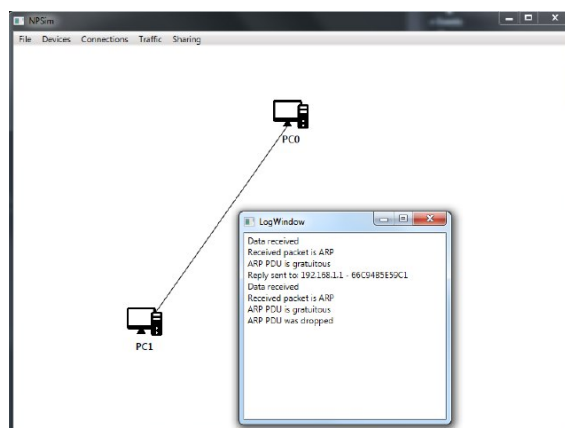


Figure 18: Application that acts as a server.

erties of devices and protocols made it possible to formulate the requirements that the designed simulator must meet.

Designed and developed the structure of the program code and the main architecture of the system.

Classes for interaction with the user and classes for the operation of the application, for communication between applications, are described.

The methodology for using the created application is described. The processes of creating a project, creating devices, connecting them to a network, creating traffic between devices, viewing a log, and communicating between devices were described and shown.

The designed software meets the requirements and is sufficiently fast, without taking up large resources of the computer on which it is running. We see the expansion of the functionality of this simulator as a prospect for further research.







ACKNOWLEDGEMENTS

This work was carried out thanks to the named scholarship of the Verkhovna Rada of Ukraine for young scientists – doctors of sciences for the year 2022.

REFERENCES

- (2023). Getting Started with GNS3. <https://docs.gns3.com/docs/>.
- Adeniji, O. D., Ayomide, M. O., and Ajagbe, S. A. (2023). A Model for Network Virtualization with OpenFlow Protocol in Software-Defined Network. In Rajakumar, G., Du, K.-L., Vuppapapati, C., and Beligianis, G. N., editors, *Intelligent Communication Technologies and Virtual Mobile Networks*, volume 131 of *Lecture Notes on Data Engineering and Communications Technologies*, pages 723–733, Singapore. Springer Nature Singapore. https://doi.org/10.1007/978-981-19-1844-5_57.
- Balyk, N., Vasylenko, Y., Oleksiuk, V., and Shmyger, G. (2019). Designing of Virtual Cloud Labs for the Learning Cisco CyberSecurity Operations Course. In Ermolayev, V., Mallet, F., Yakovyna, V., Kharchenko, V. S., Kobets, V., Kornilowicz, A., Kravtsov, H., Nikitchenko, M. S., Semerikov, S., and Spivakovsky, A., editors, *Proceedings of the 15th International Conference on ICT in Education, Research and Industrial Applications. Integration, Harmonization and Knowledge Transfer. Volume II: Workshops, Kherston, Ukraine, June 12-15, 2019*, volume 2393 of *CEUR Workshop Proceedings*, pages 960–967. CEUR-WS.org. http://ceur-ws.org/Vol-2393/paper_338.pdf.
- Čabarkapa, D. (2015). Application of Cisco Packet Tracer 6.2 in teaching of advanced computer networks. <https://doi.org/10.13140/RG.2.1.4881.6802>.
- Elnaggar, A. (2015). OSI layers. <https://doi.org/10.13140/RG.2.1.3457.7362>.
- Feig, R. (1994). Computer Networks: The OSI Reference Model. <http://web.archive.org/web/20000511022430/http://www.rad.com/networks/1994/osi/osi.htm>.
- Jesin, A. (2014). *Packet Tracer Network Simulator*. Packt Publishing, Birmingham. <https://www.scribd.com/book/272083120/Packet-Tracer-Network-Simulator>.
- Lee, W. (2013). The Evolution of the Networking Skills Gap in Asia/Pacific. White paper, IDC Information and Data. https://www.cisco.com/c/dam/assets/csrf/pdf/IDC_Skills_Gap_-_AsiaPacific.pdf.
- Sun, J., Wo, T., Liu, X., Cheng, R., Mou, X., Guo, X., Cai, H., and Buyya, R. (2022). CloudSimSFC: Simulating Service Function chains in Multi-Domain Service Networks. *Simulation Modelling Practice and Theory*, 120:102597. <https://doi.org/10.1016/j.simpat.2022.102597>.
- Vakaliuk, T. A., Yefimenko, A., Bolotina, V., Bailiuk, Y., Pokotylo, O., and Didkivska, S. (2020). Using Massive Open Online Courses in Teaching the Subject “Computer Networks” to the Future IT Specialists. In Sokolov, O., Zholtkevych, G., Yakovyna, V., Tarasich, Y., Kharchenko, V., Kobets, V., Burov, O., Semerikov, S., and Kravtsov, H., editors, *Proceedings of the 16th International Conference on ICT in Education, Research and Industrial Applications. Integration, Harmonization and Knowledge Transfer. Volume II: Workshops, Kharkiv, Ukraine, October 06-10, 2020*, volume 2732 of *CEUR Workshop Proceedings*, pages 665–676. CEUR-WS.org. <http://ceur-ws.org/Vol-2732/20200665.pdf>.
- Wei, X., Huang, W., and Yang, H. (2022). A Boltzmann machine optimizing dynamic routing for FANETs. *Soft Computing*, 26(22):12385–12391. <https://doi.org/10.1007/s00500-022-07104-w>.

Ultrasonic Cleaning of Ore Particles and Disintegration of Flocculation Formations

Vladimir Morkun¹^a, Natalia Morkun¹^b, Vitalii Tron²^c, Oleksandra Serdiuk²^d,
Iryna Haponenko³^e and Alona Haponenko³^f

¹Faculty of Engineering Sciences, Bayreuth University, Universitätsstraße, 30, Bayreuth, 95447, Germany

²Department of Automation, Computer Science and Technology, Kryvyi Rih National University,
11 Vitalii Matusevych Str., Kryvyi Rih, 50027, Ukraine

³Research Department, Kryvyi Rih National University,
11 Vitalii Matusevych Str., Kryvyi Rih, 50027, Ukraine

{morkunv, nmorkun}@gmail.com, {vtron, serdiuk}@knu.edu.ua, {a.haponenko, haponenko}@protonmail.com

Keywords: Ultrasonic Cleaning, Ore Particles, Disintegration, Flocculation, Ore Processing.

Abstract: The research is aimed at increasing efficiency of magnetite concentrate flotation by cleaning the surface of useful component particles through disintegrating ore flocculated formations. The generalized model of bubble motion dynamics with time-dependent pressure and bubble size is presented. Computer modelling of bubbles behaviour under the action of ultrasonic radiation is performed. The high-energy ultrasound power is calculated to maintain cavitation modes in the iron ore slurry. The research into flocculation and deflocculation considers the dependence of magnetic susceptibility on duration of magnetization. The modelling results enable the conclusion that in order to improve quality of cleaning ore particles before flotation, it is advisable to apply a spatial effect to the iron ore slurry by means of high-energy ultrasound of 20 kHz in the cavitation mode modulated by high-frequency pulses of 1 MHz to 5 MHz.

1 INTRODUCTION


In the liquid medium, some physical, chemical and physicochemical processes occur including cavitation, radiation pressure and ultrasonic flows under the influence of ultrasound (Gubin et al., 2017; Morkun et al., 2014). Since liquids are sensitive to stretching forces, therefore, under powerful ultrasonic oscillations, compression and liquefaction zones arise in the liquid. During the wave phase, which creates liquefaction, there are many gaps in the form of cavitation bubbles in the liquid, which close abruptly in the subsequent phase of compression.


Different effects of ultrasound on individual minerals, are used to achieve high dispersion (Soyama and Korsunsky, 2022; Golik et al., 2015; Morkun et al., 2017), for example, for grinding schistose min-


erals (graphite, molybdenite). The process of grinding molybdenite under excessive static pressure results in manufacturing a product, the dispersion of which is 2-3 times higher than that of the product obtained under atmospheric pressure (Soyama and Korsunsky, 2022).


Application of ultrasound to processing ore raw materials has been an urgent research problem for a long time. In particular, introduction of ultrasound into the water system of ore processing provides specific activation based on two physical phenomena – acoustic cavitation and acoustic wind (Ambedkar et al., 2011; Ambedkar, 2012; Morkun et al., 2015a; Morkun and Morkun, 2018). Gas discharge in acoustic cavitation is most preferable at lower frequency within 20kHz-40kHz, while the acoustic wind dominates at frequencies above 400kHz and 1MHz in ultrasonic and megasonic systems, respectively (Ambedkar et al., 2011).


The experiment results in (Harrison et al., 2002) reveal an increase in the clean coal yield from 3 % to 10 %, greater production of clean coal and a decrease in the content of sulfur, mercury, ash and moisture in the processed coal. These results are associated with


^a <https://orcid.org/0000-0003-1506-9759>

^b <https://orcid.org/0000-0002-1261-1170>

^c <https://orcid.org/0000-0002-6149-5794>

^d <https://orcid.org/0000-0003-1244-7689>

^e <https://orcid.org/0000-0002-0339-4581>

^f <https://orcid.org/0000-0003-1128-5163>

ultrasonic shock waves generated by bubble cavitation that contributes to breaking natural relationships between coal and ash-forming mineral impurities and cleaning of coal particles from impurities. Cavitation also enhances removal of unwanted particles of clay, slime and oxidation products covering the surface of coal.

Application of the above methods is a promising approach to improving efficiency of technological processes of iron ore beneficiation (Morkun et al., 2015b,c).

The research aims to increase efficiency of flotation of magnetite concentrates by disintegrating ore flocculated formations and cleaning particle surfaces. To achieve the set aim, it is necessary to investigate peculiarities of formation of cavitation modes in iron ore slurry by applying high-energy ultrasound.

2 MATERIALS AND METHODS

Let us consider mathematical description of cavitation processes in the heterogeneous medium. The generalized model of bubble motion dynamics dependent on the pressure time and the size of bubbles is presented as a Rayleigh-Plesset equation (Gubin et al., 2017; Kozubková et al., 2012). Solving the Rayleigh-Plesset equation for a certain pressure value $p_\infty(t)$ enables obtaining the value of the bubble radius $dR_b(t)$

$$\frac{dR_b}{dt} = \sqrt{\frac{2}{3} \frac{p_{vap}(t) - p_\infty(t)}{\rho_1}}, \quad (1)$$

where R_b is the bubble radius, μm ; p_∞ is pressure in the medium at perpetuity, Pa; p_{vap} is vapour pressure, Pa; ρ_1 is liquid density, kg/m^3 .

The results of Singhal et al. (Singhal et al., 2002) suggests a cavitation model based on a complete cavitation model. The density of the mixture is defined as

$$\rho = \alpha \rho_{vap} + (1 - \alpha) \rho_1, \quad (2)$$

where α is the volumetric fraction of vapour; ρ_{vap} is vapour density, kg/m^3 ; ρ_1 is liquid density, kg/m^3 . The ratio between density of the mixture and the volumetric fraction of vapour α has the form:

$$\frac{\partial}{\partial t}(\rho) = -(\rho_1 - \rho_{vap}) \frac{\partial}{\partial t}(\alpha), \quad (3)$$

where ρ is density of the mixture, kg/m^3 ; α is the volumetric fraction of vapour; ρ_{vap} is vapour density, kg/m^3 ; ρ_1 is liquid density, kg/m^3 . The volumetric fraction of vapour α is determined from f as

$$\alpha = f \frac{\rho}{\rho_{vap}}. \quad (4)$$

According to the cavitation model proposed in (Schnerr and Sauer, 2001), the equation for the particle volumetric fraction of vapour α is obtained from the expression

$$R = \frac{\partial}{\partial t}(\rho_{vap} \alpha) + \frac{\partial}{\partial x_j}(\rho_{vap} \alpha \bar{u}_j), \quad (5)$$

where R is the evaporation rate, kg/h .

$$R = \frac{\rho_{vap} \rho_1}{\rho} \left(\frac{\partial \alpha}{\partial t} + \frac{\partial (u_j \alpha)}{\partial x_j} \right) \quad (6)$$

When substituting equation (5) in (6) we obtain

$$R = \frac{\rho_{vap} \rho_1}{\rho} \alpha (1 - \alpha) \frac{3}{R_b} \sqrt{\frac{2}{3} \frac{(p_{vap} - p)}{\rho_1}} \quad (7)$$

The bubble radius is determined from the expression

$$R_b = \left(\frac{\alpha}{1 - \alpha} \frac{3}{4\pi} \frac{1}{n_b} \right)^{\frac{1}{3}}. \quad (8)$$

Also in this model, the only parameter to be determined is the number of spherical bubbles in the volume of liquid n_b .

Equation (7) is also used to simulate the condensation process. The final form of the model is as follows:

if $p \leq p_{vap}$

$$R_e = \frac{\rho_v \rho_1}{\rho} \alpha (1 - \alpha) \frac{3}{R_b} \sqrt{\frac{2}{3} \frac{(p_{vap} - p)}{\rho_1}}. \quad (9)$$

if $p \geq p_{vap}$

$$R_c = \frac{\rho_v \rho_1}{\rho} \alpha (1 - \alpha) \frac{3}{R_b} \sqrt{\frac{2}{3} \frac{(p - p_{vap})}{\rho_1}}. \quad (10)$$

If ultrasonic frequency is small ($< 1\text{MHz}$) and pressure amplitude is much smaller than the atmospheric static pressure (101 kPa), a bubble will be in the state of stable cavitation (Hu, 2013), i.e. fluctuate around its initial radius in the periodic mode periodically. This process should be described using an empirical equation based on the simplified Keller-Herring model (Carvell and Bigelow, 2011)

$$R_0 \cong 3 \{MHz\} \frac{\mu m}{f_0^{lin}}, \quad (11)$$

where R_0 is the radius of the bubble, μm ; μ is the shearing viscosity coefficient, f_0^{lin} is ultrasonic frequency, MHz.

It should be noted that at higher pressure, the bubble reaction also largely depends on the ultrasonic field pressure amplitude and, therefore, equation (11) is no longer possible in this ‘‘inertial cavitation’’ scenario.

There are expressions in (Carvell and Bigelow, 2011) to calculate the optimal initial radius of the bubble for maximum expansion depending on ultrasonic frequency and pressure amplitude

$$R_{optimal} = \frac{1}{\sqrt{0.0327F^2 + 0.0679F + 16.5P^2}}, \quad (12)$$

where P is the pressure amplitude for the ultrasonic sinusoidal wave, MPa; f is frequency, MHz; $R_{optimal}$ is the optimal bubble radius, μm .

For example, if $f = 1\text{MHz}$, $P = 1\text{MPa}$, the optimal bubble radius is 0.2454m .

Calculation covers the frequency range, MHz, pressure amplitudes, MPa and radii, μm used in modelling (Hu, 2013) (table 1). It should be noted that at $f = 0.5\text{MHz}$ and pressure $P = 8.0\text{MPa}$ the initial radius is $R = 30.75\text{nm}$.

After converting dependence (12), we get a square equation that includes the function of optimal frequency for a certain size of bubbles from where $F(R)$ at the known pressure P can be determined from the expression

$$F(R) = \frac{-0.068 \pm \sqrt{0.068^2 - 4 \cdot 0.034 \cdot (6.5P^2 - \frac{1}{R})}}{2 \cdot 0.033}. \quad (13)$$

where $R_{optimal}$ is the optimal bubble size, μm ; $F()$ is frequency of high-energy ultrasound, MHz.

Consequently, the cavitation mode with the known bubble size is formed by impacting the slurry with high-energy ultrasound with $F(R_{optimal})$ frequency.

We denote the function of distributing bubbles by size by $f(R)$, then the value $f(R)dR$ determines the fraction of bubbles within the size range of R to $R + dR$.

Table 2 demonstrates the value of the function used in calculations.

The obtained dependences allow determining optimal frequency of high-energy ultrasound to maintain cavitation in the iron ore slurry depending on parameters of its components. Therefore, to form controlled cavitation processes and acoustic flows in the iron ore slurry, it is necessary to model dynamic effects of high-energy ultrasound in the heterogeneous medium.

3 RESULTS AND DISCUSSION

Bubble behavior under the influence of ultrasonic radiation is modelled by using a specialized software package Bubblesim in MATLAB (Hoff et al., 2000).

Dynamics of air bubble sizes during the modelling process is determined through the modified Rayleigh-Plesset equation (Hoff, 2001):

$$\ddot{a}a + \frac{3}{2}\dot{a}^2 + \frac{p_0 + p_i(t)p_L}{\rho} - \frac{a}{\rho c}\dot{p}_L = 0 \quad (14)$$

where a is the bubble radius, m; p_0 is hydrostatic pressure, Pa; p_i is acoustic pressure, Pa; p_L is pressure on the bubble surface, Pa; ρ is fluid density, kg/m^3 ; c is the sound speed, m/s.

The following dependence is used to determine the value of the bubble surface pressure p_L :

$$p_L = -4\eta_L \frac{\dot{a}}{a} - (T_2 - T_1) + p_g \left(\frac{a_e}{a}\right)^{3k} \quad (15)$$

where η_L is the internal friction coefficient; T_1 , T_2 are tension of the inner and outer bubble walls, respectively; p_g is internal pressure of gas bubbles, Pa; k is the gas constant of the polytropic process.

The modelling results with nonlinear effects of high-energy ultrasound considered are presented in (figure 1): the driving pulse (figure 1, a), changes of the bubble radius (figure 1, b), the signal spectrum (figure 1, c).

During the study, the radiation pressure amplitude is 0.3MPa , while the ultrasound frequency changes and makes 1MHz , 3MHz , 5MHz .

To model the process of ultrasonic signal propagation in the liquid medium when changing the sound propagation rate and density, the 1st and 2nd-order k-space method is used based on the 1st-order linear equations (Tabei et al., 2002; Mast et al., 2001).

To apply the k-space method to the system of the 1st-order equations describing wave propagation, the 2nd-order k-space operator can be used by dividing it into parts associated with each spatial direction. For a two-dimensional case, this procedure is performed as follows

$$\frac{\partial p(r,t)}{\partial (c_0 \Delta t)_x^+} \equiv F^{-1} \left(ik_x e^{ik_x \Delta x / 2} \frac{\sin(c_0 \Delta t k / 2)}{c_0 \Delta t k / 2} F(p(r,t)) \right); \quad (16)$$

$$\frac{\partial p(r,t)}{\partial (c_0 \Delta t)_y^+} \equiv F^{-1} \left(ik_y e^{ik_y \Delta y / 2} \frac{\sin(c_0 \Delta t k / 2)}{c_0 \Delta t k / 2} F(p(r,t)) \right);$$

$$\frac{\partial p(r,t)}{\partial (c_0 \Delta t)_x^-} \equiv F^{-1} \left(ik_x e^{ik_x \Delta x / 2} \frac{\sin(c_0 \Delta t k / 2)}{c_0 \Delta t k / 2} F(p(r,t)) \right);$$

$$\frac{\partial p(r,t)}{\partial (c_0 \Delta t)_y^-} \equiv F^{-1} \left(ik_y e^{ik_y \Delta y / 2} \frac{\sin(c_0 \Delta t k / 2)}{c_0 \Delta t k / 2} F(p(r,t)) \right);$$

Table 1: Parameters of ultrasonic cavitation modes.

f, MHz	P, MPa								
	0.01	0.1	0.3	0.5	0.7	1.0	3.0	5.0	8.0
0.5	4.779	2.197	0.809	0.489	0.350	0.245	0.082	0.049	0.031
1.0	3.127	1.940	0.794	0.486	0.349	0.245	0.082	0.049	0.031
3.0	1.414	1.228	0.710	0.465	0.341	0.242	0.081	0.049	0.031
5.0	0.929	0.869	0.615	0.435	0.328	0.238	0.081	0.049	0.031

Table 2: Values of the function of distributing bubbles by size.

$R, m \times 10^{-6}$	3	5	10	20	50
$f(R), m^{-1}$	0.0054	0.0273	0.0545	0.330	0.545
$R, m \times 10^{-4}$	1.5	2.0	2.5	3.0	3.5
$f(R), m^{-1} \times 10^{-3}$	49	21.2	10.9	6.5	4.1

so that

$$\begin{aligned} \left(\frac{\partial p(r,t)}{\partial (c_0 \Delta t)^+ x} \frac{\partial p(r,t)}{\partial (c_0 \Delta t)^- x} + \frac{\partial p(r,t)}{\partial (c_0 \Delta t)^+ y} \frac{\partial p(r,t)}{\partial (c_0 \Delta t)^- y} \right) p(r,t) = \\ = \left(\nabla^{(c_0 \Delta t)} \right)^2 p(r,t) \quad (17) \end{aligned}$$

Spatial-frequency components k_x and k_y are determined so that $k^2 = k_x^2 + k_y^2$. The use of equation operators (16) in (15) enables formation of the 1st-order k-space method which is equivalent to equation (14). Application of exponential coefficients from equation (16) requires evaluation of ultrasonic wave velocities u_x and u_y at the grid points at intervals $\Delta x/2$ and $\Delta y/2$, respectively. The resulting algorithm has the form

$$\begin{aligned} \frac{u_x(r_1, t^+) - u_x(r_1, t^-)}{\Delta t} &= \frac{1}{\rho(r_1)} \frac{\partial p(r,t)}{\partial (c_0 \Delta t)^+ x}; \\ \frac{u_y(r_2, t^+) - u_y(r_2, t^-)}{\Delta t} &= \frac{1}{\rho(r_2)} \frac{\partial p(r,t)}{\partial (c_0 \Delta t)^+ y}; \\ \frac{p(r, t + \Delta t) - p(r, t)}{\Delta t} &= \\ &= -\rho(r) c(r)^2 \left(\frac{\partial u_x(r_1, t^+)}{\partial (c_0 \Delta t)^- x} + \frac{\partial u_y(r_2, t^+)}{\partial (c_0 \Delta t)^- y} \right) \quad (18) \end{aligned}$$

where

$$\begin{aligned} r_1 \equiv (x + \Delta x/2, y), \quad r_2 \equiv (x, y + \Delta y/2), \\ t^+ \equiv t + \Delta t/2, \quad t^- \equiv t - \Delta t/2. \quad (19) \end{aligned}$$

In equation (18), the coefficients c_0 and ρ_0 are replaced spatially and transformed by values of the sound speed and density $c(r)$ and $\rho(r)$. Spatial distribution in equation (18) is implicitly introduced into spatial derivatives of the operators considered. For example, operators

$$\partial / \partial (c_0 \Delta t)^+ x$$

and

$$\partial / \partial (c_0 \Delta t)^- x$$

determined by formula (16) correspond to derivatives calculated after spatial shifts according to the Fourier transformation shift property $\Delta x/2$ and $-\Delta x/2$, respectively.

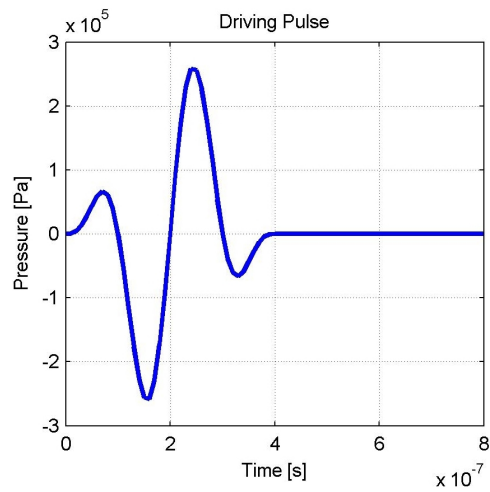
High-energy ultrasound power, which allows maintaining cavitation modes in the iron ore slurry, is calculated on the basis of the above results of studying distribution of the ultrasonic pulse front by using HI-FUSimulator v1.2 (Soneson, 2011). The calculation results are given in figures 3, 4, 5, 6, 7.

The modelling results enable us to conclude that in order to improve quality of cleaning ore particles before flotation, it is advisable to apply a spatial effect to the iron ore slurry by means of high-energy ultrasound of 20kHz in the cavitation mode modulated by high-frequency pulses of 1 MHz - 5 MHz.

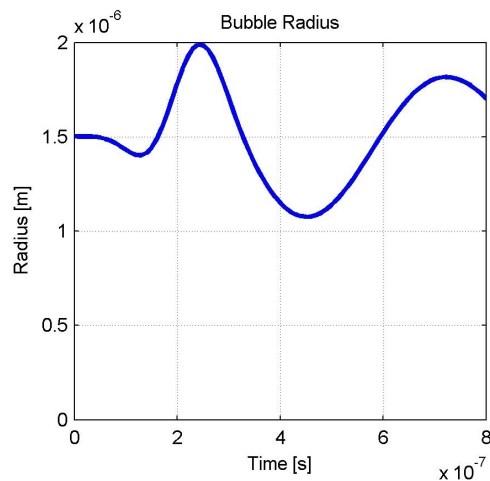
At the same time, the reasons for forming flocs from particles of magnetite iron ore slurry, which being beneficiated move relative to each other and interact with their poles, include movement of ferromagnetic particles in the magnetic field to reduce total magnetostatic energy (energy of free poles) (Karmazin and Karmazin, 2005). This phenomenon is an integral part of beneficiation of fine materials with significant magnetic properties and directly affects efficiency of beneficiation. The size of flocs can vary from 2 to 1000 diameters of the particles forming them.

The phenomenon of fluctuations of monopolar blast furnace boundaries under the action of ultrasonic waves propagating along them is explained by the fact that ultrasound causes variable mechanical stresses in iron particles, which leads to an increase in magnitude of magneto-elastic energy U_d generally determined from the expression (Vlasko-Vlasov and Tikhomirov, 1991)

$$U_d = -\sigma \cdot \lambda \quad (20)$$



(a)



(b)



(c)

Figure 1: Modelling results of cavitation processes under high-energy ultrasound.

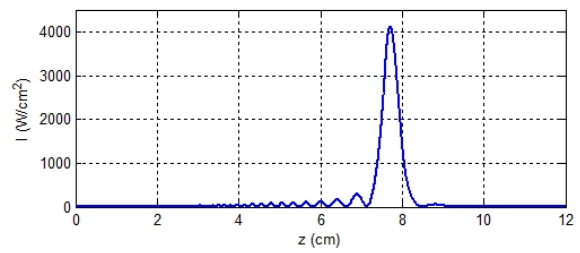


Figure 2: Radial intensity in the ultrasound focus.

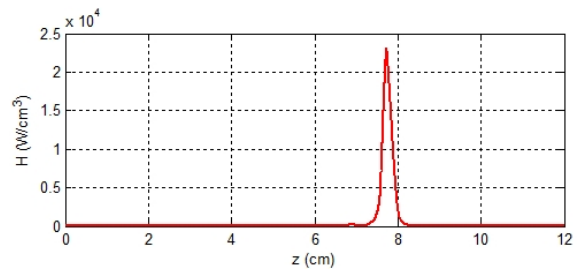


Figure 3: Intensity in the ultrasound focus.

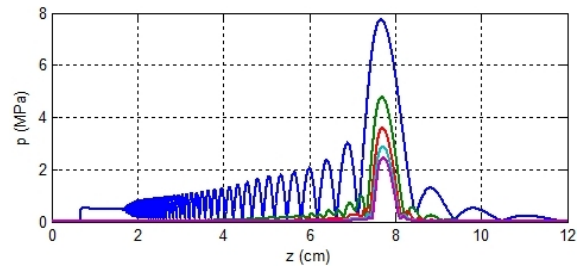


Figure 4: Axial distribution of pressure of the first five harmonics of ultrasonic radiation.

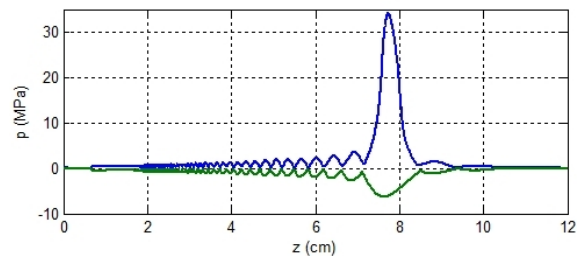


Figure 5: Axial pressure peaks in ultrasonic radiation.

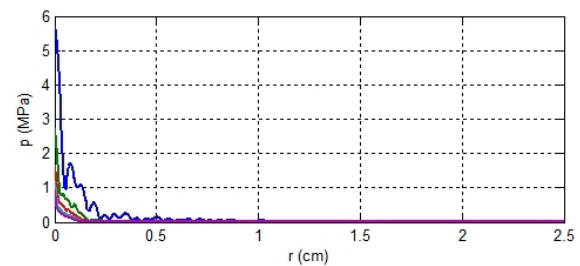


Figure 6: Distribution of radial pressure of the first five harmonics in the ultrasonic radiation focus.

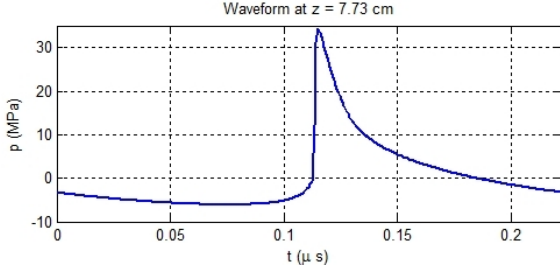


Figure 7: Shape of the ultrasonic wave along the radiation axis at the distance ($z=7.73$ cm), which corresponds to the peak intensity.

where λ is magnetostriction; σ is tension.

According to the Akulov anisotropy law, the expression for U_d has the following form (Chikazumi, 2009):

$$U_d = -\sigma \cdot \left(a_1 \sum_{i=1,2,3} \left(S_i^2 \beta_i^2 - \frac{1}{3} \right) + a_2 \sum_{i \neq j} (S_i S_j \beta_i \beta_j) \right) \quad (21)$$

To observe the condition

$$\frac{\partial (U_K + U_D + U_H)}{\partial \alpha} = 0 \quad (22)$$

where U_K is magnetic anisotropy energy of a crystal; U_H is energy of the external magnetic field.

According to expressions (20)–(22), if energy U_H changes, magnetism of the particles increases.

Interaction of magnetic masses in flocculation is described in accordance with the Coulomb law to determine the strength of flocculated formations F_{fl} (Karmazin and Karmazin, 2005):

$$F_{fl} = \sigma_{fl} S = k \chi^2 H^2 s^2 / (\mu_0 r^2) \quad (23)$$

where σ_{fl} is the floccule strength, S is the area of the floccule cross section, k is the coefficient specifying the coordinate of the point of magnetic mass concentration, ξ is magnetic susceptibility, H is intensity of the magnetic field, r is the distance of interaction.

The strength of floccules is determined by the expression (Karmazin and Karmazin, 2005):

$$\sigma_{fl} = k J^2 / (1 - \chi N)^2 \quad (24)$$

where k is the proportionality coefficient; J is floccule magnetization; N is the floccule demagnetization coefficient. This characteristic is also evaluated by the expression of ferromagnetic energy:

$$F_{fl} = -\frac{dU}{dx} = -\frac{d(BHV)}{dx} = -0.5 BHV = -0.5 \mu H^2 s; \quad \sigma_{fl} = 0.5 \mu H^2. \quad (25)$$

When studying flocculation and deflocculation, one should consider the dependence of magnetic susceptibility γ_c on duration of magnetization t .

The dependence of the flocculation degree Ψ and the field intensity looks like (Karmazin and Karmazin, 2005):

$$\Psi = k_1 H_0^2 + \Delta \psi \delta(H - H_{kr}) + (1 + \psi_2) (1 - \exp(-k_2 (H - H_{kr}))), \quad (26)$$

where H_0 is initial intensity of the magnetic field which causes equilibrable reversible flocculation; $\Delta \psi = \Psi_1 - \Psi_2$ is an increase in the flocculation degree due to the avalanche process; $\Psi_1 - \Psi_2$ are flocculation degrees at the beginning and at the end of the avalanche process, respectively, which are functions of concentration, the formfactor, size and magnetic susceptibility of flocculating particles; H_{kr} is critical field tension causing avalanche flocculation $H_0 < H_{kr}$; k_1 , k_2 are intensity coefficients presented as functions of concentration, magnetic susceptibility, the formfactor, the Reynolds parameter for the hydromechanical mode of the medium motion, particle size dependent on time [$k_2 = f(C, N, \mathfrak{K}, Re, d, t)$]; $\delta(H - H_{kr})$ is the Dirac function from tension; $\int_{H_{kr}-\Delta}^{H_{kr}+\Delta} \delta(H - H_{kr}) dH = 1$, where Δ is a small number.

The dependence of size of the narrow fraction particle extracted from the floccule (flocculation degree) E obtained in (Karmazin and Karmazin, 2005; Chikazumi, 2009), shows a significant dependence of flocculation on the content of the ferromagnetic component in the iron ore slurry:

$$E = 1 - e \left(-\frac{r_0 v_0 t}{\int_{r_0}^{R_f} \exp(-k \chi d (r_0^{-1} - r^{-1}) / (3\pi \mu D_t)) r dr} \right) \quad (27)$$

noindent where r_0 is the radius of the floccule; v_0 is the speed of particles of a narrow fraction near the surface of the floccule; t is flocculation time; D_t is the turbulent diffusion coefficient. It should be noted that with decreased size, magnetic susceptibility of the magnetic sharply decreases, and the coercive force increases sharply, which is explained by approximation to the monodomain size of magnetite, that complicating the flocculation process.

When implementing this approach, the ultrasonic wave radiator should be able to vary frequency during measurements in a fairly wide range. In practice, this can be done by means of the ultrasonic phased array. While developing its design, the influence of the distance between elements, wavelength and the number of elements on controllability and efficiency of ultrasonic radiation are investigated. Optimal parameters of the ultrasonic phased array are selected by indicators that characterize its directional diagram (Morkun et al., 2015b,c).

Analysis of the research results enables concluding that in order to increase efficiency of the flotation

process by disintegrating flocculated ore formations, it is advisable to exert a spatial effect on the iron ore slurry including a combination of high-energy ultrasound and the pulsed magnetic field of descending intensity.

The modelling results enable concluding that to improve quality of ore particles cleaning before flotation, it is advisable to apply a spatial effect to the iron ore slurry. This includes a combination of high-energy ultrasound of 20 kHz in the cavitation mode modulated by high-frequency pulses within 1 MHz-5 MHz and the pulsed magnetic field of descending intensity. The next stage involves calculation of characteristics of these effects and determination of the device parameters to disintegrate flocculated ore formations in the slurry flow on the basis of the ultrasonic phased array.

4 CONCLUSIONS

To increase efficiency of magnetite concentrates flotation by disintegrating flocculated ore formations and cleaning the particle surface, it is advisable to use nonlinear effects of the high-energy ultrasonic field to form and maintain cavitation processes and acoustic flows in the iron ore slurry.

Investigation into cavitation patterns results in dependences obtained to determine optimal frequency of high-energy ultrasound aimed to maintain cavitation processes in the iron ore slurry depending on parameters of its components.



Based on the modelling results, it is established that in order to improve quality of ore particles cleaning before flotation, a spatial effect should be exerted on the iron ore slurry, which includes a combination of 20kHz high-energy ultrasound in the cavitation mode modulated by high-frequency pulses of 1 MHz-5 MHz and the pulsed magnetic field of descending intensity.

REFERENCES

- Ambedkar, B. (2012). *Ultrasonic Coal-Wash for De-Ashing and De-Sulfurization: Experimental Investigation and Mechanistic Modeling*. Springer Theses. Springer Berlin, Heidelberg. <https://doi.org/10.1007/978-3-642-25017-0>.
- Ambedkar, B., Nagarajan, R., and Jayanti, S. (2011). Investigation of High-Frequency, High-Intensity Ultrasonics for Size Reduction and Washing of Coal in Aqueous Medium. *Ind. Eng. Chem. Res.*, 50(23):13210–13219. <https://doi.org/10.1021/ie200222w>.
- Carvell, K. J. and Bigelow, T. A. (2011). Dependence of optimal seed bubble size on pressure amplitude at therapeutic pressure levels. *Ultrasonics*, 51(2):115–122. <https://doi.org/10.1016/j.ultras.2010.06.005>.
- Chikazumi, S. (2009). *Physics of Ferromagnetism*, volume 94 of *International Series of Monographs on Physics*. Oxford University Press, Oxford, 2 edition.
- Golik, V., Komashchenko, V., Morkun, V., and Zaalishvili, V. (2015). Enhancement of lost ore production efficiency by usage of canopies. *Metallurgical and Mining Industry*, 7(4):325–329. https://www.metaljournal.com.ua/assets/MML_2014_6/MML_2015_4/047-GolikKomashchenkoMorkunZaalishvili.pdf.
- Gubin, G. V., Tkach, V. V., and Ravinskaya, V. O. (2017). Application of ultrasound for cleaning the surface of altered mineral particles before flotation [Primene-nie ul'trazvuka dlja ochistki poverhnosti izmenennykh mineral'nykh chastic pered flotaciej]. *The quality of mineral raw materials*, 1:341–349.
- Harrison, C. D., Raleigh, Jr., C. E., and Vujnovic, B. J. (2002). The use of ultrasound for cleaning coal. In *Proceedings of the 19th Annual International Coal Preparation Exhibition and Conference*, volume 1, page 61–67. http://web.archive.org/web/20190713150249if_/http://www.bixbydental.com:80/about/news/coalultrasound.pdf.
- Hoff, L. (2001). *Acoustic Characterization of Contrast Agents for Medical Ultrasound Imaging*. Springer Dordrecht. <https://doi.org/10.1007/978-94-017-0613-1>.
- Hoff, L., Sontum, P. C., and Hovem, J. M. (2000). Oscillations of polymeric microbubbles: Effect of the encapsulating shell. *The Journal of the Acoustical Society of America*, 107:2272–2280. <https://doi.org/10.1121/1.428557>.
- Hu, Z. (2013). Comparison of Gilmore-Akulichev equation and Rayleigh-Plesset equation on the rapetic ultrasound bubble cavitation. Master's thesis, Iowa State University. <https://doi.org/10.31274/etd-180810-3261>.
- Karmazin, V. V. and Karmazin, V. I. (2005). *Magnetic, electrical and special methods of mineral processing*. Publishing house MGTU.
- Kozubková, M., Rautová, J., and Bojko, M. (2012). Mathematical Model of Cavitation and Modelling of Fluid Flow in Cone. *Procedia Engineering*, 39:9–18. XI-IIth International Scientific and Engineering Conference "Hermetic Sealing, Vibration Reliability and Ecological Safety of Pump and Compressor Machinery" - "HERVICON-2011". <https://doi.org/10.1016/j.proeng.2012.07.002>.
- Mast, T. D., Souriau, L. P., Liu, D.-L. D., Tabei, M., Nachman, A. I., and Waag, R. C. (2001). A k-space method for large-scale models of wave propagation in tissue. *IEEE Transactions on Ultrasonics, Ferroelectrics, and Frequency Control*, 48(2):341–354. <https://doi.org/10.1109/58.911717>.
- Morkun, V. and Morkun, N. (2018). Estimation of the Crushed Ore Particles Density in the Pulp Flow Based on the Dynamic Effects of High-Energy Ultrasound.

- Archives of Acoustics*, 43(1):61–67. <https://doi.org/10.24425/118080>.
- Morkun, V., Morkun, N., and Pikilnyak, A. (2014). The adaptive control for intensity of ultrasonic influence on iron ore pulp. *Metallurgical and Mining Industry*, 6(6):8–11. https://www.metaljournal.com.ua/assets/MMI_2014_6/2-MorkunPikilnyak.pdf.
- Morkun, V., Morkun, N., and Tron, V. (2015a). Distributed closed-loop control formation for technological line of iron ore raw materials beneficiation. *Metallurgical and Mining Industry*, 7(7):16–19. https://www.metaljournal.com.ua/assets/Journal/english-edition/MMI_2015_7/003Vladimir%20Morkun%2016-19.pdf.
- Morkun, V., Morkun, N., and Tron, V. (2015b). Distributed control of ore beneficiation interrelated processes under parametric uncertainty. *Metallurgical and Mining Industry*, 7(8):18–21. https://www.metaljournal.com.ua/assets/Journal/english-edition/MMI_2015_8/004Morkun.pdf.
- Morkun, V., Morkun, N., and Tron, V. (2015c). Model synthesis of nonlinear nonstationary dynamical systems in concentrating production using Volterra kernel transformation. *Metallurgical and Mining Industry*, 7(10):6–9. https://www.metaljournal.com.ua/assets/Journal/english-edition/MMI_2015_10/001Morkun.pdf.
- Morkun, V., Semerikov, S., Hryshchenko, S., and Slovak, K. (2017). Environmental geo-information technologies as a tool of pre-service mining engineer's training for sustainable development of mining industry. In Ermolayev, V., Bassiliades, N., Fill, H., Yakovyna, V., Mayr, H. C., Kharchenko, V. S., Peschanenko, V. S., Shyshkina, M., Nikitchenko, M. S., and Spivakovsky, A., editors, *Proceedings of the 13th International Conference on ICT in Education, Research and Industrial Applications. Integration, Harmonization and Knowledge Transfer, ICTERI 2017, Kyiv, Ukraine, May 15-18, 2017*, volume 1844 of *CEUR Workshop Proceedings*, pages 303–310. CEUR-WS.org. <https://ceur-ws.org/Vol-1844/10000303.pdf>.
- Schnerr, G. H. and Sauer, J. (2001). Physical and Numerical Modeling of Unsteady Cavitation Dynamics. In *CMF-2001, 4th International Conference on Multiphase Flow. New Orleans, USA, May 27 - June 1, 2001*. <https://www.researchgate.net/publication/296196752>.
- Singhal, A. K., Athavale, M. M., Li, H., and Jiang, Y. (2002). Mathematical Basis and Validation of the Full Cavitation Model. *Journal of Fluids Engineering*, 124(3):617–624. <https://doi.org/10.1115/1.1486223>.
- Soneson, J. (2011). High intensity focused ultrasound simulator. <https://www.mathworks.com/matlabcentral/fileexchange/30886-high-intensity-focused-ultrasound-simulator>.
- Soyama, H. and Korsunsky, A. M. (2022). A critical comparative review of cavitation peening and other surface peening methods. *Journal of Materials Processing Technology*, 305:117586. <https://doi.org/10.1016/j.jmatprotec.2022.117586>.
- Tabei, M., Mast, T. D., and Waag, R. C. (2002). A k-space method for coupled first-order acoustic propagation equations. *The Journal of the Acoustical Society of America*, 111(1):53–63. <https://doi.org/10.1121/1.1421344>.
- Vlasko-Vlasov, V. K. and Tikhomirov, O. A. (1991). Oscillations of monopolar domain walls in the field of ultrasonic waves. *Solid State Physics*, 33(12):3498–3501. <https://journals.ioffe.ru/articles/22125>.

NFTs: An Overhyped Gimmick or a Promising Technology of the 21st Century

Savelii Lukash¹, Nonna N. Shapovalova¹ ^a and Andrii M. Striuk^{1,2} ^b

¹*Department of Simulation and Software Engineering, Kryvyi Rih National University, 11 Vitalii Matusevych Str., Kryvyi Rih, 50027, Ukraine*

²*Academy of Cognitive and Natural Sciences, 54 Gagarin Ave., Kryvyi Rih, 50086, Ukraine*
{SaveliiLukash, shapovalovann09, andrey.n.striuk}@gmail.com

Keywords: NFT, Non-Fungible Token, Blockchain, Cryptocurrency, Crypto, Web3, Decentralized Application, DApp, Decentralized Finance, DeFi.

Abstract: Non-fungible tokens are the rising technology of the 21st century that is generally overlooked and considered to be impractical. This paper aims to analyze the current state of NFT technology, as well as provide reasonable applications for modern problems and ideas for further development and adoption of this technology. Several live and in-development examples of such projects were provided in this article together with their description and reasoning for the advantages of decentralized approach. Readers of this article are encouraged to consider NFTs as a viable tool for traditional as well as yet unsolved problems.

1 INTRODUCTION

The rise of blockchain and cryptocurrency can be considered the greatest innovation of how people handle money since the introduction of centralized banking (Soloviev and Belinskiy, 2018). Being a decentralized, distributed ledger that securely holds the information on digital transactions it has already started to disrupt traditional business models and financial systems, providing an alternative to traditional banking. Since the first release of Bitcoin in 2009 the industry has gone long way and has attracted a huge number of new users, developers and investors. In the world of ever-growing monopolies, the decentralized finance is a breath of fresh air and a world of infinite possibilities.

The number of crypto holders increases year by year and new successful startups launch regularly. It is estimated that over 6.5 million people, 15.72% of Ukraine's total population, currently own cryptocurrency as of 2021 (table 1) (TripleA, 2023). This number has, undoubtedly, drastically increased in 2022 due to the ongoing events, which have complicated the traditional ways of managing finances, for instance, the ban of P2P transfers from hryvnia payment cards to foreign cards that was passed on 29 Septem-

Table 1: Crypto owners by country (sorted by the percentage of population).


Country	Number of crypto owners	Percentage of the population
Vietnam	20,210,834	20.27%
Ukraine	6,516,114	15.72%
United States	46,020,521	13.74%
South Africa	7,712,116	12.45%
Kenya	6,101,599	11.60%
Pakistan	26,457,317	11.50%
Nigeria	22,332,791	10.34%


ber 2022 and took effect from 5 October 2022 (National Bank of Ukraine, 2022).

Blockchain, however, can be used not only in order to send international payments with record low commissions and speed, but also to mint and trade non-fungible tokens (NFTs).

2 THE NATURE OF NFTs

A non-fungible token (NFT) is a record on blockchain which is associated with a particular digital or physical asset. Unlike regular fungible tokens (such as Bitcoin, Tether, Ether, Solana) it has no equal counterpart. That is, 1 Tether coin is always equal to any other 1 Tether coin (in case of traditional finance 1 USD is always the same as any other 1 USD),

^a  <https://orcid.org/0000-0001-9146-1205>

^b  <https://orcid.org/0000-0001-9240-1976>

whereas any given NFT does not have an equal counterpart, hence the name “non-fungible”. The ownership of an NFT is recorded in the blockchain, and can be transferred by the owner, allowing NFTs to be sold and traded. Usually NFTs contain references to images (art, generated characters, photos, animated GIFs, or any other image), videos, music, etc. (figure 1) (Ozone Networks, 2023).

Technically, it is possible for everyone to right click an NFT art on any website and save it to the hard drive, then use it as a regular image file – set it as a screensaver, print it out or even go as far as to set it as a profile picture on Twitter (as many online trolls do).

However, the main point of NFTs is not that only the owner gets to view the artwork, rather they are the one, who have the ownership of it. The ownership, in turn, can be easily verified thanks to the transparent nature of blockchain. All relevant data, such as transaction history, price and other attributes of an NFT are also publicly available.

A good analogy for NFTs could be conventional pieces of art. Such paintings as Mona Lisa by Leonardo da Vinci do not exist in one single copy, instead, it can be found everywhere: decorating various establishments, on merchandise, in movies, on desktop wallpapers and so on. However the original is the one that bears the real value, both artistic and material. NFTs are a lot alike in this matter. Although instead of experts who determine the original it is the blockchain and its users, who all agree on what the original is, who it belongs to and what is its price.

No matter the benefits of this rising technology its reputation still lags behind. NFTs are associated with many controversies and are often considered to be a gimmick and are expected by many to fade into oblivion rather soon. It cannot be denied that this reputation is well deserved, since the technology is clearly ahead of its time and is just starting to see truly practical applications.

For instance, an American influencer Logan Paul bought an NFT from Azuki’s NFT collection for \$623 000, which is worth \$10 today (figure 2) (Paul, 2022). It is the deals like this than make people wonder if NFTs have any practicality.

3 PRACTICAL USE CASES

Having experience of working in various NFT projects as a developer, in this article I would like to provide you various ideas and examples of how we can make NFTs useful and wipe off the questionable reputation of this technology.

3.1 Fund Raising and Charity

The most obvious way that also removes most questions concerning the artistic value of an NFT is, of course, fund raising.

There are several great projects that are also extremely actual that raise money for the support of Ukrainian people, various funds, volunteers and, for sure, the Armed Forces of Ukraine.

One of such projects is MetaHistory NFT museum (figure 3), which is widely regarded and backed by such organization as the Ministry of Digital Transformation of Ukraine.

Their “WARLINE” collection (Meta History: Museum of War, 2022) follows a chronology of events of the Ukrainian history of modern times. Each token is a real news piece from an official source and an illustration from artists, both Ukrainian and international. This helps not only to raise funds and raise awareness. But also to record the history in a way, that can neither be altered, nor destroyed.

One other project is a landing page for a partnership between Usyk Foundation and Blockasset. The website was launched a couple of weeks before the “Oleksandr Usyk vs Anthony Joshua II” boxing match, which was a great way to gain attention. (More than that, the glorious victory of Oleksandr Usyk vastly improved sales). On this landed page a collection of 2000 unique NFTs featuring Oleksandr Usyk were being sold, each priced at \$200. This helped to raise \$400 000 for medical and hygiene supplies, food and much more. Blockasset has also benefited, as more people got interested in the project in general and in Usyk NFT collection in particular.

The collaboration on raising funds has ended. Regular Blockasset NFTs, featuring Oleksandr Usyk and other athletes, can still be purchased on such platforms as Magic Eden (figure 4) (Blockasset, 2022).

3.2 Decentralized Digital Assets Marketplace

Another great use case for NFTs is creating and trading unique content, which has not only artistic, but also practical value and can be used in commercial or non-commercial purposes. The examples of such content are photos, music, video clips and so on.

At the moment there a lot of such online marketplaces to be found. Such popular services as Envato (Envato, 2023), Shutterstock (Shutterstock, 2023) and Epidemic Sound (Epidemic Sound, 2022) have existed for quite a long time and have gathered thousands of creators, clients and pieces of content.

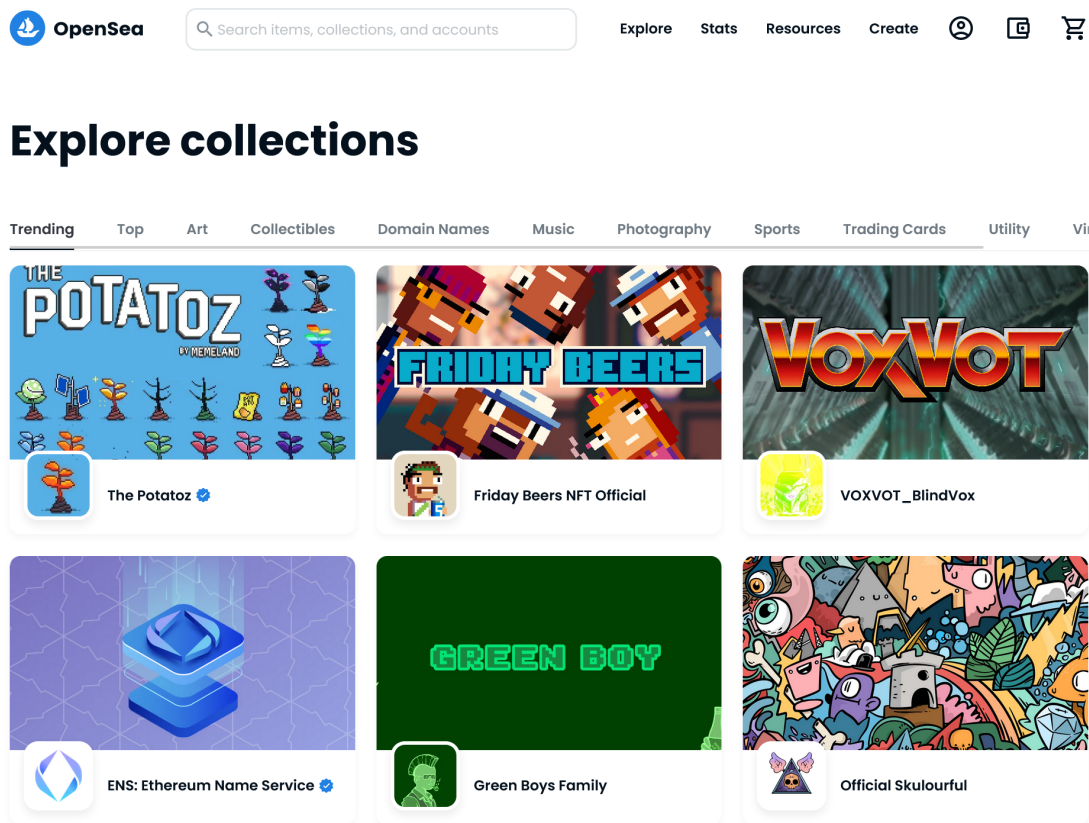


Figure 1: NFT examples from OpenSea, one of the largest non-fungible token marketplaces.

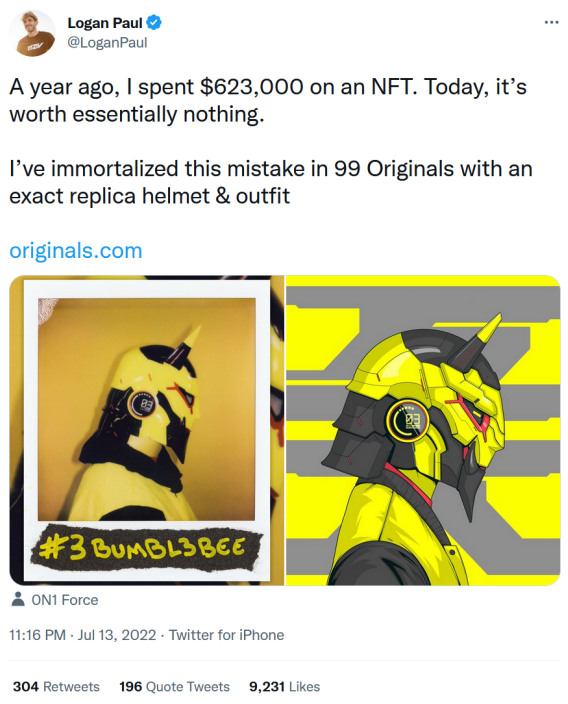


Figure 2: A tweet by Logan Paul on his NFT purchase.

Such marketplaces can also be implemented using Web3 technologies. All these assets will benefit from transparent copyright law protection thanks to the transparent nature of blockchain, and users and creators can perform payments using cryptocurrency.

One of such projects is an NDA¹ project I am currently working on. Since it is completely confidential the good way to describe it is to talk about its closest competitor – Releap.

Releap is a music distribution protocol where artists can publish their tracks as a set of NFTs to be discovered, enjoyed and traded on chain (figure 5) (Rel, 2022).

This project aims to empower emerging and major artists with new ways of gaining exposure, engaging with fans and monetizing their work. With Releap its possible to do such things as:

- Mint music NFTs that can interact with any NFT DApp² (e.g. NFT exchanges, lending or renting protocols) in the Solana ecosystem.
- Discover new music from our growing creator community and directly support creators that user

¹NDA – non-disclosure agreement

²DApp – decentralized application

WARLINE

A chronology of events of the Ukrainian history of modern times, set in stone. The NFTs are facts accompanied by personal reflections. The formula of each NFT is clear and simple: each token is a real news piece from an official source and an illustration from artists, both Ukrainian and international.

Відверта хронологія подій новітньої історії України. Експонати — це факти, супроводжені емоційними спогадами. Формула експонату проста і прозора, кожен токен — реальне новинне повідомлення з офіційних джерел та ілюстрація до нього від художників — як українських, так і світових.

By Hour
By Day
By Drop
All Arts
On Sale
Newest first ▾

Day 189

31 Aug 2022

Day 188 ▾



20:13

#0709

Yesterday, President @BillClinton and I spoke about the importance of strengthening democracy, making sure Ukraine has the assistance it needs, supporting people, and growing resilient economies. Thanks for the...

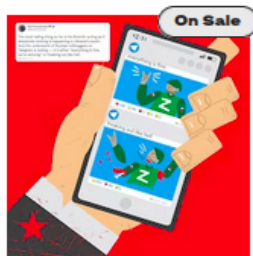
@JustinTrudeau

Buy NFT See details

Day 188

30 Aug 2022

Day 187 ▾ Day 189 ▴



20:46

#0708

The most telling thing so far is the Kremlin acting as if absolutely nothing is happening in Ukraine's south. And the underworld of Russian milbloggers on Telegram is boiling — it's either "everything is fine, we're winning" or freaking...

@IAPonomarenko

Buy NFT See details

Day 187

29 Aug 2022

Day 186 ▾ Day 188 ▴



21:39

#0707

⚡ Zelensky: The legend of 'Russia the great country' must be forgotten. Zelensky said that "when Russia was strong, it was as the Soviet Union, including Ukraine, Kazakhstan, Belarus, and the Baltic states." That time is...

@KyivIndependent

Buy NFT See details



12:59

#0706

BREAKING: The counteroffensive on the ground begins. The #Ukrainian Army have broken through the first line of #Russia's defense in #Kherson. Most of the key bridges are rendered defunct, obstructing the supply of...

@KyivPost

Figure 3: MetaHistory NFT museum "WARLINE" collection page.

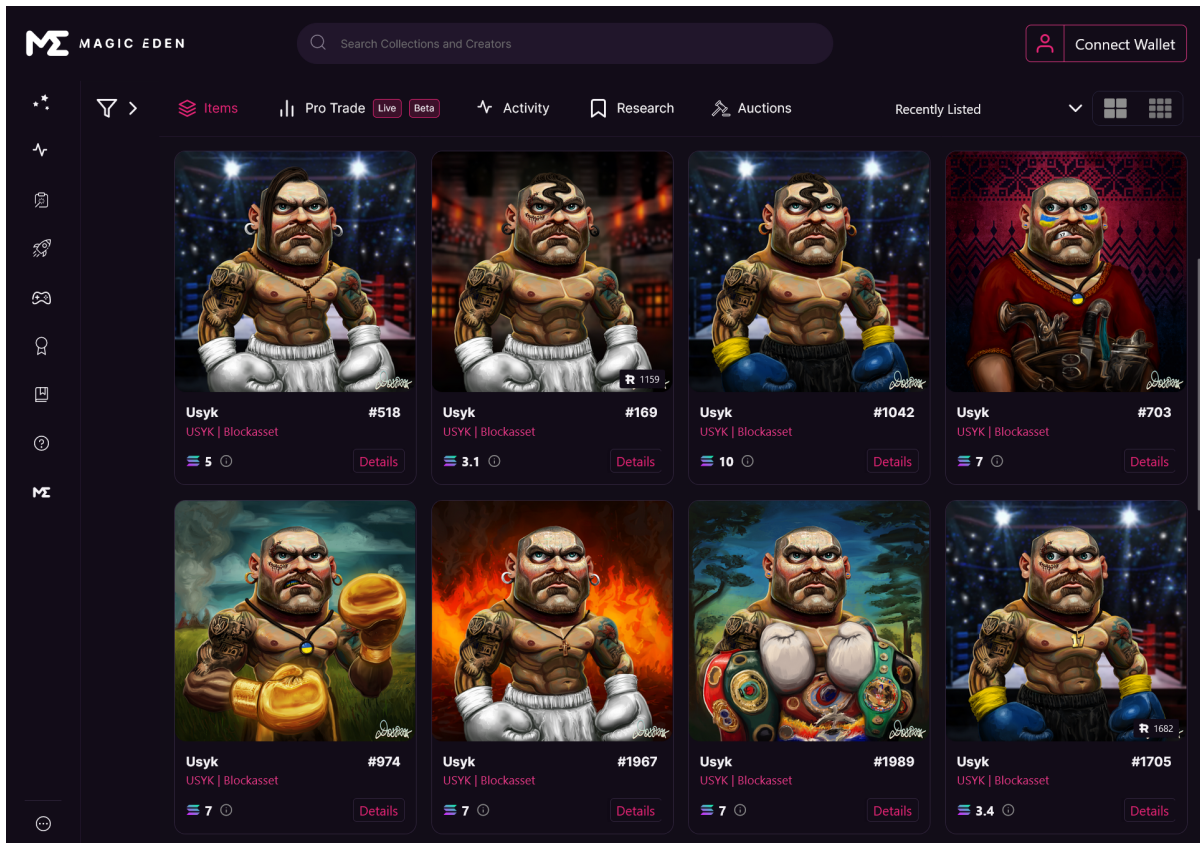


Figure 4: Usyk NFT collection page on Magic Eden.

loves.

- Buy and sell Solana music NFTs on Releap Exchange.
- Interact with music-loving community through public posts and comments.
- Engage with collectors who have bought user’s NFTs through gated posts using Releap Circles.

The same model of using NFTs for original content can also be applied to photos, videos, art and any other digital assets.

3.3 Documents and Certificates

The problem of issuing and verifying documents digitally is widely regarded, as of today. A great leap in this field can be contributed to the Ministry of Digital Transformation of Ukraine with their project Diia (Diia, 2022), which was launched in 2020 and since then has been helping Ukrainian citizens to use digital documents in their smartphones instead of physical ones for identification and sharing purposes. Also, the Diia portal allows access to over 50 governmental services, all within the click of mouse.

The disadvantage of such service is its centralized nature, where users heavily depend on the IT team of Diia to keep everything stable, working as expected and have 24/7 uptime. To mitigate these drawbacks we could also make a good use of blockchain and NFTs to emit, distribute and validate various types of documents and certificates in a decentralized manner.

Thanks to the nature of blockchain it would be easy to establish a specific account that would be associated with a particular governmental or non-governmental institution. This institution could emit documents or certificates by means of minting NFTs.

The ideal documents or certificates for this use case are the ones that do not contain sensitive information, such as: diplomas, certificates, awards, tickets, invitations, and others.

Other documents, such as driver’s licence could be modified for Web3 to only contain non-sensitive information, such as the date of issue and vehicle types that the barer is capable of conducting.

Documents, that contain sensitive information could be still managed in a centralized manner.

There is number of advantages of the decentralized approach in document management, among

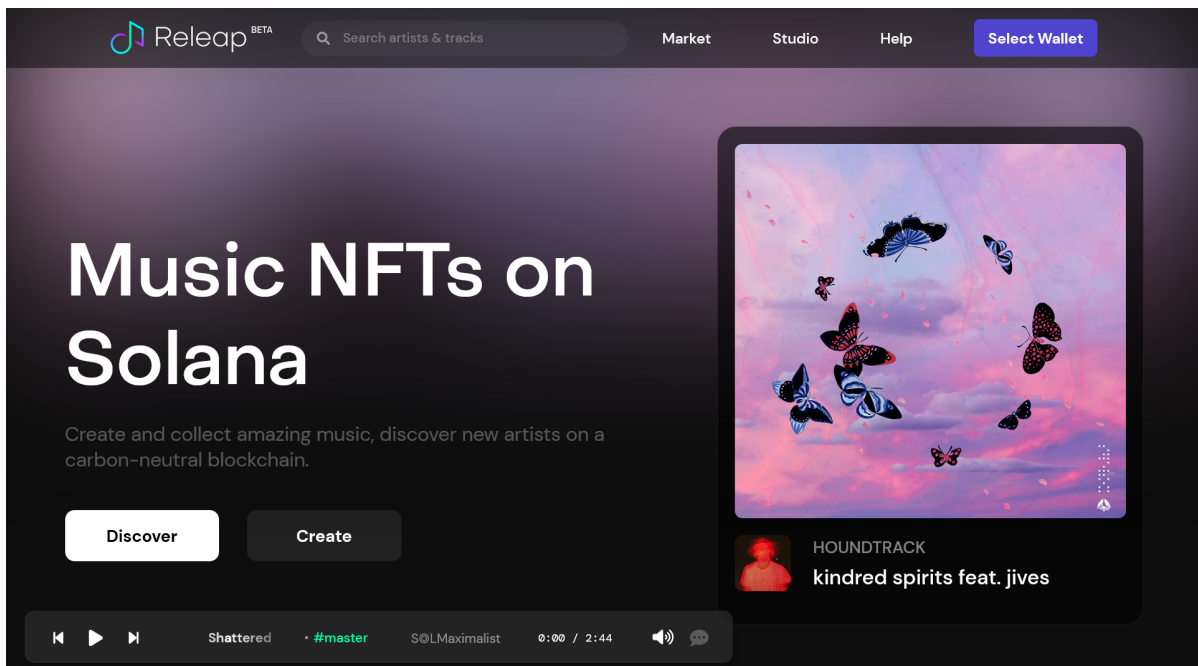


Figure 5: Releap – a platform for music NFTs on Solana.

them:

- Web3-based authentication
- transparency
- ease of validation
- impossibility to counterfeit
- absence of reliance on one specific web service

Such application of blockchain is yet to see light. Ukraine is the first country in the world to implement electronic passports, so it is, for sure, early to discuss a Web3 implementation for something that is yet to come to the majority of the world.

On the other hand non-governmental documents and certificates are rather common. Innovative online platforms use NFTs in order to issue diplomas for their online courses (especially when the course is about Web3 technologies). And ecosystems, such as Blockasset (Athlete-verified NFT and token ecosystem, 2023) use NFTs to provide exclusive access to content (videos, interviews, behind-the-scenes clips) and allow users to have a chat with their favourite athlete in Discord.

4 CONCLUSION

As of today NFTs are associated with many controversies and are often considered to be a short-lasting gimmick and a subject for speculation. However it

appears to be not an issue of the technology itself, but its use case. There is a wide range of options when it comes to NFTs that bring the advantages of decentralized applications into previously existing fields, some of which were described in this article:

- fund raising and charity
- decentralized digital assets marketplace
- documents and certificates

There are many other use cases of NFTs which were not mentioned in this article. Basically almost everything we know today can be implemented in a decentralized manner, what is required is a correct and thoughtful implementation.

All in all, non-fungible tokens make a perspective and promising technology which proves an important and universal point – it is not a technology that should be feared or praised, rather its application.

REFERENCES

- (2022). Releap - Social NFT Platform on Solana. <https://beta.releap.io/>.
- Athlete-verified NFT and token ecosystem (2023). Blockasset. <https://www.blockasset.co>.
- Blockasset (2022). Magic Eden - NFT Marketplace: USYK — Blockasset. <https://magiceden.io/marketplace/usyk>.

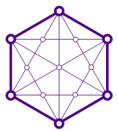
- Diia (2022). Government services online. <https://diia.gov.ua/>.
- Envato (2023). Envato - Top digital assets and services. <https://www.envato.com/>.
- Epidemic Sound (2022). Royalty Free Music for video creators. <https://www.epidemicsound.com>. [Online; accessed 28-October-2022].
- Meta History: Museum of War (2022). Warline: A chronology of events of the Ukrainian history. <https://metahistory.gallery/collection/warline>.
- National Bank of Ukraine (2022). The National Bank of Ukraine is taking measures to ease demand in the FX market's cash segment and protect international reserves, and clarifying some provisions. <https://tinyurl.com/4r3bh9uy>.
- Ozone Networks (2023). OpenSea, the largest NFT marketplace. <https://opensea.io/>.
- Paul, L. (2022). A tweet on NFT purchase. <https://twitter.com/loganpaul/status/1547314126698995713>.
- Shutterstock (2023). Stock Images, Photos, Vectors, Video, and Music. <https://www.shutterstock.com>.
- Soloviev, V. N. and Belinskiy, A. (2018). Complex Systems Theory and Crashes of Cryptocurrency Market. In Ermolayev, V., Suárez-Figueroa, M. C., Yakovyna, V., Mayr, H. C., Nikitchenko, M. S., and Spivakovsky, A., editors, *Information and Communication Technologies in Education, Research, and Industrial Applications - 14th International Conference, ICTERI 2018, Kyiv, Ukraine, May 14-17, 2018, Revised Selected Papers*, volume 1007 of *Communications in Computer and Information Science*, pages 276–297. Springer. https://doi.org/10.1007/978-3-030-13929-2_14.
- TripleA (2023). Global Cryptocurrency Ownership Data 2023. <https://triple-a.io/crypto-ownership-data/>.

AUTHOR INDEX

Antoniuk, D.	63	Kuzmenko, O.	41	Saiapin, V.	5
Bobrov, E.	57	Levchenko, A.	41	Serdiuk, O.	78
Chernysh, O.	50	Levkivskyi, V.	41	Shapovalova, N.	86
Chyzhmotria, O.	63	Lukash, S.	86	Striuk, A.	86
Haponenko, A.	57, 78	Mamyrbayev, O.	13	The, Q.	19, 27, 34
Haponenko, I.	57, 78	Marchuk, G.	41	Tkachuk, A.	50
Hrynevych, M.	50	Medvediev, M.	50	Tron, V.	57, 78
Khairova, N.	13	Morkun, N.	57, 78	Vakaliuk, T.	50, 63
Kontsedailo, V.	63	Morkun, V.	57, 78	Ybytayeva, G.	13
Kryvohyzha, V.	63	Mukhsina, K.	13	Zhumazhanov, B.	13
Kupin, A.	5	Osadchuk, Y.	5	Zubov, D.	5

SUPPORTED BY:

PUBLISHED BY:



ACADEMY OF COGNITIVE
AND NATURAL SCIENCES



Copyright © 2023 by SCITEPRESS -
Science and Technology Publications,
Lda. Under CC license (CC BY-NC-ND 4.0)
ISBN: 978-989-758-653-8